The Artificial Metabolic Organ: Nanorobotic Nutritional Self-Sufficiency

Robert A. Freitas Jr.
Senior Research Fellow, Institute for Molecular Manufacturing
CEO, Nanofactory Corporation

Abstract. The artificial metabolic organ (AMO) is a compact special-purpose diamondoid nanofactory, intended to be implanted in the human body, that can efficiently recycle metabolic waste products into nutrients. By this means, the user becomes a nutritionally self-sufficient entity needing only air, water, and occasional access to electrical power and a few grams per day of stored supplemental minerals to survive indefinitely at metabolic activity power levels ranging from 100 W (basal) to 500 W. The metabolic organ is ~2441 gm in mass and ~1266 cm^3 in volume (smaller than liver) and installed in the central abdomen with proximal access to the two renal veins and the renal ureters exiting both kidneys. It can efficiently extract waste molecules from both blood and urine, chemically transform these wastes into nutrient molecules, then release the nutrient molecules back into the bloodstream, creating a closed-circuit nutrient recycling system. Device power draw ranges from ~200 W to supply basal-level nutritional recycling for ~1 day before recharging the embedded flywheel battery, up to ~578 W at the peak exercise level for ~8 hours of continuous activity, which exhausts the onboard battery. The user can eat and digest food as normal if desired, but at a monetary cost ~25 times higher than today's cost of the electricity needed to power the device.

Cite as: Freitas RA Jr. The Artificial Metabolic Organ: Nanorobotic Nutritional Self-Sufficiency. IMM Report No. 62, September 2025; http://www.imm.org/Reports/rep062.pdf.

Table of Contents

1. Introduction

Human beings eat food for many reasons. The primary biological function of eating is to supply chemical energy for cellular respiration that supports basal metabolism, physical activity, thermoregulation, and biosynthesis. Shared meals are also central to human social structures, from family dinners to religious feasts, with food rituals helping to reinforce group identity and cohesion. Cuisine encodes cultural heritage, beliefs, and practices, with specific foods marking celebrations, mourning, or rites of passage. Eating is linked to emotional regulation, reward pathways (dopamine, opioids), and stress response – comfort foods, emotional eating, and celebratory feasts are common across cultures – and the acquisition and sharing of food can serve as courtship behavior or status display, possibly shaping the course of human evolution.[1]

The nutritional demands of the human body impose significant constraints on human survival, ranging from the immediate exigency to eat sufficient food every day in order to survive, to the larger impact of this persistent necessity such as the entire enterprise of agriculture, food distribution, cooking, and related activities. Setting aside the many obvious social benefits of eating, **is it possible for human beings to become fully nutritionally self-sufficient and independent of the need to eat food every day?**

The concept of the "food pill"[2] – a single oral capsule that could replace traditional meals by delivering complete nutrition – truly originated in early 20th-century science fiction and was popularized by futurist speculation during the early- to mid-1900s.[3] One of the first was L. Frank Baum, whose earliest children's novel *The Master Key* (1901)[4] described a box of tablets: "Within each tablet are stored certain elements of electricity which are capable of nourishing a human body for a full day. All you need do is to toss one into your mouth each day and swallow it. It will nourish you, satisfy your hunger and build up your health and strength. The ordinary

---

[1] Kaplan H, Hill K, Lancaster J, Hurtado AM. A theory of human life history evolution: Diet, intelligence, and longevity. Evol Anthropol. 2000; 9(4):156-185; https://www.unm.edu/~jlancas/KaplanHillLancasterHurtado_2000_LHEvolution.pdf.

[2] The earliest satirical mention may be James Payn's "The Fatal Curiosity; or, A Hundred Years Hence," published in Dec 1877 in Belgravia, A London Magazine, describing the matter of a sheep's lozenge: "My dear husband... actually took a whole one, as though it had been a cough lozenge.... He forgot, you see, that each lozenge was the concentration of an entire sheep (with the trifling exception of the wool and teeth), and the consequence was he became so enormously strong that he was positively dangerous..."[*] The earliest non-satirical mention may be an article titled 'Food of the Future" published by the newspaper Indiana Progress (Indiana PA) on 1 Jan 1896: "Given the formula for our food, says Berthelot, the father of the artificial food idea, and why not prescribe it from the chemist's? Surely the nitrogen and carbon of the beefsteak may not be as grateful to the palate if absorbed from a capsule or masticated in a tiny tablet, but the bones and the blood, the flesh and the sinews will be just as well supplied with their essential material, their own special foods, provided always the prescription is right in proportion...."[†]

[*] https://www.flyingcarsandfoodpills.com/-a-hundred-years-hence.

[†] https://web.archive.org/web/20080129104455/http://www.paleofuture.com/2007/05/food-of-future-indiana-progress-1896.html.

[3] https://www.flyingcarsandfoodpills.com/synthetic-food-of-the-future

[4] https://en.wikipedia.org/wiki/The_Master_Key_(Baum_novel).

food of mankind is more or less injurious; this is entirely beneficial. Moreover, you may carry enough tablets in your pocket to last for months." [5] Baum later returned to the food pill idea in one of his popular Oz books[6] in which he describes a "Square Meal Tablet", each one containing, in condensed form, "a dish of soup, a fried fish, a mutton pot-pie, lobster salad, charlotte russe and lemon jelly – all made into one little tablet that you can swallow without trouble".[7] There was an appearance of food pills that substitute for a roast beef dinner[8] in the 1930 musical comedy film *Just Imagine*.[9] The idea gained renewed attention in the 1950s and 1960s, fueled by space race optimism and NASA's development of compact astronaut rations.[10] Media representations, including *The Jetsons* (1962)[11] and *2001: A Space Odyssey* (1968)[12] reinforced the notion that highly compressed nutrition was just around the corner.

However, past technical analyses have consistently revealed major obstacles to the food pill concept. First, the sheer bulk of nutrients required for human survival cannot realistically be compressed into a single pill. A typical adult may need 2000-2500 kcal/day. Since pure fat (the most calorically dense macronutrient) only supplies ~9 kcal/gm, meeting this caloric requirement would require over 220 grams of fat alone, far exceeding the mass of any conventional pill, as has been noted in the technical literature.[13] Essential vitamins, minerals, amino acids, and fiber all have varying absorption requirements and cannot be delivered effectively in one bolus form. Studies of total parenteral nutrition (TPN), which bypasses the gut entirely, show that maintaining human health without enteral[14] feeding requires continuous infusion of carefully balanced macronutrients and micronutrients in liquid form.[15] Thus, while the food pill remains a

---

[5] https://www.flyingcarsandfoodpills.com/baums-magic-pills.
[6] https://en.wikipedia.org/wiki/The_Patchwork_Girl_of_Oz.

[7] L. Frank Baum. The Patchwork Girl of Oz, The Reilly & Lee Co., Chicago, 1913, p. 308.

[8] Michael Ann Dobbs. Remember when we thought we'd get all our nutrition from pills and bars? Gizmodo.com, 7 May 2012; https://gizmodo.com/remember-when-we-thought-wed-get-all-our-nutrition-from-5908332.

[9] https://en.wikipedia.org/wiki/Just_Imagine_(film).
[10] https://en.wikipedia.org/wiki/Space_food.
[11] https://en.wikipedia.org/wiki/The_Jetsons.
[12] https://en.wikipedia.org/wiki/2001:_A_Space_Odyssey.

[13] Young VR, Pellett PL. Plant proteins in relation to human protein and amino acid nutrition. Am J Clin Nutr. 1994 May;59(5 Suppl):1203S-1212S; https://medicosadventistas.org/wp-content/uploads/2018/09/Plan-protein-in-relation-to-human-protein-1.pdf.

[14] https://en.wikipedia.org/wiki/Enteral_administration.

[15] Nightingale JM, Lennard-Jones JE, Gertner DJ, Wood SR, Bartram CI. Colonic preservation reduces need for parenteral therapy, increases incidence of renal stones, but does not change high prevalence of gall stones in patients with a short bowel. Gut. 1992 Nov;33(11):1493-7; https://pmc.ncbi.nlm.nih.gov/articles/PMC1379534/. Boullata JI, Carrera AL, Harvey L, Escuro AA, Hudson L, Mays A, McGinnis C, Wessel JJ, Bajpai S, Beebe ML, Kinn TJ, Klang MG, Lord L, Martin K, Pompeii-Wolfe C, Sullivan J, Wood A, Malone A, Guenter P; ASPEN Safe Practices for Enteral Nutrition Therapy Task Force, American Society for Parenteral and Enteral Nutrition. ASPEN Safe Practices for

compelling symbol of futuristic efficiency, the traditional scientific consensus views it as implausible.

This paper proposes a new approach to the challenge of human nutritional self-sufficiency called the **artificial metabolic organ** or AMO. The AMO is a compact special-purpose nanofactory, composed of atomically precise nanomachinery and embedded in the human body. It would have full bloodstream access and the ability to efficiently extract waste molecules from both blood and urine, chemically transform these wastes into nutrient molecules, then release the nutrient molecules back into the bloodstream, creating a closed-cycle nutrient recycling system and effectively a "zero-waste human". This is possible in principle because all nutrients enter the bloodstream via ingestion, digestion, and absorption of food in the stomach and the alimentary canal, with the exception of oxygen which enters the bloodstream via the lungs. Similarly, all waste products enter the bloodstream by diffusion or active transport out of the cytoplasm of trillions of metabolically active cells throughout the human body. Advanced molecular nanotechnology will be required to implement this, but ongoing research suggests it's theoretically feasible: an AMO could be fabricated and deployed in the future once the technical details of atomically precise molecular manufacturing[16] have been mastered.

There would be many practical advantages to users possessing an implanted artificial metabolic organ, including:

(1) **Weight management**. An AMO could provide automated weight management – users should be able to control their weight very precisely, explicitly setting a desired target weight which would then be managed automatically by the AMO.

(2) **Hunger control**. An AMO could provide automated control of hunger, since the AMO would let users dial down their hunger as low as desired, or even to zero, so they would not feel hungry, would experience no symptoms of starvation, and would remain satiated and energetic even after not eating any solid food for weeks.

(3) **Sports performance enhancement**. An AMO could assist in recreational or competitive sports, enabling record athletic performances using otherwise unaugmented natural human bodies. An AMO could let users exercise their body far more vigorously and for longer times, making it easier to become and stay physically fit.

(4) **Resilience to food scarcity and disaster survival**. In famine, pandemic, supply-chain collapse, or being stranded (e.g., remote travel, disaster zones), an AMO makes you nutritionally self-sufficient, needing only air, water, and electricity, dramatically increasing survival odds and reducing anxiety about food security. First responders, military, or field

---

Enteral Nutrition Therapy [Formula: see text]. JPEN J Parenter Enteral Nutr. 2017 Jan;41(1):15-103; https://pubmed.ncbi.nlm.nih.gov/27815525/.

[16] Drexler KE. Nanosystems: Molecular Machinery, Manufacturing, and Computation. John Wiley & Sons, New York, 1992; https://www.amazon.com/dp/0471575186/. Freitas RA Jr., Merkle RC. A Nanofactory Roadmap: Research Proposal for a Comprehensive Diamondoid Nanofactory Development Program. IMM Report No. 58, 2008/2025; http://www.imm.org/Reports/rep058.pdf.

workers could operate longer in austere environments without needing regular food resupply, improving mission endurance and reducing logistic tails.

(5) **Reduction of gastrointestinal discomfort and eating-related disorders**. For people with problematic digestion, food intolerances, or inflammatory gut conditions, an AMO could supply nutrition without triggering flare-ups while still allowing normal eating optionally.

(6) **Temporary management of metabolic disorders**. The AMO could enable temporary management of metabolic disorders,[17] which are commonly regarded as treatable by nutrition management. Such treatment would only be temporary, because in an era in which AMOs are available metabolic diseases should be completely curable via advanced nanorobotics.[18]

(7) **Cognitive optimization and stable mental energy**. Tight control over metabolite and nutrient levels could smooth blood glucose and micronutrient fluctuations, reducing "brain fog," mood swings, and fatigue – appealing to knowledge workers, students, and anyone who wants consistent mental performance without relying on stimulants or frequent meals.

(8) **Elimination of eating-related time overhead**. The AMO frees people from having to plan, prepare, shop for, and consume meals. That reclaimed time could be valuable for busy professionals, caregivers, or people seeking more unstructured life hours. Of course, humans may still choose to eat for pleasure or social reasons; the AMO simply makes eating biologically unnecessary.[19]

(9) **Dramatically reduced cost and environmental footprint of nutrition**. Over the long run and assuming widespread implementation, individuals could sharply cut their food bills and the associated carbon / land / water footprint of conventional agriculture, since most "nutrition" would be recycled internally by the AMO rather than produced externally and transported.

(10) **Speedier recovery from illness, injury, or surgery**. By ensuring continuous optimal nutrient supply even when appetite is poor or digestion is impaired, an AMO could speed healing, reduce complications from malnutrition during convalescence, and allow elective procedures with lower nutritional risk.

---

[17] https://en.wikipedia.org/wiki/Metabolic_disorder.

[18] Freitas RA Jr. Chapter 23. Comprehensive Nanorobotic Control of Human Morbidity and Aging, Section 6.2.5, "Hormonal, Metabolic and Genetic Disease". In: Fahy GM, West MD, Coles LS, Harris SB, eds, The Future of Aging: Pathways to Human Life Extension, Springer, New York, 2010, pp. 685-805; http://www.nanomedicine.com/Papers/Aging.pdf.

[19] The existence of AMO technology will raise interesting cultural questions, such as: Will family dinners become obsolete? How will AMOs affect the joy of cooking, cuisine, and food culture? Who can get AMOs and what will it cost? What is the impact on personal time and lifestyle, toilet paper consumption, house and building design, municipal sewage systems, human waste pollution and the natural environment of vastly reducing the need for regular bowel movements?

The essential human nutritional requirements that must be supplied by the artificial metabolic organ, including glucose, proteins, lipids, micronutrients and oxygen, are summarized in Section 2. The biochemical waste products generated by human metabolism, including carbon dioxide, four nitrogen-rich chemicals (urea, creatinine, uric acid, and hippuric acid), a half-dozen metabolic microwastes, and 14 mineral microwastes, are then identified in Section 3. There is also a catch-all category we've dubbed "miscwastium" that serves as a representative composite of some unknown number of waste molecule types that collectively appear to have the approximate chemical formula ~$C_{19}H_{15}O_{10}$ in order to balance the total numbers of nutrient atoms with the total numbers of waste atoms for each chemical element.

After that, the structure and operation of the proposed artificial metabolic organ, which is designed to convert waste molecules into nutrient molecules and provide essentially complete endogenous nutrient recycling,[20] is detailed in Section 4, followed by our overall conclusions in Section 5.

[20] The metabolic organ may be thought of as a self-refueling zero-emission human body, crudely analogous to the zero-emission self-refueling automobile recently described in another publication: Freitas RA Jr. Zero-Emission Gasoline-Powered Automobiles. IMM Report No. 57, 8 Apr 2025; http://www.imm.org/Reports/rep057.pdf.

2. Human Metabolic Nutrient Requirements

Assuming no oral food intake, standard parenteral (intravenous feeding) guidelines recommend macronutrient infusion rates that meet basal energy needs while avoiding metabolic complications,[21] while providing all nutrients that are considered "essential".[22] Carbohydrate is generally provided in amounts up to 50-60% of total daily calories and should not exceed 7.2 gm/kg/day (504 gm/day) to minimize the occurrence of fatty liver and hyperglycemia.[23] More typical parenteral rates specify (1) initiating **glucose** at 2.5-3.0 mg/kg/min (250-300 gm/day and then advancing to a steady state of 4-6 mg/kg/min (400-600 gm/day),[24] (2) infusing protein as **amino acids** at 0.8-1.5.0 gm/kg/day (56-105 gm/day),[25] and (3) injecting 1-2 gm/kg/day (70-140 gm/day) in the form of **lipids**, or 25-30% of the total calories.[26] Additionally, **micronutrients** are essential chemicals required in small quantities, typically vitamins, dietary minerals, and trace elements in milligram–gram amounts, totaling on the order of ~10 gm/day as a sum of the typical Recommended Daily Allowances (RDAs).

Table 1 summarizes the estimated mass consumption rate of intravenous nutrients for a resting 70 kg human male at the basal ~100 watt (~2000 kcal/day) metabolic rate, consistent with the standard parenteral guidelines. This is the rate at which the metabolic organ would have to supply nutrients to a resting 70 kg male to permanently maintain life and health. Note that a 2000 kcal/day food intake is generally regarded as sufficient to sustain a person who goes about the

---

[21] https://www.merckmanuals.com/professional/nutritional-disorders/nutritional-support/parenteral-nutrition-pn.

[22] Chipponi JX, Bleier JC, Santi MT, Rudman D. Deficiencies of essential and conditionally essential nutrients. Am J Clin Nutr. 1982 May;35(5 Suppl):1112-6; https://pubmed.ncbi.nlm.nih.gov/6805293/.

[23] Madsen H, Frankel EH. The hitchhiker's guide to parenteral nutrition management for adult patients. Practical Gastroenterology, Jul 2006, pp. 46-68; https://med.virginia.edu/ginutrition/wp-content/uploads/sites/199/2015/11/MadsenArticle-July-06.pdf.

[24] https://www.ashp.org/-/media/assets/pharmacy-practice/resource-centers/Clinical-Pharmacy-Resources/Nutrition-Support/2016-MCM/MCM16-335-Strategies-for-Successful-Parenteral-nutrition.pdf.

[25] The recommended daily allowance (RDA) for protein is 0.8 gm per day per kg of body weight (https://www.health.harvard.edu/blog/how-much-protein-do-you-need-every-day-201506188096), hence (0.8 gm/kg-day) (70 kg) = 56 gm/day. But this should be regarded as a lower bound, and practical recommendations often suggest 0.8-1.5 gm/kg/day,[*] or 56-105 gm/day for stable 70 kg adult patients. In estimating the whole-body nitrogen balance of all nutrients (**Section 2**) and wastes (**Section 3**), an allocation of ~**100 gm/day** of amino acids appears sufficient to prevent negative nitrogen balance.

[*] e.g., "Table 1. Macronutrients", ASPEN Recommendations on Appropriate Parenteral Nutrition Dosing for Adult Patients, American Society for Parenteral and Enteral Nutrition (ASPEN), 2019 (17 Nov 2020); https://nutritioncare.org/wp-content/uploads/2024/12/Appropriate-Dosing-for-PN.pdf.

[26] Hamdan M, Puckett Y. Total Parenteral Nutrition. StatPearls [Internet], 4 Jul 2023; https://www.ncbi.nlm.nih.gov/books/NBK559036/.

typical everyday activities of life, excluding purposeful vigorous exercise or physically demanding work.

All nutrient requirements are keyed to the 100 watt basal metabolic rate. As the metabolic rate increases, perhaps due to engaging in vigorous physical exercise, the energy and nutrient consumption will rise accordingly. The impact of this is discussed in Section 4.3.8. More generally, nutrient needs scale with body size and activity, and the AMO would be programmable or adaptive to the individual's requirements.

Table 1. Approximate intravenous nutrient requirements for a resting 70 kg male human body at the ~100 watt basal metabolic rate

Molecular Component	Human Requirement (gm/day)	Approximate Caloric Content (kcal/day)	Discussed in:
Glucose ($C_6H_{12}O_6$)	400	~1360	Section 2.1
Proteins	100	~400	Section 2.2
Lipids (incl. ~4.2 gm/day carrier)	74.2	~640	Section 2.3
Micronutrients	10.8	~0	Section 2.4
Subtotal, Solid Nutrients	585	~2000	
Oxygen (O_2)	719	0	Section 2.5
Total Nutrients	**1304**	**~2000**	

2.1 Glucose

In human nutrition there are no other true "essential" carbohydrates beyond the requirement for glucose ($C_6H_{12}O_6$; 180.1 gm/mole) itself. Any other carbohydrate the body needs (e.g., fructose for glycolysis, ribose for nucleotides, etc.) can be synthesized internally from glucose or from gluconeogenic precursors such as amino acids, glycerol, or lactate. Glucose remains the sole essential carbohydrate substrate and all other monosaccharides, disaccharides, and polysaccharides are non-essential because the human body can interconvert them as needed. No additional carbohydrate mass is strictly required beyond the stated 400 gm/day of glucose.

Virtually all of the glucose that reaches the body's metabolizing cells originates in (and is carried by) the blood, and from there diffuses into the interstitial fluid bathing each cell. There is no alternative "direct" route – no other fluid compartment that bypasses the vascular system – so 100% of the extracellular glucose supply to cells is bloodborne. Glucose reaches metabolizing cells by the following pathway:

(1) **Intestinal absorption.** Dietary glucose is taken up by enterocytes[27] in the small intestine and exported into the portal vein, which carries it first to the liver.

(2) **Hepatic handling.** The liver either stores some as glycogen or releases it back into the systemic circulation as needed, maintaining blood-glucose homeostasis.

(3) **Systemic delivery.** In the arterial blood, glucose travels dissolved in plasma. At each tissue capillary bed it diffuses across the capillary wall into the interstitial fluid, from which it enters cells via GLUT transporters.

(4) **Local gluconeogenesis.** A small fraction of glucose is also produced by the kidneys (and to a much lesser extent other tissues) via gluconeogenesis[28] and is released directly into the blood, but even this "new" glucose still reaches target cells via the bloodstream.

In the absence of enteral (oral) carbohydrate intake in hospital settings or during parenteral feeding, an intravenous infusion of dextrose (glucose) can fully meet the body's essential glucose requirement. Parenteral dextrose is rapidly taken up by tissues, oxidized to CO_2 and H_2O, and exerts a protein-sparing effect by preventing glycogen depletion and muscle proteolysis.[29]

2.2 Protein

In healthy adults virtually no intact dietary protein molecules cross into the blood. All proteins ingested as food are first broken down in the stomach and small intestine by gastric and pancreatic proteases into free amino acids[30] and small peptides[31] such as dipeptides[32] and tripeptides,[33] whereupon these small peptides are transported across enterocyte apical membranes (at the brush border lining the small intestine)[34] via the PepT1 H+/peptide co-transporter and then exit across the basolateral membrane into the mesenteric capillaries.[35] Inside enterocytes in the

---

[27] https://en.wikipedia.org/wiki/Enterocyte.

[28] Gerich JE. Role of the kidney in normal glucose homeostasis and in the hyperglycaemia of diabetes mellitus: therapeutic implications. Diabet Med. 2010 Feb;27(2):136-42; https://pmc.ncbi.nlm.nih.gov/articles/PMC4232006/.

[29] https://dailymed.nlm.nih.gov/dailymed/fda/fdaDrugXsl.cfm?setid=f2379398-a07b-417e-a022-f7b41f962067.

[30] https://en.wikipedia.org/wiki/Amino_acid.
[31] https://en.wikipedia.org/wiki/Peptide.
[32] https://en.wikipedia.org/wiki/Dipeptide.
[33] https://en.wikipedia.org/wiki/Tripeptide.

[34] Miner-Williams WM, Stevens BR, Moughan PJ. Are intact peptides absorbed from the healthy gut in the adult human? Nutr Res Rev. 2014 Dec;27(2):308-29; https://pubmed.ncbi.nlm.nih.gov/25623084/.

[35] Basile EJ, Launico MV, Sheer AJ. Physiology, Nutrient Absorption. StatPearls [Internet}, 28 Oct 2023; https://www.ncbi.nlm.nih.gov/books/NBK597379.

intestinal walls, all absorbed peptides are cleaved by cytosolic peptidases into free amino acids before they exit the cell. Only these free amino acids are then transported across the basolateral membrane into the portal vein, whereupon they pass through the liver (where some are used or modified), and then flow into the systemic arterial circulation. Once in the arterial blood, amino acids diffuse through the capillary wall into the interstitial fluid and are taken up by cells via specific amino-acid transporters.[36] Aside from the tiny, mostly negligible paracrine release of locally synthesized peptides, every gram of exogenous protein-derived amino acid that reaches internal bodily tissues must ride in the blood plasma (and hence pass through capillaries into the interstitium) before being taken up by cells.

Note that while no intact dietary peptides directly enter the arterial circulation, the blood plasma nevertheless carries a rich variety of endogenous peptides generated metabolically by the body's tissues, including:

(1) **Peptide hormones** synthesized by endocrine cells and secreted into the blood. such as insulin, glucagon, atrial natriuretic peptide (ANP), angiotensin II, vasopressin (ADH), oxytocin, cholecystokinin (CCK), glucagon-like peptide-1 (GLP-1), growth hormone-releasing hormone, and many others;[37]

(2) **Cytokines and chemokines**, which are immune-modulating peptides released by leukocytes and other cells, such as interleukins (IL-6, IL-1β), tumor necrosis factor-α (TNF-α), interferons, and many others;

(3) **Peptide growth factors and neuropeptides**, such as epidermal growth factor (EGF), brain-derived neurotrophic factor (BDNF), neuropeptide Y (NPY), and substance P; and

(4) **Proteolytic fragments** or the "peptidome",[38] consisting of low-abundance peptide fragments generated by the controlled proteolysis of larger plasma proteins such as fibrinogen, albumin, and chromogranins.[39]

These plasma-resident peptides range in size from a few amino acids (e.g., angiotensin II is an octapeptide) up to several hundred amino acids (e.g., pro-hormone precursors and split fragments). Their combined mass in the blood is extremely small – typically in the microgram to milligram range at any moment – and their net daily flux is likewise on the order of

---

[36] Souba WW, Pacitti AJ. How amino acids get into cells: mechanisms, models, menus, and mediators. JPEN J Parenter Enteral Nutr. 1992 Nov-Dec;16(6):569-78; https://pubmed.ncbi.nlm.nih.gov/1494216/.

[37] https://en.wikipedia.org/wiki/Peptide_hormone.

[38] Dufresne J, Bowden P, Thavarajah T, Florentinus-Mefailoski A, Chen ZZ, Tucholska M, Norzin T, Ho MT, Phan M, Mohamed N, Ravandi A, Stanton E, Slutsky AS, Dos Santos CC, Romaschin A, Marshall JC, Addison C, Malone S, Heyland D, Scheltens P, Killestein J, Teunissen C, Diamandis EP, Siu KWM, Marshall JG. The plasma peptidome. Clin Proteomics. 2018 Dec 1;15:39; https://pmc.ncbi.nlm.nih.gov/articles/PMC6271647/pdf.

[39] https://en.wikipedia.org/wiki/Granin#Chromogranins.

micrograms/day to milligrams/day, negligible compared to the much larger ~100 gm/day flux of free amino acids. All are produced endogenously and need not be provided nutritionally.

In the absence of enteral protein intake (i.e., no food), supplying the full spectrum of amino acids intravenously (as is done in Total Parenteral Nutrition or TPN)[40] can meet all of the body's essential protein needs. In clinical practice, standard adult TPN formulations provide a mixture of all 11 essential amino acids[41] plus non-essential ones at a total rate of 0.8-1.5 gm/kg-day,[42] or ~100 gm/day for a 70 kg person. These intravenous amino-acid solutions are taken up directly by tissues without the need for gastrointestinal digestion and fully substitute for dietary protein in supporting tissue maintenance, repair, enzyme and hormone synthesis, and other vital functions.

For maintenance of truly normal plasma amino-acid profiles and to minimize the metabolic burden of *de novo* synthesis, parenteral and dietary protein sources are usually formulated to supply all the standard amino acids, not just the classic essentials. Clinical parenteral nutrition practice uses "balanced" amino-acid mixtures that include both essential[43] and non-essential amino acids (typically excluding only glutamine and arginine in older formulations,[44] though modern admixtures now include conditionally essential ones as well).[45]

Table 2 lists a hypothetical 100 gm/day "balanced" amino-acid mixture based on two well-established patterns: (1) **essential amino acids** are assigned according to the 2007 WHO/FAO/UNU adult "maintenance" scoring pattern (mg of each essential amino acid per gm of protein),[46] and (2) **nonessential amino acids** are apportioned roughly in proportion to their

---

[40] Hamdan M, Puckett Y. Total Parenteral Nutrition. StatPearls [Internet], 4 Jul 2023; https://www.ncbi.nlm.nih.gov/books/NBK559036/.

[41] https://en.wikipedia.org/wiki/Essential_amino_acid.

[42] "Table 1. Macronutrients", ASPEN Recommendations on Appropriate Parenteral Nutrition Dosing for Adult Patients, American Society for Parenteral and Enteral Nutrition (ASPEN), 2019 (17 Nov 2020); https://nutritioncare.org/wp-content/uploads/2024/12/Appropriate-Dosing-for-PN.pdf.

[43] An essential amino acid is one that is required by an organism but cannot be synthesized *de novo* by it, and therefore must be supplied in its diet. Of the 20 standard protein-producing amino acids, nine cannot be endogenously synthesized by humans: histidine, isoleucine, leucine, lysine, methionine, phenylalanine, threonine, tryptophan, and valine; https://en.wikipedia.org/wiki/Essential_amino_acid.

[44] Yarandi SS, Zhao VM, Hebbar G, Ziegler TR. Amino acid composition in parenteral nutrition: what is the evidence? Curr Opin Clin Nutr Metab Care. 2011 Jan;14(1):75-82; https://pmc.ncbi.nlm.nih.gov/articles/PMC3071792/pdf.

[45] Hamdan M, Puckett Y. Total Parenteral Nutrition. StatPearls [Internet], 4 Jul 2023; https://www.ncbi.nlm.nih.gov/books/NBK559036/.

[46] "Dietary Protein Quality Evaluation in Human Nutrition," FAO Food and Nutrition Paper 92, Food and Agriculture Organization of the United Nations, Rome, 2013; https://www.fao.org/ag/humannutrition/35978-02317b979a686a57aa4593304ffc17f06.pdf..

relative abundance in whole-egg protein (mg amino acid per 100 gm protein),[47] scaled so that total nonessentials + essentials = 100 gm. Note that asparagine and glutamine are typically not included in parenteral amino-acid solutions[48] because they deamidate and are synthesized endogenously.

Table 2. Estimated daily amino acid requirements for a resting 70 kg male human body at the ~100 watt basal metabolic rate (e = essential), with molecular weights in [gm/mole]

Amino Acid	Requirement (gm/day)	Amino Acid	Requirement (gm/day)
Alanine [89.1]	8.40	Phenylalanine (e) [165.2]	2.34
Arginine [174.2]	9.20	Proline [115.1]	6.30
Aspartate [133.1]	15.05	Serine [105.1]	10.75
Cysteine (e) [121.2]	0.64	Threonine (e) [119.1]	2.40
Glutamate [147.1]	19.10	Tryptophan (e) [204.2]	0.60
Glycine [75.1]	5.00	Tyrosine (e) [181.2]	1.76
Histidine (e) [155.2]	1.70	Valine (e) [117.2]	2.90
Isoleucine (e) [131.2]	2.30	Asparagine [150.1]	0 (synth. endogenously)
Leucine (e) [131.2]	5.20	Glutamine [146.2]	0 (synth. endogenously)
Lysine (e) [146.2]	4.70		
Methionine (e) [149.2]	1.66	**Total**	**100.00**

The synthesis component of the artificial metabolic organ (Section 4.1) could manufacture all essential amino acids plus any other amino acids deemed advisable (all are water-soluble), then release them directly into the bloodstream in a carefully metered manner.

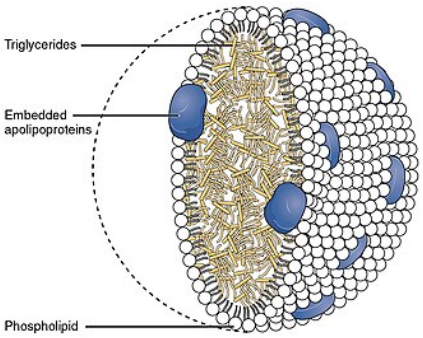

2.3 Lipids

Lipids are a broad group of organic compounds which include fats, waxes, sterols, fat-soluble vitamins (such as vitamins A, D, E and K), monoglycerides, diglycerides, phospholipids, and others, whose function includes storing energy, signaling, and acting as structural components of cell membranes.[49] Linoleic acid, aka. “LA”

[47] “The Eggceptional egg, nutritional facts and figures,” Hendrix Genetics, 7 Feb 2022; https://layinghens.hendrix-genetics.com/en/articles/eggceptional-egg-nutritional-facts-and-figures.

[48] https://www.accessdata.fda.gov/drugsatfda_docs/label/2020/019018Orig1s036lbl.pdf.

[49] https://en.wikipedia.org/wiki/Lipid.

($C_{18}H_{32}O_2$; 280.5 gm/mole), and α-linolenic acid, aka. "ALA" ($C_{18}H_{30}O_2$; 278.4 gm/mole), are the only fatty acids that humans cannot synthesize *de novo*, thus are the sole essential fatty acids[50] and sufficient to supply all essential lipid precursors. Essential fatty acids are packaged into chylomicrons (image, above)[51] and are distributed throughout the body via the bloodstream.

In clinical practice, neither free fatty acids (FFAs) nor whole chylomicrons are administered intravenously because of solubility, stability and safety issues. Specifically, unbound FFAs are poorly soluble in blood, strongly detergent-like, and rapidly bind to albumin, preventing the achievement of a stable, high-dose intravenous infusion of FFAs alone without hemolysis or toxicity. Similarly, harvesting or infusing intact chylomicrons risks triggering immune reactions and is technically impractical, and they are too large (100-1000 nm) and heterogeneous for safe clinical intravenous use. It would be possible to enzymatically remodel harvested chylomicrons, but that merely re-creates what pharmaceutical lipid emulsions already offer in a standardized form.

Instead, in clinical settings the essential-fatty-acid requirement is supplied intravenously by a sterile, oil-in-water emulsion of long-chain triglycerides – i.e., a parenteral lipid emulsion (PLE) – which functions much like a synthetic, pre-homogenized and phospholipid-stabilized "chylomicron" but is safe, uniform, and approved for IV use. A typical PLE such as Intralipid® (Baxter Healthcare Corp.) consists of ~20% soybean oil triglycerides of five molecular types,[52] 1.2% egg-lecithin emulsifier including six phospholipid types,[53] and 2.25% glycerol by mass, in an aqueous carrier (76.55%). These lipids are typically delivered via 200-500 nm emulsion droplets that circulate in blood plasma after intravenous injection. Endothelial lipoprotein lipase hydrolyzes the triglycerides at capillary beds, releasing free LA and ALA locally, which then diffuse into cells or bind to albumin for transport to distal tissues.

As detailed in **Table 3**, providing the ~70 gm/day minimum daily lipid requirement of the two essentials for a resting 70 kg male at the 100 watt basal metabolic rate might require intravenous

---

[50] Innis SM. Essential fatty acid requirements in human nutrition. Can J Physiol Pharmacol. 1993 Sep;71(9):699-706; https://pubmed.ncbi.nlm.nih.gov/8313234/. See also: https://en.wikipedia.org/wiki/Essential_fatty_acid.

[51] https://en.wikipedia.org/wiki/Chylomicron.

[52] These include linoleic acid (44-62% by mass, assume 53%; 280.5 gm/mole), oleic acid (19-30%, assume 25%; 282.5 gm/mole), palmitic acid (7-14%, assume 10%; 256.4 gm/mole), α-linolenic acid (4-11%, assume 8%; 278.4 gm/mole), and stearic acid (1.4-5.5%, assume 4%; 284.5 gm/mole); https://dailymed.nlm.nih.gov/dailymed/fda/fdaDrugXsl.cfm?setid=a69c82da-15ba-4d4d-8d7f-871dc3981eb8.

[53] The purified egg-yolk phosphatides (1.2% of the emulsion) consist almost entirely of six glycerophospholipids, including phosphatidylcholine (71% by mass; ~776 gm/mole), phosphatidylethanolamine (18.3%; 664.0-768.1 gm/mole), lysophosphatidylcholine (3.3%; 467.6-537.7 gm/mole), sphingomyelin (2.3%; 674.5-829.3 gm/mole), lysophosphatidylethanolamine (1.1%; 453.5-501.6 gm/mole), and phosphatidylinositol (4.0%; 886.6 gm/mole); Blesso CN. Egg phospholipids and cardiovascular health. Nutrients. 2015 Apr 13;7(4):2731-47; https://pmc.ncbi.nlm.nih.gov/articles/PMC4425170/pdf.

injection of ~74.23 gm/day of emulsion,[54] including 70 gm/day of five triglycerides (range 256-285 gm/mole), 4.2 gm/day of six emulsifier phospholipids (range 454-887 gm/mole), and 10-70 mg/day of alkaline buffer – e.g., ~30 mg/day of sodium hydroxide (NaOH; 40.0 gm/mole)[55] or ~70 mg/day of tromethamine, aka. THAM ($C_4H_{11}NO_3$; 121.1 gm/mole)[56] – to keep the emulsion within its specified pH window (6.0-8.9), without which the emulsion would be physically unstable and potentially harmful to infuse. (Lipid emulsions become unstable at low pH leading to droplet coalescence, increased large-droplet fraction, and risk of fat-embolism and phlebitis,[57] and an overly acidic infusate can irritate or damage vascular endothelium and even promote red-cell hemolysis on contact.[58])

The synthesis component of the artificial metabolic organ (Section 4.1) could manufacture all necessary lipid components and combine them to make synthetic "chylomicrons" similar to those which pharmaceutical lipid emulsions already offer in a standardized form, and release them into the human bloodstream.

---

[54] For the traditional bulk chemical preparation of the emulsion,[*] the five triglycerides are first melted and mixed into a single oil phase, the phospholipids are dissolved in the aqueous phase (with glycerol and buffer), and then the oil phase is dispersed into submicron droplets upon high-shear homogenization (e.g., via microfluidizer or high-pressure homogenizer), whereupon the amphiphilic phospholipid molecules spontaneously migrate to the oil-water interface, forming a monolayer around each droplet. For the preparation considered here, the synthesis component (**Section 4.1**) of the metabolic organ would assemble the ingredients of the emulsion by combining nanoscale aliquots of pure molecules in a manner that avoids emulsion stability and solubility issues.

[*] Hippalgaonkar K, Majumdar S, Kansara V. Injectable lipid emulsions-advancements, opportunities and challenges. AAPS PharmSciTech. 2010 Dec;11(4):1526-40; https://pmc.ncbi.nlm.nih.gov/articles/PMC3011075/pdf.

[55] https://registrasiobat.pom.go.id/files/assesment-reports/01701847415.pdf.

[56] https://pubchem.ncbi.nlm.nih.gov/compound/6503. At such a low buffer dose, tromethamine would be fully biocompatible with no expected undesirable side effects.

[57] https://www.clinicalnutritionespen.com/article/S1751-4991(09)00004-3/fulltext and https://www.accessdata.fda.gov/drugsatfda_docs/label/2023/017643s083%2C018449s050s051%2C019942s021%2C020248s027s028lbl.pdf.

[58] https://www.accessdata.fda.gov/drugsatfda_docs/label/2023/017643s083%2C018449s050s051%2C019942s021%2C020248s027s028lbl.pdf.

Table 3. Estimated daily lipid requirements for a resting 70 kg male human body at the ~100 watt basal metabolic rate (e = essential)			
Emulsion Component	**Requirement (gm/day)**	**Emulsion Component**	**Requirement (gm/day)**
Linoleic acid (e)	37.1	Lysophosphatidylcholine	0.14
Oleic acid	17.5	Sphingomyelin	0.10
Palmitic acid	7.0	Lysophosphatidylethanolamine	0.05
α-Linolenic acid (e)	5.6	Phosphatidylinositol	0.17
Stearic acid	2.8	NaOH	0.03
Phosphatidylcholine	2.97		
Phosphatidylethanolamine	0.77	**Total**	**74.23**

2.4 Micronutrients

Micronutrients are essential chemicals required by humans in small quantities to regulate physiological functions of cells and organs. Human micronutrients take one of three forms: vitamins,[59] trace elements,[60] and dietary minerals.[61] **Table 4** provides a list of known or suspected micronutrients and their estimated daily requirements for a 70 kg male human, typically the highest U.S. Recommended Dietary Allowances (RDA) or Adequate Intake (AI).[62]

Since all micronutrients are distributed via the circulation, the synthesis component of the artificial metabolic organ (Section 4.1) could manufacture all 28 components and release them into the bloodstream in a controlled manner, perhaps with pulsed timing to ensure safety and in sufficient quantities to satisfy minimal nutritional requirements consistent with human health.

2.4.1 Vitamins

Most of the 13 essential vitamins listed in **Table 4** cannot be synthesized by the human body and must be provided nutritionally.[63]

---

[59] Vitamins are essential organic molecules, other than amino acids or fatty acids, that commonly function as enzymatic cofactors, metabolic regulators or antioxidants; humans require thirteen vitamins in their diet. https://en.wikipedia.org/wiki/Vitamin.

[60] https://en.wikipedia.org/wiki/Trace_element.
[61] https://en.wikipedia.org/wiki/Mineral_(nutrient).
[62] https://en.wikipedia.org/wiki/Nutrient#Deficiencies_and_toxicity.

[63] **Vitamin D3** is the only true vitamin that humans make in substantial quantity from UVB exposure of 7-dehydrocholesterol in skin.[*] **Niacin (B3)** can be synthesized from tryptophan in the liver, converting ~60 mg Trp to 1 mg of niacin, though vitamins B2, B6, and iron are required for the process.[†] Trace amounts of

Table 4. Estimated essential daily micronutrient requirements[64] for a resting 70 kg male human body at the ~100 watt basal metabolic rate, with molecular weights in [gm/mole]

Micronutrient	Requirement (mg/day)	Micronutrient	Requirement (mg/day)
Potassium[65] [39.1]	3400	Vit. B6 [169.2]	1.1-1.3
Chloride [35.5]	2300	Vit. B1 (thiamin) [265.4]	1.0-1.2
Sodium [23.0]	2300	Copper [63.5]	0.7-0.9
Calcium [40.1]	800-1000	Vit. A [286.5]	0.625-0.900
Phosphorus [31.0]	580-700	Vit. B9 (folate) [441.4]	0.32-0.40
Choline [104.2]	550	Vit. K [450.7]	0.12
Magnesium [24.3]	350-420	Iodide [126.9]	0.095-0.150
Vit. C [176.1]	75-90	Selenium [79.0]	0.045-0.055
Vit. B3 (niacin) [123.1]	12-16	Chromium [52.0]	0.035
Vit. E (α-tocopherol) [430.7]	12-15	Molybdenum [95.9]	0.034-0.045
Zinc [65.4]	9.4-11	Vit. B7 (biotin) [244.3]	0.03
Iron[66] [55.8]	1	Vit. D [384.6]	0.010-0.015
Vit. B5 (pantothenic acid) [219.2]	5	Vit. B12 (cobalamin) [1355.4]	0.0020-0.0024
Manganese [54.9]	2.3		
Vit. B2 (riboflavin) [376.4]	1.1-1.3	**Total**	**10.4-10.8** (gm/day)

Water-soluble vitamins (B1, B2, B3, B5, B6, B7, B9, B12, and C) circulate free or loosely protein-bound (e.g., PLP-albumin, transcobalamin-B12) in blood plasma, then enter cells via

---

Vitamins B2 and **B7** are produced by gut microbiota;[‡] however, absorption sites (distal ileum/colon) and low quantities ensure that diet remains the primary source.

[*] https://en.wikipedia.org/wiki/Vitamin_D#Biosynthesis.

[†] https://en.wikipedia.org/wiki/Nicotinic_acid#Biosynthesis.

[‡] Said HM. Recent advances in transport of water-soluble vitamins in organs of the digestive system: a focus on the colon and the pancreas. Am J Physiol Gastrointest Liver Physiol. 2013 Nov;305(9):G601-10; https://pmc.ncbi.nlm.nih.gov/articles/PMC3840235/.

[64] https://en.wikipedia.org/wiki/Nutrient#Deficiencies_and_toxicity.

[65] https://en.wikipedia.org/wiki/Potassium#North_America.

[66] Most adult parenteral nutrition formulations don't routinely include large amounts of iron. Iron is usually added separately to match normal basal losses of ~1 mg/day. In practice, adult men on exclusive parenteral feeding receive ~1 mg of elemental iron per day.[*] The U.S. RDA for iron in men ranges for 6-11 mg/day because on average only ~12% of total iron ingested is taken up.[†]

[*] Forbes A. Iron and parenteral nutrition. Gastroenterology. 2009 Nov;137(5 Suppl):S47-54; https://www.gastrojournal.org/article/s0016-5085(09)01451-6/fulltext.

[†] Piskin E, Cianciosi D, Gulec S, Tomas M, Capanoglu E. Iron Absorption: Factors, Limitations, and Improvement Methods. ACS Omega. 2022 Jun 10;7(24):20441-20456; https://pmc.ncbi.nlm.nih.gov/articles/PMC9219084/.

facilitated transporters or endocytosis.[67] Fat-soluble vitamins (A, D, E, and K) are packed into chylomicrons (large lipoprotein particles) produced by intestinal enterocytes;[68] once in the plasma, they transfer to various lipoprotein classes (VLDL, LDL, HDL) or bind to specific carrier proteins (e.g., RBP4 for vitamin A, DBP for vitamin D) for delivery to target cells. The synthesis component of the artificial metabolic organ should manufacture fat-soluble vitamins for release into plasma via emulsions as previously described for lipids in Section 2.3.

2.4.2 Choline

Choline $[(CH_3)_3NCH_2CH_2OH]^+$ is also listed as an essential nutrient in **Table 4**.[69] The cholines are a family of water-soluble quaternary ammonium compounds, and choline is the parent compound of the cholines class.[70] Choline wasn't initially classified as essential because the human body can produce it in small amounts,[71] e.g., through phosphatidylcholine metabolism,[72] but healthy humans on choline-deficient diets develop fatty liver, liver damage, and muscle damage, so most choline normally comes from the diet.[73] All dietary (and endogenous) choline ultimately travels to cells exclusively via the bloodstream – either as free choline in plasma or (for lipid-derived choline) first in chylomicrons to the liver and then released into blood. For parenteral patients, choline is usually supplied intravenously as a soluble salt (e.g., a 25 mg/cm^3 sterile aqueous solution of choline chloride),[74] mixed with the glucose and amino acid components of the injection. Because choline is water-soluble, it then circulates freely in plasma and is taken up by tissues via the same transporters used for enterally absorbed choline.

2.4.3 Sodium, Potassium, Chloride, and Iodide

In human blood, Na^+, K^+, Cl^- and I^- are transported almost exclusively as free ions dissolved in plasma water, with little meaningful protein binding. For parenteral patients, these elements are typically supplied as water-soluble salts (e.g., KCl, NaCl, KI, NaI, and $CaCl_2$, $MgCl_2$, choline chloride, etc.) that are added directly to the intravenous supply.[75]

---

[67] Lykstad J, Sharma S. Biochemistry, Water Soluble Vitamins. StatPearls [Internet], 6 Mar 2023; https://www.ncbi.nlm.nih.gov/books/NBK538510/.

[68] https://synapse.patsnap.com/article/what-is-the-mechanism-of-fat-soluble-vitamin.
[69] https://en.wikipedia.org/wiki/Nutrient#Deficiencies_and_toxicity.
[70] https://en.wikipedia.org/wiki/Choline.
[71] https://lpi.oregonstate.edu/mic/other-nutrients/choline#sources.
[72] https://en.wikipedia.org/wiki/Choline#Biosynthesis.
[73] https://lpi.oregonstate.edu/mic/other-nutrients/choline.
[74] https://www.mdpi.com/2072-6643/16/12/1873.
[75] https://en.wikipedia.org/wiki/Parenteral_nutrition#Total_parenteral_nutrition.

2.4.4 Calcium and Magnesium

Ca^{2+} circulates as ~45% ionized, ~40% albumin-bound, and ~15% complexed with anions;[76] only the ionized fraction is biologically active and diffuses into cells. Mg^{2+} circulates as 60-70% ionized, 20-30% protein-bound, and 10-20% complexed;[77] only the ionized fraction is immediately available for cellular uptake. For parenteral patients, calcium is often provided as calcium gluconate but calcium chloride ($CaCl_2$) is also used when central access and rapid repletion are required; magnesium is usually provided as magnesium sulfate or magnesium chloride ($MgCl_2$), added directly to the intravenous supply.

2.4.5 Phosphorus

Inorganic phosphate is transported in the plasma in three forms: (1) ionized (free $H_2PO_4^-$ / HPO_4^{2-}) and immediately available to cells (~45%), (2) protein-bound to albumin or globulins and acting as a buffer reservoir (~15%), and (3) complexed with Ca^{2+}, Mg^{2+}, Na^+, or small organic anions such as citrate or lactate (~40%).[78] For parenteral patients, phosphorus is usually provided as aqueous solutions of sodium phosphate (Na_2HPO_4 or NaH_2PO_4) and/or potassium phosphate (K_2HPO_4 or KH_2PO_4), added directly to the intravenous supply, thus delivering ionized inorganic phosphorus to blood plasma, just as if it had been absorbed enterally through the gut. It may be necessary to pulse the delivery of calcium and phosphorus separately to avoid precipitation of $Ca_3(PO_4)_2$ or other calcium-phosphate salts if free Ca^{2+} and phosphate concentrations exceed solubility.

2.4.6 Zinc

In healthy humans, 70-85% of plasma zinc is tightly bound to albumin, with most of the remainder (10-30%) bound to α_2-macroglobulin or other high-molecular-weight proteins (e.g., α_1-acid glycoprotein). Only a very small fraction (<5%) is loosely complexed with low-molecular-weight ligands such as histidine or cysteine. Free (unbound) Zn^{2+} comprises essentially 0% of total plasma zinc at equilibrium. For parenteral patients, zinc chloride[79] or zinc sulfate can be added directly to the intravenous supply.

---

[76] Burtis CA, Ashwood ER, Bruns DE (eds.). *Tietz Textbook of Clinical Chemistry and Molecular Diagnostics*, 5th ed., Philadelphia, PA: Elsevier Saunders; 2012, Section: "Calcium", Table 32-2 (p. 787), "Plasma Calcium Distribution in Adults"; https://www.amazon.com/Textbook-Clinical-Chemistry-Molecular-Diagnostics/dp/0323089852.

[77] Gröber U, Schmidt J, Kisters K. Magnesium in Prevention and Therapy. Nutrients. 2015 Sep 23;7(9):8199-226; https://pmc.ncbi.nlm.nih.gov/articles/pmid/26404370/.

[78] https://derangedphysiology.com/main/cicm-primary-exam/body-fluids-and-electrolytes/Chapter-122/distribution-phosphate-body-fluid-compartments.

[79] https://labeling.pfizer.com/ShowLabeling.aspx?id=4675.

2.4.7 Iron

Essentially all plasma iron[80] is bound to the glycoprotein transferrin (>99% of the "exchangeable" pool), which carries two Fe^{3+} ions per molecule under physiologic pH. Free (unbound) Fe^{3+} is virtually 0% of the plasma iron pool because uncomplexed iron would catalyze free-radical formation.[81] Iron is not typically included directly in standard parenteral infusions because free iron and simple iron salts such as $FeCl_3$ precipitate readily and promote oxidative injury. Instead, intravenous iron is administered as a carbohydrate-coated complex such as iron dextran, ferric gluconate ($C_{66}H_{121}Fe_2NaO_{65}$),[82] iron sucrose ($C_{12}H_{29}Fe_5Na_2O_{23}$),[83] or ferric carboxymaltose. Once infused, these iron-carbohydrate complexes are taken up by reticuloendothelial macrophages via endocytosis. Fe^{3+} is released in the acidic endolysosome, whereupon the Fe^{3+} is reduced to Fe^{2+} and used to refill ferritin stores or exported via ferroportin to bind transferrin.[84]

2.4.8 Manganese

Mn does not normally exist in free form in plasma, but rather as (1) transferrin-bound Mn, primarily Mn^{3+} (~50%), (2) α_2-macroglobulin and similar high-MW proteins (20-55%), (3) albumin-bound as Mn^{2+} (~5%), and (4) small-anion complexes such as Mg-citrate (<5%).[85] For parenteral patients, the only safe and practical way to deliver Mn intravenously is as manganese chloride ($MnCl_2$) which dissociates immediately to Mn^{2+} (the physiologic cation) and its anion (Cl^-) once in plasma.[86]

2.4.9 Copper

About 75-95% of circulating Cu is bound to ceruloplasmin[87] and 5-25% is in a non-ceruloplasmin pool (e.g., albumin, α_2-macroglobulin, low-MW ligands). Free Cu^{2+} in plasma is normally ~0% because unbound copper is rapidly sequestered to prevent free-radical generation. For parenteral patients, copper chloride ($CuCl_2$) is the preferred source for intravenous administration;[88] copper

---

[80] https://en.wikipedia.org/wiki/Serum_iron.
[81] https://sickle.bwh.harvard.edu/iron_transport.html.
[82] https://en.wikipedia.org/wiki/Sodium_ferric_gluconate_complex.
[83] https://en.wikipedia.org/wiki/Iron_sucrose.
[84] https://en.wikipedia.org/wiki/Iron_preparation.

[85] Scheuhammer AM, Cherian MG. Binding of manganese in human and rat plasma. Biochim Biophys Acta. 1985 Jun 18;840(2):163-9; https://pubmed.ncbi.nlm.nih.gov/3995083/. O'Neal SL, Zheng W. Manganese Toxicity Upon Overexposure: a Decade in Review. Curr Environ Health Rep. 2015 Sep;2(3):315-28; https://pmc.ncbi.nlm.nih.gov/articles/PMC4545267/pdf.

[86] "Manganese (OTC)"; https://reference.medscape.com/drug/mncl2-manganese-344440#0. See also: "Trace Elements for Injection"; https://pdf.hres.ca/dpd_pm/00055580.PDF.

[87] https://en.wikipedia.org/wiki/Ceruloplasmin.
[88] https://pubchem.ncbi.nlm.nih.gov/compound/Cupric-Chloride.

sulfate ($CuSO_4$) is an acceptable alternative but less commonly used due to acid-base considerations. Upon infusion, these salts dissociate fully to free Cu^{2+}, which then binds albumin and is incorporated into ceruloplasmin for physiologic delivery.

2.4.10 Selenium

Selenoprotein P, a liver-synthesized glycoprotein containing multiple selenocysteine residues, carries ~50% of plasma selenium.[89] Glutathione peroxidases (GPx) and related selenoenzymes in plasma account for another ~30% of circulating Se, albeit as very low-molecular-weight proteins or enzyme complexes, while the remaining ~20 % is bound loosely to albumin or present as small inorganic selenide/selenite intermediates.[90] Plasma "free" inorganic Se is minimal (<5%) since most is protein-bound. For parenteral patients, the standard for intravenous administration is sodium selenite (Na_2SeO_3), which dissociates to SeO_3^{2-} and Na^+ in solution; once infused, SeO_3^{2-} is taken up by the liver, converted into selenide, and incorporated into selenoproteins.[91]

2.4.11 Chromium

Transferrin transports ~80% of circulating Cr^{3+},[92] while albumin[93] and low-molecular-weight complexes[94] such as Cr–citrate or "chromodulin" carry the remaining 15-20%). Free (unbound) Cr^{3+} is ~0% because unchelated Cr^{3+} is rapidly sequestered to avoid redox reactions. Chromium chloride ($CrCl_3$) in aqueous solution is the usual trace-element parenteral additive – upon infusion, $CrCl_3$ dissociates to Cr^{3+} plus $3Cl^-$, and the Cr^{3+} immediately binds to transferrin or albumin in plasma.

---

[89] Toyama T, Kaneko T, Arisawa K, Saito Y. Metal-binding properties of selenoprotein P – its relation to structure and function. Metallomics Res 2022; 2(3):rev-18-rev-27; https://www.jstage.jst.go.jp/article/metallomicsresearch/2/3/2_MR202209/_html. See also: https://www.sciencedirect.com/science/article/abs/pii/S0891584922005500.

[90] Deagen JT, Butler JA, Zachara BA, Whanger PD. Determination of the distribution of selenium between glutathione peroxidase, selenoprotein P, and albumin in plasma. Anal Biochem. 1993 Jan;208(1):176-81; https://pubmed.ncbi.nlm.nih.gov/8434786/.

[91] https://books.rsc.org/books/edited-volume/1109/chapter-abstract/925423/Selenium-in-Parenteral-Nutrition.

[92] Deng G, Wu K, Cruce AA, Bowman MK, Vincent JB. Binding of trivalent chromium to serum transferrin is sufficiently rapid to be physiologically relevant. J Inorg Biochem. 2015 Feb;143:48-55; https://pubmed.ncbi.nlm.nih.gov/25528477/.

[93] https://www.chl.co.nz/test/chromium-plasma/.

[94] https://en.wikipedia.org/wiki/Low-molecular-weight_chromium-binding_substance.

2.4.12 Molybdenum

Molybdate (MoO_4^{2-}) is the predominant circulating species at physiological pH (~7.4).[95] More specifically, 70-80% of plasma molybdate transiently associates with erythrocytes via anion exchangers (DIDS-sensitive), facilitating an enterohepatic-like shuttle.[96] A small fraction (15-20%) is loosely bound to albumin, with the remainder (5-10%) forming complexes with other small anions such as phosphate or sulfate. At any moment, 5-10% of plasma Mo is present as truly free MoO_4^{2-} while the rest is protein- or RBC-associated. Sodium molybdate (Na_2MoO_4) or ammonium molybdate ($(NH_4)_2MoO_4$) in sterile solution are the usual parenteral additives,[97] both of which dissociate to MoO_4^{2-} and their respective counter-ions (Na^+ or NH^{4+}) upon infusion.

2.5 Oxygen

For virtually all metabolizing cells in the body, the only source of molecular oxygen is the blood, either bound to hemoglobin or dissolved in plasma. There are only a few small avascular tissues that obtain O_2 directly by diffusion from their surrounding fluids or the atmosphere, bypassing the systemic circulation:

(1) **Corneal epithelium** (the transparent "window" of the eye) is completely avascular. Its primary oxygen source is atmospheric O_2 dissolved in the tear film,[98] which then diffuses through the epithelium.

(2) **Articular cartilage** (in joints) has no blood vessels and relies on oxygen diffusing in from the synovial fluid.[99]

(3) **Ocular lens** and the **outermost epidermis** likewise receive oxygen only by diffusion from the aqueous humor or ambient air, respectively (though these are minor in mass and metabolic rate).

---

[95] https://www.sciencedirect.com/topics/nursing-and-health-professions/molybdate.

[96] Gimenez I, Garay R, Alda JO. Molybdenum uptake through the anion exchanger in human erythrocytes. Pflugers Arch. 1993 Aug;424(3-4):245-9; https://pubmed.ncbi.nlm.nih.gov/8414913/.

[97] https://lpi.oregonstate.edu/mic/minerals/molybdenum.

[98] https://www.sciencedirect.com/topics/medicine-and-dentistry/tear-film; https://en.wikipedia.org/wiki/Cornea#Structure.

[99] Gibson JS, Milner PI, White R, Fairfax TP, Wilkins RJ. Oxygen and reactive oxygen species in articular cartilage: modulators of ionic homeostasis. Pflugers Arch. 2008 Jan;455(4):563-73; https://pubmed.ncbi.nlm.nih.gov/17849146/.

These avascular regions collectively represent negligible oxygen consumption compared to the rest of the body, so for all practical purposes, 100% of the O_2 used by systemic tissues – skeletal muscle, brain, heart, liver, etc. – is delivered via blood.

Approximately 98.5% of the oxygen content of whole blood (i.e., 2.4-3.2 x 10^{-4} gm/cm^3 arterial, 1.6-2.3 x 10^{-4} gm/cm^3 venous) is reversibly bound to hemoglobin in red blood cells, with only about 1.5% is carried as physically dissolved O_2 in the blood plasma (i.e., ~3.9 x 10^{-6} gm/cm^3 arterial, ~1.6 x 10^{-6} gm/cm^3 venous).[100] All oxygen taken up by tissue cells must be in the dissolved form in the plasma. Only dissolved oxygen can diffuse across the capillary and cell membranes. Hemoglobin's role is to offload O_2 into the plasma, maintaining the dissolved O_2 partial pressure that drives diffusion into tissues. No oxygen ever crosses directly from hemoglobin in the red cell into the tissue cell. All oxygen used by intracellular mitochondria comes from the dissolved pool in plasma at the tissue capillary interface. That dissolved pool is continuously replenished by hemoglobin unloading under the tissue PO_2 gradient, with perhaps ~97% of the O_2 ultimately consumed by cells originating from the hemoglobin-bound reservoir and ~3% having been dissolved in plasma and never bound to hemoglobin.

Due to oxygen's relatively low solubility in water, it is not possible to dissolve significantly more O_2 in the blood plasma, nor would it be wise to attempt to do so as this would risk effervescence and gas bubble embolism.[101] The metabolic organ must inject oxygen into the blood primarily by reoxygenating red cells in the functioning circulation.

Table 5 gives an estimate of the amount of molecular oxygen that must be consumed to metabolize each of the three principle nutrient materials (glucose, amino acids, and lipids) in the amounts that must be produced by the metabolic organ (**Table 1**), and the amount of carbon dioxide waste and metabolic water (~12 fluid ounces per day) that will be produced when those nutrients are metabolized in the body.

---

[100] Freitas RA Jr. Nanomedicine, Volume I: Basic Capabilities. Landes Bioscience, Georgetown, TX, 1999, Appendix B, "Concentrations of Human Blood Components"; http://www.nanomedicine.com/NMI/AppendixB.htm.

[101] Freitas RA Jr. Nanomedicine, Volume I: Basic Capabilities. Landes Bioscience, Georgetown, TX, 1999, Section 9.2.6, "Effervescence and Crystallescence"; http://www.nanomedicine.com/NMI/9.2.6.htm.

Table 5. Estimated daily O_2 requirement and metabolic CO_2 / H_2O generation for a resting 70 kg male human body at the ~100 watt basal metabolic rate

Macronutrient	Amount provided (gm/day)	O_2 consumed (gm/day)	CO_2 produced (gm/day)	H_2O produced[102] (gm/day)
Glucose[103]	400	427	587	240
Amino acids[104]	100	116	128	40
Lipids[105]	70	176	169	75
Micronutrients	10	~0	~0	~0
Totals	**580**	**719**	**884**	**355**

[102] The mass of metabolic water created per gm of substrate is ~0.60 gm/gm of glucose, ~0.40 gm/gm of protein, and ~1.07 gm/gm of lipid. Edney EB. Metabolic Water. In: Water Balance in Land Arthropods. Zoophysiology and Ecology, vol 9. Springer, Berlin, 1977; https://link.springer.com/chapter/10.1007/978-3-642-81105-0_8.

[103] The metabolic consumption of glucose according to $C_6H_{12}O_6 + 6\ O_2 \rightarrow 6\ CO_2 + 6\ H_2O$ has a respiratory quotient RQ = 1.0 (https://en.wikipedia.org/wiki/Respiratory_quotient), hence metabolizing 400 gm/day of glucose consumes (6) (32 gm/mole O_2) (400 gm/day glucose) / (180 gm/mole glucose) = 427 gm/day O_2 and produces (6) (44 gm/mole CO_2) (400 gm/day glucose) / (180 gm/mole glucose) = 587 gm/day CO_2 and (6) (18 gm/mole H_2O) (400 gm/day glucose) / (180 gm/mole glucose) = 240 gm/day H_2O.

[104] The metabolic consumption of amino acids has an Atwater energy of 17 kJ/gm (https://en.wikipedia.org/wiki/Food_energy) and a respiratory quotient RQ = 0.8 (https://en.wikipedia.org/wiki/Respiratory_quotient), hence metabolizing 100 gm/day of amino acids consumes (100 gm/day amino acids) (17 kJ/gm amino acids) (32 gm/mole O_2) / (470 kJ/mole O_2)[*] = 116 gm/day O_2 and produces (0.8) (44 gm/mole CO_2) (116 gm/day O_2) / (32 gm/mole O_2) = 128 gm/day CO_2.
[*] The oxycaloric equivalent in cultured mammalian cells is –470 kJ/mole O_2 (i.e. 470 kJ of heat dissipated per mole O_2) under fully aerobic glucose-oxidizing conditions. Gnaiger E, Kemp RB. Anaerobic metabolism in aerobic mammalian cells: information from the ratio of calorimetric heat flux and respirometric oxygen flux. Biochim Biophys Acta. 1990 Apr 26;1016(3):328-32; https://pubmed.ncbi.nlm.nih.gov/2184896/.

[105] The metabolic consumption of lipids has an Atwater energy of 37 kJ/gm (https://en.wikipedia.org/wiki/Food_energy) and a respiratory quotient RQ = 0.7 (https://en.wikipedia.org/wiki/Respiratory_quotient), hence metabolizing 70 gm/day of lipids consumes (70 gm/day lipids) (37 kJ/gm lipids) (32 gm/mole O_2) / (470 kJ/mole O_2) = 176 gm/day O_2 and produces (0.7) (44 gm/mole CO_2) (176 gm/day O_2) / (32 gm/mole O_2) = 169 gm/day CO_2.

3. Human Metabolic Waste Generation

Table 6 summarizes the overall estimated mass production rate of waste molecules for a standard 70 kg male human body at the basal ~100 watt (~2000 kcal/day) metabolic rate. These waste products are further detailed in the Sections that follow. The primary waste molecules produced by the human body are carbon dioxide and four nitrogenous waste molecules generated during the breakdown of protein. The total mass rate for waste generation reported in **Table 6** equals to the total mass rate for nutrients reported in **Table 1**, ensuring that elemental outflows equal inflows at steady state. In summary, an average person produces roughly 1.3 kg of metabolic waste per day (mostly CO_2 and water). The AMO must capture or otherwise deal with these wastes to complete the recycling loop – each waste is a crucial reservoir of essential elements for recycled nutrients.

Table 6. Estimated molecular waste generation for a resting 70 kg male human body at the ~100 watt basal metabolic rate, with molecular weights in [gm/mole]

Molecular Component	Waste Generation (gm/day)	Discussed in:
Carbon Dioxide (CO_2) [44]	884	**Table 5**, Sec. 4.2.2
Metabolic Water (H_2O) [18]	355	**Table 5**
Urea (H_2NCONH_2)[106] [60.1]	28.08	Section 3.2
Creatinine ($C_4H_7N_3O$)[107] [113.1]	1.6	Section 3.3
Uric acid ($C_5H_4N_4O_3$) [168.1]	0.5	Section 3.4
Hippuric acid ($C_9H_9NO_3$) [179.2]	0.8	Section 3.5
Metabolic Microwastes		Section 3.6
Sulfate anion (SO_4^{2-}) [96.1]	1.58	Section 3.6.1
Ammonium ion (NH_4^+) [18]	0.6	Section 3.6.2
Phosphate ion ($H_2PO_4^{3-}$) [97]	2.74	Section 3.6.3
Bilirubin ($C_{33}H_{36}N_4O_6$) [584.7]	0.3	Section 3.6.4
Bile acids ($C_{24}H_{40}O_5$) [408.6] & ($C_{24}H_{40}O_4$) [392.6]	0.5	Section 3.6.5
Free cholesterol ($C_{27}H_{46}O$) [386.7]	1.0	Section 3.6.6
Mineral Microwastes	9.45	Section 3.7
Subtotal	1270.2	
Miscwastium (~$C_{19}H_{15}O_{10}$) [403.0]	~17.9	Section 3.8
Total Wastes	**1304.1**	

[106] Urinary urea excretion averages 20-35 gm/day in adults, with 27 gm/day a reasonable midpoint; http://ordspub.epa.gov/ords/eims/eimscomm.getfile?p_download_id=498574.

[107] Average daily creatinine production is about 1.6 gm; https://www.news-medical.net/health/Urine-Composition-Whats-Normal.aspx.

3.1 Carbon Dioxide

Carbon dioxide, the principal metabolic waste product of the human body, is discussed at length in Section 4.2.2. (The AMO captures CO_2 from the blood before it is exhaled.)

3.2 Urea

Almost 80% of the nitrogen excreted in humans is in the form of urea (H_2NCONH_2). The urea cycle[108] occurs primarily in the liver, processed by mitochondrial and cytosolic enzymes in the periportal hepatocytes.[109] (A small amount of urea cycle activity also occurs in renal cortex cells, but quantitatively the liver is the major source.) Once formed, urea diffuses out of the hepatocytes and into the hepatic vein, then enters the systemic circulation and travels in the bloodstream dissolved in plasma. It is freely soluble (no protein binding) and moves down its concentration gradient toward the kidneys. Blood plasma entering the kidney typically carries ~300 mg/L of urea under healthy basal conditions, while blood plasma exiting the kidney contains ~270 mg/L.[110]

Urinary urea excretion typically averages 20-35 gm/day in adults, with 27 gm/day often taken as a reasonable midpoint.[111] It is also common to assume proteins (and amino acids) are ~16% nitrogen by weight,[112] in which case the estimated urea production is ~(16% gm N/gm protein) (100 gm/day protein) (60.1 gm/mole urea) / (2) (14 gm/mole for nitrogen) ~ 34.3 gm/day urea. Nutrient nitrogen intake is exactly balanced with nitrogen wastes if we assume ~**27.58 gm/day** for urinary urea generation. A vascular- or renal-contacting nanodevice should be able to recover virtually all of this waste urea. But there is also 0.2-0.3 gm/day of urea lost in sweat at rest,[113]

---

[108] https://en.wikipedia.org/wiki/Urea_cycle.

[109] Barmore W, Azad F, Stone WL. Physiology, Urea Cycle. StatPearls [Internet], 8 May 2023; https://www.ncbi.nlm.nih.gov/books/NBK513323/.

[110] Van Stone JC. Peripheral venous blood is not the appropriate specimen to determine the amount of recirculation during hemodialysis. ASAIO J. 1996 Jan-Feb;42(1):41-5; https://pubmed.ncbi.nlm.nih.gov/8808457/.

[111] Urinary urea excretion averages 20-35 gm/day in adults, with 27 gm/day taken as a reasonable midpoint; http://ordspub.epa.gov/ords/eims/eimscomm.getfile?p_download_id=498574.

[112] Richter M, Baerlocher K, Bauer JM, Elmadfa I, Heseker H, Leschik-Bonnet E, Stangl G, Volkert D, Stehle P; on behalf of the German Nutrition Society (DGE). Revised Reference Values for the Intake of Protein. Ann Nutr Metab. 2019;74(3):242-250; https://pmc.ncbi.nlm.nih.gov/articles/PMC6492513/.

[113] Sweat urea concentration is measured* at 22.2 mmol/L ~ 1.33 gm/L; resting (non-exercise) sweat volume is 0.1-0.3 L/day, giving 0.13-0.40 gm/day of urea lost in sweat. During exercise or high-temperature exposure, sweat losses can rise up to several grams of urea, but 0.2-0.3 gm/day is typical in a sedentary state.
* Huang CT, Chen ML, Huang LL, Mao IF. Uric acid and urea in human sweat. Chin J Physiol. 2002 Sep 30;45(3):109-15; https://pubmed.ncbi.nlm.nih.gov/12817713/.

and 0.2-0.4 gm/day of urea can be lost to fecal (gastrointestinal) and pulmonary excretion, collectively totaling ~**0.5 gm/day** non-urinary urea loss under basal resting conditions.[114] It will be difficult to conveniently recover and recycle this portion of the waste urea stream. The total urea production is therefore ~28.08 gm/day.

3.3 Creatinine

Creatinine ($C_4H_7N_3O$) arises from the non-enzymatic cyclization of creatine and phosphocreatine within skeletal muscle, at a nearly constant rate proportional to muscle mass.[115] Once formed in muscle fibers, creatinine diffuses into the interstitial fluid and thence into the blood plasma, where it dissolves freely. It is not protein-bound and circulates as a free cation dissolved in the plasma water to the kidneys, in typical serum concentration 6-12 mg/L.[116] Creatinine excretion in male urine is typically 14-26 mg/kg-day,[117] or 0.98-1.82 gm/day (typically ~**1.6 gm/day**) for a 70 kg person. Virtually all (>99%) creatinine is removed by the kidneys and thus can be recovered from the urine or directly from blood plasma prior to renal filtration. There is also ~**4 mg/day** of creatinine lost in feces[118] and **0.4 mg/day** lost in sweat at rest[119] that will be difficult to conveniently recover and recycle.

3.4 Uric Acid

Uric acid ($C_5H_4N_4O_3$) is the end-product of purine (adenine and guanine) nucleotide catabolism. Nucleotides are degraded to hypoxanthine and xanthine in many tissues, but the rate-limiting enzymes – xanthine dehydrogenase/oxidase (XDH/XO) – are most highly expressed in liver hepatocytes, with additional activity in vascular endothelium and gut. At physiological pH, uric acid exists almost entirely as the urate anion ($C_5H_3N_4O_3^-$). Urate is highly soluble in plasma water with no covalent protein binding. Perhaps 7-15 % of urate is loosely bound to plasma

---

[114] https://en.wikipedia.org/wiki/Urea-to-creatinine_ratio#Technique.
[115] https://en.wikipedia.org/wiki/Creatinine.

[116] Hosten AO. Chapter 193. BUN and Creatinine. In: Walker HK, Hall WD, Hurst JW, eds., Clinical Methods: The History, Physical, and Laboratory Examinations, 3rd Edition, Butterworths, Boston, 1990; https://www.ncbi.nlm.nih.gov/books/NBK305.

[117] https://www.ucsfhealth.org/medical-tests/creatinine-urine-test.

[118] Goldman R. Creatinine Excretion in Renal Failure. Proc Soc Exp Biol and Med. 1954;85(3):446-448; https://www.ebm-journal.org/journals/experimental-biology-and-medicine/articles/10.3181/00379727-85-20912/pdf.

[119] Sweat creatinine concentration is measured at ~20 μmol/L ~ 2 mg/L;* resting (non-exercise) sweat volume is ~0.2 L/day, giving ~0.40 mg/day of creatinine lost in sweat.
* Adelaars S, Konings CJAM, Cox L, Boonen E, Mischi M, Bouwman RA, van de Kerkhof D. The correlation of urea and creatinine concentrations in sweat and saliva with plasma during hemodialysis: an observational cohort study. Clin Chem Lab Med. 2024 Jan 23;62(6):1118-1125; https://pubmed.ncbi.nlm.nih.gov/38253354/.

proteins (primarily albumin),[120] while the remaining 85-93% **c**irculates free, mostly in association with Na^+ or K^+ cations, typically 25-80 mg/L in male blood.[121] While most uric acid simply diffuses in plasma, some cells (e.g., adipocytes, endothelial cells) can uptake or efflux urate, modulating local concentrations.[122] About 70% of the daily uric acid load is eliminated via the kidneys while ~30% is secreted into the gut lumen and intestinally excreted in feces.[123] The normal excretion rate for adult males is ~**315 mg/day** (range 270-360 mg/day) in urine,[124] ~**158 mg/day** (range 135-180 mg/day) in the feces,[125] and ~**0.8 mg/day** lost in sweat.[126] The ~158.8 mg/day of uric acid lost to feces and sweat will be difficult to conveniently recover and recycle unless they can be extracted directly from blood plasma prior to intestinal or dermal filtration.

Uric acid probably should not be thought of purely as a waste molecule. The loss of uricase in higher primates parallels the similar loss of the ability to synthesize Vitamin C (ascorbic acid), which means that urate might partially substitute for ascorbate[127] – uric and ascorbic acids are both potent antioxidants, and it's estimated that over half the antioxidant capacity of human blood plasma comes from hydrogen urate ion[128] – so the metabolic organ must be designed to maintain uric acid within an optimum range, not targeting complete removal (producing hypouricemia).[129]

---

[120] Bertolini J, Masarei JR. The binding of urate by plasma proteins. Aust J Exp Biol Med Sci. 1979 Feb;57(1):51-60; https://pubmed.ncbi.nlm.nih.gov/475669/.

[121] https://en.wikipedia.org/wiki/Uric_acid#Humans.

[122] So A, Thorens B. Uric acid transport and disease. J Clin Invest. 2010 Jun;120(6):1791-9; https://pmc.ncbi.nlm.nih.gov/articles/PMC2877959/pdf.

[123] So A, Thorens B. Uric acid transport and disease. J Clin Invest. 2010 Jun;120(6):1791-9; https://pmc.ncbi.nlm.nih.gov/articles/PMC2877959/pdf.

[124] Kok DJ, Poindexter J, Pak CY. Calculation of titratable acidity from urinary stone risk factors. Kidney Int. 1993 Jul;44(1):120-6; https://core.ac.uk/download/pdf/82078021.pdf.

[125] Hosomi A, Nakanishi T, Fujita T, Tamai I. Extra-renal elimination of uric acid via intestinal efflux transporter BCRP/ABCG2. PLoS One. 2012;7(2):e30456; https://pmc.ncbi.nlm.nih.gov/articles/PMC3277506/.

[126] Sweat uric acid concentration is measured* at 24.5 μmol/L ~ 4.12 mg/L; resting (non-exercise) sweat volume is ~0.2 L/day, giving ~0.8 mg/day of uric acid lost in sweat.
* Huang CT, Chen ML, Huang LL, Mao IF. Uric acid and urea in human sweat. Chin J Physiol. 2002 Sep 30;45(3):109-15; https://pubmed.ncbi.nlm.nih.gov/12817713/.

[127] Proctor P. Similar functions of uric acid and ascorbate in man? Nature. 1970 Nov 28;228(5274):868; https://www.nature.com/articles/228868a0.pdf.

[128] Maxwell SR, Thomason H, Sandler D, Leguen C, Baxter MA, Thorpe GH, Jones AF, Barnett AH. Antioxidant status in patients with uncomplicated insulin-dependent and non-insulin-dependent diabetes mellitus. Eur J Clin Invest. 1997 Jun;27(6):484-90; https://pubmed.ncbi.nlm.nih.gov/9229228/.

[129] https://en.wikipedia.org/wiki/Hypouricemia.

3.5 Hippuric Acid

Hippuric acid ($C_9H_9NO_3$) is produced via a host–microbe co-metabolic pathway: dietary and endogenously derived aromatic compounds[130] (e.g. polyphenols, phenylalanine, toluene) are first converted by the gut microbiota into benzoic acid, which is absorbed across the intestinal epithelium into portal blood.[131] In hepatocytes (and to a lesser extent in renal and intestinal cells) benzoic acid is activated to benzoyl-CoA by a CoA-ligase and then conjugated with glycine via glycine N-acyltransferase (GLYAT) in the mitochondrial matrix, yielding hippuric acid (N-benzoylglycine).[132] At physiological pH (~7.4), hippuric acid exists predominantly as the hippurate anion ($C_9H_8NO_3^-$). It is highly water-soluble and travels freely dissolved in plasma, mostly as sodium and potassium hippurate salts, with no significant protein binding. Circulating concentrations are typically in the micromolar range, and hippurate is carried in the bloodstream from the liver mainly to the kidneys for elimination.[133]

About **700 mg/day** of hippuric acid is excreted in the urine of healthy adults,[134] ranging from 0.34 gm/day (1.89 mmol/day) for healthy adults on low polyphenol diets[135] up to 0.74-1.4 gm/day on high polyphenol diets (i.e., heavy consumption of black or green tea).[136] Pharmacokinetic data from a tracer-dose study[137] shows that ~80% of an administered hippuric-acid–forming dose is recovered in urine and ~20% in feces within 24 h, so it may be reasonable to infer another ~**150 mg/day** of hippuric acid that is lost through fecal excretion. Minute amounts of hippuric acid are also excreted in sweat, ~**0.2 mg/day**.[138] Again, the ~150.2 mg/day of hippuric acid lost to feces

---

[130] Mainly plant-derived phenolic compounds, as found in fruit juice, tea, and wine; https://en.wikipedia.org/wiki/Hippuric_acid.

[131] Pero RW. Health consequences of catabolic synthesis of hippuric acid in humans. Curr Clin Pharmacol. 2010 Feb;5(1):67-73; https://pubmed.ncbi.nlm.nih.gov/19891605/.

[132] https://en.wikipedia.org/wiki/GLYAT. See also: https://reactome.org/content/detail/R-HSA-159566.
[133] https://healthmatters.io/understand-blood-test-results/hippuric-acid.

[134] Toromanović J, Kovac-Besović E, Sapcanin A, Tahirović I, Rimpapa Z, Kroyer G, Sofić E. Urinary hippuric acid after ingestion of edible fruits. Bosn J Basic Med Sci. 2008 Feb;8(1):38-43; https://pmc.ncbi.nlm.nih.gov/articles/PMC5724873/pdf.

[135] Mulder TP, Rietveld AG, van Amelsvoort JM. Consumption of both black tea and green tea results in an increase in the excretion of hippuric acid into urine. Am J Clin Nutr. 2005 Jan;81(1 Suppl):256S-260S; https://www.sciencedirect.com/science/article/pii/S0002916523275140.

[136] Clifford MN, Copeland EL, Bloxsidge JP, Mitchell LA. Hippuric acid as a major excretion product associated with black tea consumption. Xenobiotica. 2000 Mar;30(3):317-26; https://pubmed.ncbi.nlm.nih.gov/10752646/.

[137] Sheets LP. Imidacloprid. In: Wexler P, Anderson BD, eds., Encyclopedia of Toxicology, 2nd edition, 2005, pp.567-570; https://www.sciencedirect.com/topics/earth-and-planetary-sciences/hippuric-acid.

[138] Hippuric acid has been detected in eccrine sweat but at very low concentrations, <5 μmol/L or ≲ 0.9 mg/L;* resting (non-exercise) sweat volume is ~0.2 L/day, giving ~0.18 mg/day of hippuric acid lost in sweat.

and sweat will be hard to conveniently recover and recycle unless they can be extracted directly from blood plasma prior to intestinal or dermal filtration.

3.6 Metabolic Microwastes

There are six additional metabolic microwastes produced by a healthy normal 70 kg male human with a ~100 W basal metabolism, as detailed below.

3.6.1 Sulfate Anion

Both methionine and cysteine amino acids are ultimately catabolized (via the transsulfuration and oxidative pathways) to inorganic sulfate. Each mole of methionine or cysteine ultimately produces one mole of sulfate (SO_4^{2-}; 96.06 gm/mole), which corresponds to one mole of sulfuric-acid equivalents (H_2SO_4; 98.08 gm/mole). From **Table 2**, we use a nutrient input of 0.928 gm/day of methionine ($C_5H_{11}NO_2S$; 149.2 gm/mole) or 6.22 mmoles/day, and 0.360 gm/day of cysteine ($C_3H_7NO_2S$; 121.2 gm/mole) or 2.97 mmoles/day, which produces a total of 9.19 mmoles/day or 883 mg/day of sulfate anion, a sulfuric acid equivalent of 0.901 gm/day. The sulfate anion appears in urine almost entirely as the free sulfate anion (SO_4^{2-}), paired with Na^+ and K^+ (and to a far lesser extent NH_4^+), i.e., as sodium/potassium sulfate salts.[139] This is consistent with evidence that inorganic sulfate derived from sulfur-amino-acid catabolism (and dietary sources) is filtered and excreted by the kidney, generating 0.8-1.0 gm/day of urinary sulfate in healthy adults on a normal protein diet.[140]

Nutrient sulfur intake is exactly balanced with sulfur wastes if we assume ~**1.5279 gm/day** for urinary sulfate generation. Under normal dietary and absorptive conditions, fecal sulfate losses are <0.5 mmol/day or ~**48 mg/day**.[141] Eccrine sweat contains only trace sulfate at 83 μmol/L (8 mg/L),[142] so a resting sweat rate of ~0.2 L/day excretes ~**1.6 mg/day** of sulfate in the sweat. The total sulfate production is taken as ~1.5775 gm/day.

---

[*] Clifford MN, Copeland EL, Bloxsidge JP, Mitchell LA. Hippuric acid as a major excretion product associated with black tea consumption. Xenobiotica. 2000 Mar;30(3):317-26; https://pubmed.ncbi.nlm.nih.gov/10752646/.

[139] Hoffer LJ, Hamadeh MJ, Robitaille L, Norwich KH. Human sulfate kinetics. Am J Physiol Regul Integr Comp Physiol. 2005 Nov;289(5):R1372-80; https://journals.physiology.org/doi/full/10.1152/ajpregu.00325.2005.

[140] https://faculty.ksu.edu.sa/sites/default/files/Urine%20Analysis%20OK.pdf.

[141] Florin T, Neale G, Gibson GR, Christl SU, Cummings JH. Metabolism of dietary sulphate: absorption and excretion in humans. Gut. 1991 Jul;32(7):766-73; https://pmc.ncbi.nlm.nih.gov/articles/PMC1378993.

[142] Cole DE, Landry DA. Determination of inorganic sulfate in human saliva and sweat by controlled-flow anion chromatography. Normal values in adult humans. J Chromatogr. 1985 Feb 8;337(2):267-78; https://pubmed.ncbi.nlm.nih.gov/3988858/.

3.6.2 Ammonium Ion

Unlike almost all other solutes in the urine, ammonium ion (NH_4^+; 18 gm/mole) does not result from arterial delivery but rather is produced by the kidney, with only a portion excreted in the urine while the remainder is returned to the systemic circulation through the renal veins, whereupon systemic ammonia addition is metabolized efficiently by the liver.[143] Under basal (normal acid-base) conditions the kidney produces ammonia (NH_3/NH_4^+) via glutamine metabolism and then "splits" it roughly half/half between urinary excretion (~30 mmoles/day or **540 mg/day**) and return to the systemic circulation via renal veins (~30 mmoles/day or 540 mg/day).[144] Measured fecal NH_4^+ excretion in healthy subjects is about 1.4-2.9 mmol/day (low- vs. high-meat diet),[145] averaging ~2 mmol/day or ~**36 mg/day**. Ammonia is found in widely varying amounts in sweat at about 1-8 mmol/L (18-144 mg/L),[146] so a resting sweat rate of ~0.2 L/day excretes **4-29 mg/day** of ammonia in the sweat. A small amount of ammonia is also exhaled from the lungs with average concentration ~265 ppb (~265 x 10^{-9} atm) in normal adults,[147] or ~**1.7 mg/day**,[148] for a grand total of up to **607 mg/day**.

3.6.3 Phosphate Ion

Phosphate in the form of inorganic hydrogen-phosphate (HPO_4^{2-}) and dihydrogen-phosphate ($H_2PO_4^-$) comes entirely from the pool of filtered plasma phosphate, which itself derives both from the dietary (or parenteral) phosphate necessary for cell metabolism and from the normal breakdown of ATP, nucleic acids, phospholipids, and bone remodeling. These sources liberate organic phosphate esters which are then hydrolyzed to free inorganic phosphate and released into the extracellular fluid. Once liberated by phosphatases in cells, inorganic phosphate enters the extracellular fluid, passing into the plasma where it exists as a mixture of HPO_4^{2-} and $H_2PO_4^-$ and travels exclusively via the bloodstream (dissolved in plasma or loosely bound to proteins) to the kidneys for elimination.

---

[143] Weiner ID. Roles of renal ammonia metabolism other than in acid-base homeostasis. Pediatr Nephrol. 2017 Jun;32(6):933-942; https://pmc.ncbi.nlm.nih.gov/articles/PMC5107182/pdf.

[144] Weiner ID, Verlander JW. Renal ammonia metabolism and transport. Compr Physiol. 2013 Jan;3(1):201-20; https://pmc.ncbi.nlm.nih.gov/articles/PMC4319187/pdf.

[145] Silvester KR, Bingham SA, Pollock JR, Cummings JH, O'Neill IK. Effect of meat and resistant starch on fecal excretion of apparent N-nitroso compounds and ammonia from the human large bowel. Nutr Cancer. 1997;29(1):13-23; https://pubmed.ncbi.nlm.nih.gov/9383779/.

[146] https://www.gssiweb.org/sports-science-exchange/article/sweat-biomarkers-for-sports-science-applications. See also: https://www.physio-pedia.com/Physiology_of_Sweat.

[147] Hibbard T, Killard AJ. Breath ammonia levels in a normal human population study as determined by photoacoustic laser spectroscopy. J Breath Res. 2011 Sep;5(3):037101; https://pubmed.ncbi.nlm.nih.gov/21654023/.

[148] Assuming alveolar ventilation ~6 L/min = 8640 L/day, then (8640 L/day) (265 x 10^{-9} atm) (17 gm/mole) / (22.4 atm-L/mole) = 1.7 mg/day.

Assuming ~877 mg/day of phosphorus is provided intravenously (**Table 9**) and is 100% bioavailable with no oral intake, all excreted PO_4^{3-} must equal the ~877 mg/day supplied (equivalent to (877 mg/day) (97/31) ~ **2744.5 mg/day $H_2PO_4^-$**) in steady state, but fecal losses arise only from endogenous secretions and not from unabsorbed dietary phosphate. Under conditions of parenteral phosphate supply (no oral intake), renal phosphate excretion adjusts to match the infused load and amounts to ~90% of the daily phosphate load (e.g., ~**789 mg P/day** for a 726 mg/day IV infusion, or ~2470 mg/day $H_2PO_4^-$) with the gastrointestinal tract excreting the remainder (e.g., fecal excretion ~**82 mg P/day**, with phosphate is secreted into bile (~20 mg/day) and across enterocytes (50-80 mg/day), independent of diet),[149] and perhaps the remaining ~**6 mg P/day** in resting sweat.

3.6.4 Bilirubin

Bilirubin ($C_{33}H_{36}N_4O_6$)[150] arises continuously from normal red-blood-cell turnover (~1% of RBC mass per day), independent of diet. Aging erythrocytes undergo eryptosis[151] in the mononuclear phagocyte system (spleen, liver, and lymph nodes), in which the heme constituent of hemoglobin is reduced to bilirubin which is released into the plasma and recirculated to the liver bound to albumin, while the liberated iron is released into the plasma and recirculated bound to transferrin, a carrier protein.[152] From the liver, conjugated bilirubin is released into bile and delivered to the small intestine via the bile ducts. Adult production of bilirubin is ~ 4 mg/kg-day,[153] or **280 mg/day** for a 70 kg human. There is no urinary bilirubin excretion under normal conditions. However, a small fraction of its bacterial metabolite, urobilinogen, is filtered and excreted in urine, where it is later oxidized to urobilin (the yellow pigment in normal urine); normal urinary urobilinogen excretion is ~**4 mg/day** in adults.[154] (*In vivo*, the bladder is effectively an anaerobic reservoir, so the colorless urobilinogen remains un-oxidized until exposure to air and a rapid extraction *in situ* will capture urobilinogen alone.

3.6.5 Bile Acids

Bile[155] is required for the digestion of food and is secreted by the liver into passages that carry bile toward the hepatic duct, which joins the cystic duct (carrying bile to and from the gallbladder) to form the common bile duct which then opens into the intestine. The liver of an

---

[149] Rout P, Jialal I. Hyperphosphatemia. StatPearls [Internet], 12 Jun 2023; https://www.ncbi.nlm.nih.gov/books/NBK551586/.

[150] https://en.wikipedia.org/wiki/Bilirubin.
[151] https://en.wikipedia.org/wiki/Eryptosis.
[152] https://en.wikipedia.org/wiki/Red_blood_cell#Senescence.

[153] Kalakonda A, Jenkins BA, John S. Physiology, Bilirubin. StatPearls [Internet], 12 Sep 2022; https://www.ncbi.nlm.nih.gov/books/NBK470290/.

[154] https://www.sciencedirect.com/topics/medicine-and-dentistry/urobilinogen.
[155] https://en.wikipedia.org/wiki/Bile.

adult produces 400-800 mL/day of bile, composed of 97–98% water, 0.7% bile salts, 0.2% bilirubin, 0.51% fats (cholesterol, fatty acids, and lecithin), and 200 meq/L inorganic salts.

Bile acids[156] facilitate digestion of dietary fats and oils, serving as micelle-forming surfactants that encapsulate nutrients, facilitating their absorption.[157] Bile acids (composed mainly of 40% cholic acid,[158] or $C_{24}H_{40}O_5$ at 408.57 gm/mole, and 40% chenodeoxycholic acid[159] and 20% deoxycholic acid,[160] both $C_{24}H_{40}O_4$ at 392.58 gm/mole) are steroid acids that comprise ~80% of the organic compounds found in bile (besides phospholipids and cholesterol) and are synthesized from cholesterol in the peroxisomes of hepatocytes in the liver. Bile acids are conjugated with taurine or glycine residues to give anions called **bile salts**. These are secreted into bile canaliculi and then excreted into the intestinal duodenum, after which ~95% are enterohepatically recycled by reabsorption in the terminal ileum (being routed to the portal vein and thence back to the liver), with ~5% permanently lost in the feces (300-600 mg/day);[161] we'll assume a ~**500 mg/day** net loss in the feces. At most <**0.5 mg/day** of bile acids spill over into the systemic circulation and are subsequently excreted into urine.[162]

3.6.6. Free Cholesterol

Surplus cholesterol is either converted into bile acids or secreted as free cholesterol ($C_{27}H_{46}O$, 386.65 gm/mole)[163] in bile, whereupon it flows through the bile ducts[164] into the duodenum, and is subsequently excreted in the feces. Biliary secretion of free cholesterol into the feces is **~1000 mg/day**,[165] solubilized in mixed micelles with bile salts and phospholipid. Because cholesterol is hydrophobic and tightly bound within lipoproteins, it is almost entirely reabsorbed or metabolized

---

[156] https://en.wikipedia.org/wiki/Bile_acid.

[157] Chen I, Cassaro S. Physiology, Bile Acids. StatPearls [Internet], 1 May 2023; https://www.ncbi.nlm.nih.gov/books/NBK549765/.

[158] https://en.wikipedia.org/wiki/Cholic_acid.
[159] https://en.wikipedia.org/wiki/Chenodeoxycholic_acid.
[160] https://en.wikipedia.org/wiki/Deoxycholic_acid.

[161] Fleishman JS, Kumar S. Bile acid metabolism and signaling in health and disease: molecular mechanisms and therapeutic targets. Signal Transduct Target Ther. 2024 Apr 26;9(1):97; https://pmc.ncbi.nlm.nih.gov/articles/PMC11045871/. See also https://en.wikipedia.org/wiki/Bile_acid#Primary_bile_acids and https://www.ncbi.nlm.nih.gov/books/NBK470209/.

[162] Chiang JYL, Ferrell JM. Bile Acid Metabolism in Liver Pathobiology. Gene Expr. 2018 May 18;18(2):71-87; https://pmc.ncbi.nlm.nih.gov/articles/PMC5954621/.

[163] https://en.wikipedia.org/wiki/Cholesterol.
[164] https://en.wikipedia.org/wiki/Bile_duct.

[165] McNamara DJ. Cholesterol: Sources, Absorption, Function and Metabolism. In: Caballero B, ed., Encyclopedia of Human Nutrition, Second Edition, Elsevier, 2005, pp. 379-385; https://www.sciencedirect.com/science/article/pii/B0122266943000570.

before any can reach the urine. For practical purposes, urinary free cholesterol excretion is negligible (<**1 mg/day**) in a resting 70 kg male at basal metabolism.[166]

3.7 Mineral Microwastes

Renal excretion is the dominant route for most of these mineral elements, all of which will be present as ions in an aqueous solution environment. Given the proposed intravenous nutrient inputs as listed in **Table 4**, total excretion equals these inputs under steady-state, as shown in **Table 7**. Mostly minor non-renal routes (e.g., sweat and feces) are essentially independent of intake route and are similar to basal values. Fecal estimates reflect only endogenous secretions (e.g., sloughed cells, biliary excretions). Sweat and insensible skin losses are assumed unchanged by intravenous vs. oral routes, since plasma electrolyte levels remain within normal ranges, allowing urinary excretion to be estimated as intake – non-renal losses.

Table 7. Estimated mineral microwaste generation for a 70 kg male human body at the ~100 watt basal metabolic rate with intravenous nutrient inputs

Waste Element	Urine	Sweat	Feces	Total
Sodium[167]	2058 mg/day	230 mg/day	23 mg/day	2311 mg/day
Potassium	3283 mg/day	39 mg/day	78 mg/day	3400 mg/day
Chloride[168]	1900 mg/day	350 mg/day	50 mg/day	2300 mg/day
Iodide[169]	0.13 mg/day	0.005 mg/day	0.015 mg/day	0.15 mg/day
Calcium[170]	860 mg/day	~40 mg/day	100 mg/day	1000 mg/day
Magnesium[171]	386 mg/day	4 mg/day	30 mg/day	420 mg/day
Zinc[172]	10.25 mg/day	0.25 mg/day[179]	0.5 mg/day	11 mg/day

[166] Jüngst D, Tauber R, Osterholzer M, Karl HJ. Is urinary cholesterol determination a possible screening test for urological carcinomas? Urol Res. 1981;9(1):1-3; https://pubmed.ncbi.nlm.nih.gov/7268998/.

[167] https://nap.nationalacademies.org/read/10925/chapter/8#278.
[168] https://nap.nationalacademies.org/read/10925/chapter/8#278.
[169] https://lpi.oregonstate.edu/mic/minerals/iodine.

[170] Mathis SL, Pivovarova AI, Hicks SM, Alrefai H, MacGregor GG. Calcium loss in sweat does not stimulate PTH release: A study of Bikram hot yoga. Complement Ther Med. 2020 Jun;51:102417; https://www.sciencedirect.com/science/article/pii/S0965229919316243. Heaney RP, Recker RR. Determinants of endogenous fecal calcium in healthy women. J Bone Miner Res. 1994 Oct;9(10):1621-7; https://pubmed.ncbi.nlm.nih.gov/7817809/.

[171] Sawka MN, Montain SJ. Fluid and electrolyte supplementation for exercise heat stress. Am J Clin Nutr. 2000 Aug;72(2 Suppl):564S-72S; https://www.sciencedirect.com/science/article/pii/S0002916523067370. And https://nap.nationalacademies.org/read/1349/chapter/10#187.

[172] King JC, Shames DM, Woodhouse LR. Zinc homeostasis in humans. J Nutr. 2000 May;130(5S Suppl):1360S-6S; https://www.sciencedirect.com/science/article/pii/S0022316622140897.

Iron	0.07 mg/day	0.40 mg/day[180]	0.53 mg/day[182]	1 mg/day
Manganese[173]	0.02 mg/day	0.02 mg/day	2.26 mg/day	2.3 mg/day
Copper	0.10 mg/day[178]	0.32 mg/day[181]	0.48 mg/day	0.9 mg/day
Selenium[174]	0.0275 mg/day	~0 mg/day	0.0275 mg/day	0.055 mg/day
Chromium[175]	0.028 mg/day	0.004 mg/day	0.003 mg/day	0.035 mg/day
Molybdenum[176]	0.034 mg/day	~0 mg/day	0.011 mg/day	0.045 mg/day
Cobalt (as cobalamin)[177]	0.0002 mg/day	~0 mg/day	0.0022 mg/day	0.0024 mg/day
Totals	**8486.7 mg/day**	**664.0 mg/day**	**284.8 mg/day**	**9435.5 mg/day**

3.8 Miscwastium

The estimated total waste product generation is listed in **Table 6** (Section 3) and **Table 7** (Section 3.7). These 26 components represent our best estimate of the molecules or elements that are lost every day from a 70 kg human male body in the basal resting state. However, this list is necessarily incomplete because not all waste products are precisely known. As previously noted, the total mass rate for waste generation reported in **Table 6** differs slightly from the total mass rate for nutrients reported in **Table 1**, which should be equal at steady state. Waste generation

---

[179] Up to 0.02 mmol/L of zinc is lost in cutaneous sweat, losing ~0.25 mg/day at 0.2 L/day; https://www.physio-pedia.com/Physiology_of_Sweat.

[173] https://www.epa.gov/sites/default/files/2014-09/documents/support_cc1_magnese_healtheffects_0.pdf.
[174] https://www.atsdr.cdc.gov/toxprofiles/tp92-c3.pdf.
[175] https://en.wikipedia.org/wiki/Chromium(III)_picolinate#Biochemistry_of_chromium(III)_picolinate.
[176] https://www.atsdr.cdc.gov/toxprofiles/tp212-c3.pdf.

[177] Sobczyńska-Malefora A, Delvin E, McCaddon A, Ahmadi KR, Harrington DJ. Vitamin B_{12} status in health and disease: a critical review. Diagnosis of deficiency and insufficiency - clinical and laboratory pitfalls. Crit Rev Clin Lab Sci. 2021 Sep;58(6):399-429; https://www.tandfonline.com/doi/full/10.1080/10408363.2021.1885339. Note that most people maintain 1-5 mg of B12 stored in their liver, a multi-year supply at the indicated excretion rate.

[178] Dietary Reference Intakes for Vitamin A, Vitamin K, Arsenic, Boron, Chromium, Copper, Iodine, Iron, Manganese, Molybdenum, Nickel, Silicon, Vanadium, and Zinc. Institute of Medicine (US) Panel on Micronutrients. Washington (DC): National Academies Press (US), 2001; https://www.ncbi.nlm.nih.gov/books/NBK222312/.

[180] This estimate includes ~0.22 mg/day for cutaneous sweat and ~0.18 mg/day for skin/hair desquamation.

[181] This estimate includes ~0.12 mg/day for cutaneous sweat,[*] ~0.13 mg/day for skin/hair desquamation, and 0.07 mg/day in pulmonary droplets.
[*] https://www.physio-pedia.com/Physiology_of_Sweat.

[182] Ingalls RL, Johnston FA. Iron from gastrointestinal sources excreted in the feces of human subjects. J Nutr. 1954 Jul 10;53(3):351-63; https://www.sciencedirect.com/science/article/abs/pii/S0022316623115938.

(**Table 6**) must equal nutrient inflow (**Table 1**) or else the equilibrium body weight would change. We can balance the molecular ledger by assuming the generation of **~17.9 gm/day** of one additional waste product which appears to have the approximate chemical formula ~$C_{19}H_{15}O_{10}$ (~403.0 gm/mole). This miscellaneous waste material, designated simply as "Miscwastium", is intended to serve as a representative composite of some unknown number of waste molecules that have not yet been identified but may be specified in future work.

What is the possible identity of these unidentified waste molecules? One study[183] found tiny amounts of hundreds of volatile organic compounds in respiratory gases exhaled from the lungs. These gases diffuse from blood into alveolar air based on partial pressure gradients, and include:

(1) **acetone** (0.1-1.5 gm/day from fat metabolism; rises with diabetes or during fasting);[184]
(2) **carbon monoxide** (~0.4 gm/day, endogenous production from heme breakdown);[185]
(3) **methanol** (0.01-0.1 gm/day, endogenous production from pectin) and **ethanol** (0.01-0.1 gm/day, endogenous fermentation in small quantities);[186]
(4) **isoprene** (17 mg/day, product of cholesterol synthesis);[187]
(5) **nitric oxide** (1-20 mg/day, a vasoregulator exhaled in trace amounts);[188]
(6) **ammonia** (0.6 mg/day from ~100 ppb alveolar, with much more originating in the oral cavity);[189] and
(7) **hydrogen** (1-5 gm/day, mostly from colonic fermentation with some exiting via the lungs).

---

[183] Filipiak W, Ruzsanyi V, Mochalski P, Filipiak A, Bajtarevic A, Ager C, Denz H, Hilbe W, Jamnig H, Hackl M, Dzien A, Amann A. Dependence of exhaled breath composition on exogenous factors, smoking habits and exposure to air pollutants. J Breath Res. 2012 Sep;6(3):036008; https://pmc.ncbi.nlm.nih.gov/articles/PMC3863686/.

[184] Filipiak W, Ruzsanyi V, Mochalski P, Filipiak A, Bajtarevic A, Ager C, Denz H, Hilbe W, Jamnig H, Hackl M, Dzien A, Amann A. Dependence of exhaled breath composition on exogenous factors, smoking habits and exposure to air pollutants. J Breath Res. 2012 Sep;6(3):036008; https://pmc.ncbi.nlm.nih.gov/articles/PMC3863686/.

[185] Ryter SW, Choi AM. Carbon monoxide in exhaled breath testing and therapeutics. J Breath Res. 2013 Mar;7(1):017111. doi: 10.1088/1752-7155/7/1/017111; https://pmc.ncbi.nlm.nih.gov/articles/PMC3651886/.

[186] Lourenço C, Turner C. Breath analysis in disease diagnosis: methodological considerations and applications. Metabolites. 2014 Jun 20;4(2):465-98; https://pmc.ncbi.nlm.nih.gov/articles/PMC4101517/.

[187] https://en.wikipedia.org/wiki/Isoprene#Human_&_other_organisms.
[188] https://en.wikipedia.org/wiki/Exhaled_nitric_oxide.

[189] Smith D, Wang T, Pysanenko A, Spanel P. A selected ion flow tube mass spectrometry study of ammonia in mouth- and nose-exhaled breath and in the oral cavity. Rapid Commun Mass Spectrom. 2008;22(6):783-9; https://pubmed.ncbi.nlm.nih.gov/18275096/.

4. Nanorobotic Recycling of Essential Nutrients

Section 4.1 describes how microscale nanofactories called Nanofabricators can synthesize molecules quickly and efficiently using the techniques of positionally-controlled atomically precise mechanosynthesis, as illustrated with a simple example (ethanol molecules). Nanofabricators can do additive or subtractive mechanosynthesis, hence may be employed to synthesize complex molecules from simple ones, or to decompose complex molecules into simpler ones. We describe how a large population of Nanofabricators, if supplied with simple molecular feedstock, can produce the nutrient molecules we need in the quantities we need. This population of Nanofabricators forms one of the major components of the metabolic organ, called the Nutrient Synthesis Unit or NSU.

Section 4.2 describes the other major component of the metabolic organ, called the Waste Recovery Unit or WRU, which is charged with acquiring waste molecules from two waste streams and then presenting these molecules to the NSU to achieve essentially closed-cycle recycling. The WRU consists of two major components: (1) the Urine Extraction Subunit or UES (Section 4.2.1), which extracts a variety of waste molecules from the urine produced by the kidneys, then processes them and ships them to the NSU for mechanosynthetic recycling into nutrients; and (2) the Blood Extraction Subunit or BES (Section 4.2.2), which is primarily charged with extracting carbon dioxide molecules from the venous blood exiting the kidneys and transporting the CO_2 to the NSU to be mechanosynthetically converted into nutrient glucose molecules, but also imports oxygen molecules from the NSU (liberated by the glucose recycling reaction) to assist in CO_2 extraction and to reoxygenate red blood cells before they reach the lungs. Section 4.2.3 describes methods of acquiring and storing small amounts of essential supplemental nutrient atoms inside the metabolic organ.

Section 4.3 presents an overall description of the metabolic organ along with several important operational issues, including device reliability and redundancy (Section 4.3.1), onboard computational requirements (Section 4.3.2), the power source for the metabolic organ (Section 4.3.3), and the estimated mass, volume, and power consumption of all major components of a baseline metabolic organ intended to supply the human body with full nutrient recycling at the basal metabolic rate of ~100 W (Section 4.3.4). Section 4.3.5 discusses thermoregulation issues that arise due to the extra heat generated by the metabolic organ, and presents workable mitigations that render the metabolic organ concept feasible. Section 4.3.6 examines possible risks to the alimentary system if the metabolic organ is employed to displace all food consumption, and general biocompatibility issues are discussed in Section 4.3.7. Section 4.3.8 examines modifications to the baseline metabolic organ that would enable it to provide nutrient recycling services up to metabolic rates of ~500 W, which is followed by brief descriptions of a few optional functions (Section 4.3.9) and applications (Section 4.3.10) that could be added to the artificial metabolic organ and its uses.

4.1 Nutrient Synthesis Unit (NSU)

Human essential nutrients are considered generic biomolecules or pure elements. Generics are found in all human bodies without regard to the unique biochemical composition of different people. All nutrient biomolecules (Section 2), ranging in size from the smallest (e.g., choline at 104 gm/mole or glucose at 180 gm/mole) to the largest (i.e., Vitamin B12, aka. cobalamin, at 1355 gm/mole), can be produced using a chemical synthesis system that employs the techniques of mechanosynthesis[190] and atomically precise molecular manufacturing.[191]

As a representative example, and as detailed in a previous publication,[192] we here provide a brief description of a hypothetical mechanosynthetic synthesis unit that could produce a representative simple organic molecule – ethyl alcohol or ethanol (C_2H_5OH; 46 gm/mole) – along with tentative estimates of the mass and productivity of the nanomachinery necessary to accomplish this. It is believed that a similar set of molecular tools and reaction sequences could be devised for most simple organic molecules of interest, including carbohydrates, amino acids, and other important biomolecules containing additional key elements such as nitrogen (N), sulfur (S), and phosphorus (P), whose study is a proper subject for future research. A nanorobotic manufacturing subsystem called a **Nutrient Synthesis Unit**, composed of trillions of generic organic chemical Nanofabricators, is described in some detail below and would serve as the principal chemical synthetic component of the artificial metabolic organ.

4.1.1 Nanorobotic Chemical Nanofabricators

A generic organic chemical **Nanofabricator** builds molecules one at a time, usually on a surface via one or more tooltips that transfer reactive moieties from a source of small simple feedstock molecules (e.g., CH_4, H_2O) or surface-bound substituents (e.g., $–CH_3$, –OH, =O, –H) to the "workpiece" (i.e., the molecule that is being built). Atomically precise fabrication involves holding feedstock atoms or molecules, and a growing nanoscale workpiece, in the proper relative positions and orientations so that when they touch they will chemically bond in the desired manner. In this process, a mechanosynthetic tool is brought up to the surface of a workpiece. One or more transfer atoms are added to, or removed from, the workpiece by the tool. Then the tool is withdrawn and recharged. This process is repeated until the workpiece is completely fabricated to molecular precision with every atom in exactly the right place. Note that the transfer atoms are under positional control at all times to prevent unwanted side reactions from

---

[190] Freitas RA Jr., Merkle RC. A minimal toolset for positional diamond mechanosynthesis. J Comput Theor Nanosci. 2008;5:760-861; http://www.molecularassembler.com/Papers/MinToolset.pdf.

[191] Drexler KE. Nanosystems: Molecular Machinery, Manufacturing, and Computation. John Wiley & Sons, New York, 1992; https://www.amazon.com/dp/0471575186/. Freitas RA Jr., Merkle RC. A Nanofactory Roadmap: Research Proposal for a Comprehensive Diamondoid Nanofactory Development Program. IMM Report No. 58, 2008/2025; http://www.imm.org/Reports/rep058.pdf.

[192] Freitas RA Jr. Cell Mills: Nanofactory Manufacture of Biological Components. IMM Report No. 53, 15 June 2024; Section 2.1.2.1, "Nanorobotic Fabrication Subunits"; http://www.imm.org/Reports/rep053.pdf.

occurring. Side reactions are also prevented using proper reaction design so that the reaction energetics include energy barriers to avoid undesired pathological intermediate structures.[193]

The mechanosynthetic fabrication of most organic molecules containing the three elements carbon (C), hydrogen (H), and oxygen (O) will generally require the ability to build and join together just five basic types of organic building blocks made from these elements, including:

(1) hydrocarbon chains, e.g., $–CH_2–CH_2–$;

(2) linear esters with a carbon chain interrupted by an oxygen atom, e.g., $–RCO_2R'–$, where R and R′ = a hydrocarbon chain;

(3) cyclic phenyl and phenylene groups, e.g., $–C_6H_4R$ and $–C_6H_3RR'$, where R and R′ = CH_3, OH, or other organic side group;

(4) cyclic lactones, e.g., $–O(C=O)(CH_2)_2(CHR)–$ or $–O(C=O)(CH_2)(CHR)(CHR')–$; and

(5) simple terminating groups, e.g., $–CH_3$, –OH, =O, –H, and –COOH.

It is asserted that any organic CHO molecule, including ethanol, can be built, atom by atom or group by group, by the sequential application of a surprisingly short list of mechanosynthetic tools. As few as 2 primary tools and 6 intermediate tool states ("•" indicates a radical site) may suffice for manufacturing ethanol and many similar organic molecules:

Primary #1: H abstraction "HAbst*" tool ($•CC–C_{10}H_{15}$) to remove an H atom;
Primary #2: Ge radical "*GeRad" tool ($•GeC_9H_{15}$) for moiety transfer with weak bonding and for abstraction tool recharge reactions;

Intermediate #1: CH_3 transfer tool ($CH_3–GeC_9H_{15}$) to acquire a CH_3 group;
Intermediate #2: CH_2 donation tool ($•CH_2–GeC_9H_{15}$) to add a CH_2 group;
Intermediate #3: CH_3CH_2 donation tool ($CH_3CH_2–GeC_9H_{15}$) to add a CH_3CH_2 group;
Intermediate #4: OH donation tool ($OH–GeC_9H_{15}$) to add an OH group;
Intermediate #5: H donation tool ($H–GeC_9H_{15}$) to add an H atom; and
Intermediate #6: spent abstraction tool "HAbst-H" ($H–CC–C_{10}H_{15}$) needing recharge.

One possible minimal toolset for building linear, planar, branching, or cyclic organic molecules containing only the elements C (black), H (white), and O (red) is shown below, with the two primary tools at left (P1, P2) and six intermediate tool states at right (I1-I6). In this example, many tooltips also include Ge (yellow) atoms at the working apex or "bridgehead" position.[194]

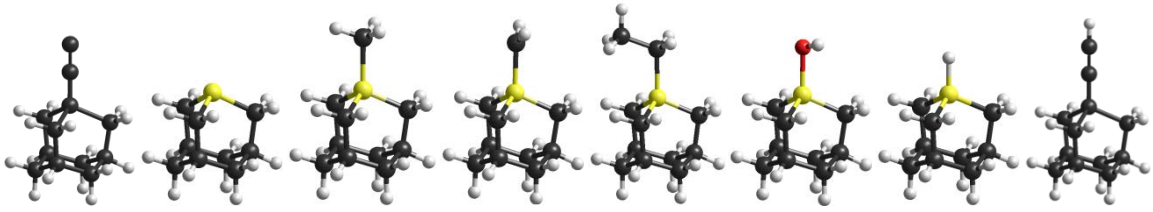

[193] Freitas RA Jr., Merkle RC. A minimal toolset for positional diamond mechanosynthesis. J Comput Theor Nanosci. 2008;5:760-861; http://www.molecularassembler.com/Papers/MinToolset.pdf.

[194] Freitas RA Jr. The Whiskey Machine: Nanofactory-Based Replication of Fine Spirits and Other Alcohol-Based Beverages. IMM Report No. 47, May 2016; http://www.imm.org/Reports/rep047.pdf.

Each of these tooltips – all built on a single adamantane cage – is attached to a larger tool handle structure (not shown) that is mounted on a reagent device that is attached, in turn, to moving conveyor belt mechanisms (images, below).[195] Note the "backing surfaces" in the mechanism illustrated at center, below – these may be used to apply large crushing forces to opposing moieties in constrained volumes to overcome reaction barriers if necessary.

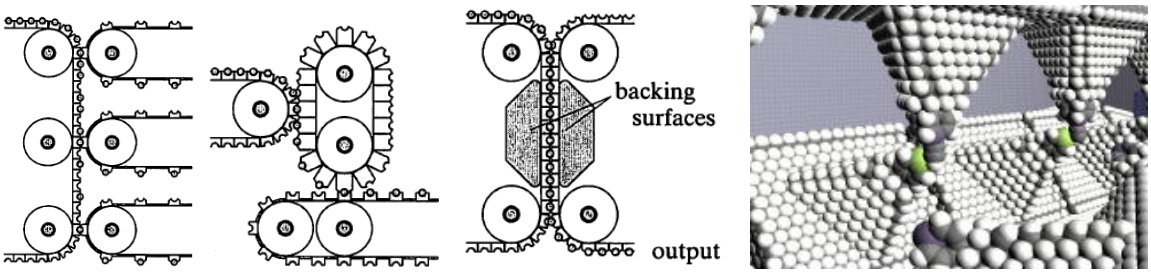

The following is a brief description of a hypothetical mechanosynthetic mill-style[196] production line that could be used to build ethanol molecules in a sealed vacuum environment, using conveyor belts to move reactive molecules at high speed and to precisely control the location and nature of the interaction between these reactive molecules. The described chemistry is believed to be plausible but has not yet been computationally or experimentally validated. Nevertheless, even if this specific set of reaction sequences and molecular tools proves flawed upon more detailed analysis, it seems highly likely that other reaction sequences and toolsets can be found that will provide a convenient path to the same result. It should be noted that the original analysis assumed all mechanosynthetic reactions would occur at liquid nitrogen (LN2) temperatures around ~77 K. Thermal motions will be (310 K / 77 K) ~ 4 times larger in a production line operated at human body temperature rather than LN2, potentially increasing the probability of mechanosynthetic misreactions and placement error, but stiffer mechanosynthetic tools can reduce thermal-driven placement error[197] and reaction pathways and processes can be selected and explicitly designed to operate sufficiently reliably in the warmer environment.

Of course, overall feasibility rests on the assumption that future developments will solve several challenging technical problems, including, most generally, constructing diamondoid machinery

---

[195] Adapted from: Drexler KE. Nanosystems: Molecular Machinery, Manufacturing, and Computation, Wiley, 1992, Figs. 13.7(b), 13.7(c), 13.7(d); https://www.amazon.com/dp/0471575186/.

[196] Drexler KE. Nanosystems: Molecular Machinery, Manufacturing, and Computation, John Wiley & Sons, New York, 1992, Section 14.4.2, "Products, building blocks, and assembly sequences"; https://www.amazon.com/dp/0471575186/.

[197] Peng J, Freitas RA Jr., Merkle RC, Von Ehr JR, Randall JN, Skidmore GD. Theoretical Analysis of Diamond Mechanosynthesis. Part III. Positional C_2 Deposition on Diamond C(110) Surface using Si/Ge/Sn-based Dimer Placement Tools. J Comput Theor Nanosci. 2006 Feb; 3:28-41; Section 3.6, "Thermal Uncertainty of Handle-Mounted Tooltips"; https://www.molecularassembler.com/Papers/JCTNPengFeb06.pdf.

with atomic precision, achieving high throughput assembly in a vacuum environment, dealing with byproduct disposal, and avoiding tip contamination or mechanosynthesis errors over trillions of cycles.

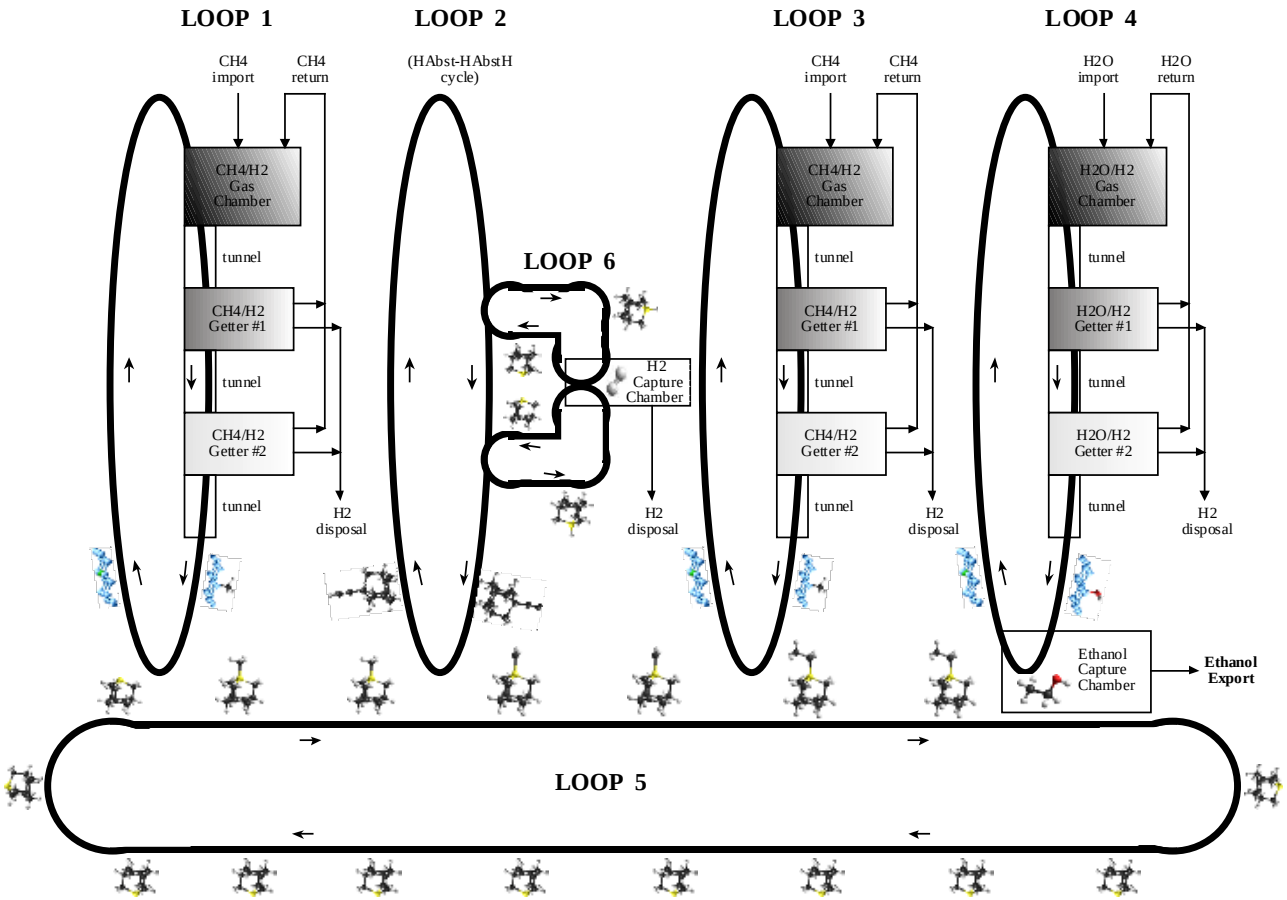

The above schematic of a hypothetical mechanosynthetic production line for ethanol molecules (black = C, white = H, yellow = Ge, red = O, blue = metal or Ge surface) has inputs of methane (CH_4) and water (H_2O) and outputs of ethanol (C_2H_5OH) and hydrogen gas (H_2).

The production line consists of six interacting continuous or stepwise-moving conveyor loops, as described below.

*** Loop 1: First methyl feedstock pickup.** A conveyor belt using carriers (image, right) having an outer coating of germanium (Ge)[198], platinum (Pt)[199], rhodium (Rh)[200], or iridium (Ir)[201] passes through a chamber containing methane gas molecules (CH_4). The coating surface strips one H off; the carrier is given enough residence time in the chamber to allow any H to migrate across the surface to

---

[198] A partially methylated germanium surface may provide a source of positionally controlled single-carbon feedstock. Such a surface can be prepared by thermal adsorption and reaction of CH_4 gas on Ge(100)[*] or by ion bombardment of clean Ge(111) at low substrate temperature (<470 K) using low-energy $\bullet CH_3$ ions, a strongly exoergic radical coupling reaction. After hydrocarbon CVD on Ge surfaces, absorption spectra indicate that bonding is mainly type sp^3 with CH, CH_2, and CH_3 bonds.[†] It may also be possible to prepare a CH_3-decorated Ge surface via conventional solution-phase chemical methylation,[‡] since methylated germanium is found in the natural environment.

[*] Murota J, Sakuraba M, Takehiro S. Atomically controlled processing for future Si-based devices. 2004 IEEE Workshop on Microelectronics and Electron Devices, Boise, ID, USA, 2004, pp. 31-34; https://ieeexplore.ieee.org/abstract/document/1297343.

[†] Franks J. Preparation and properties of diamondlike carbon films. J Vac Sci Technol A. 1989;7:2307; https://avs.scitation.org/doi/abs/10.1116/1.575933.

[‡] Sundermeyer W, Verbeek W. A Method for the Preparation of Methylmetal Compounds. Angew Chemie Intl Ed Engl. 1966 Jan;5(1):1-6; https://onlinelibrary.wiley.com/doi/abs/10.1002/anie.196600011; Mayer HP, Rapsomanikis S. Chemical methylation of germanium(II) in model aqueous solutions. Appl Organomet Chem. 1992 Apr;6(2):173-178; https://onlinelibrary.wiley.com/doi/abs/10.1002/aoc.590060210; Buriak JM. Organometallic chemistry on silicon and germanium surfaces. Chem Rev. 2002 May;102(5):1271-1308; http://www.gfmoorelab.com/uploads/4/2/3/1/42315775/buriak_chem_rev_2002.pdf.

[199] Methane impinging on Pt(111) causes methyl to adsorb at 120 K.[*] On Pt(111) surface, the dissociative chemisorption of methane to CH_3 and H is downhill by 6.5 kcal/mole. Breaking the second C-H bond to form CH_2 adsorbed on the surface is 1.2 kcal/mole uphill; forming CH adsorbed is then downhill by 21.7 kcal/mole.[†]

[*] Papp C, Trankenschuh B, Streber R, Fuhrmann T, Denecke R, Steinruck HP. Influence of steps on the adsorption of methane on platinum surfaces. J Phys Chem C. 2007 Jan 18;111(5):2177-2184; https://pubs.acs.org/doi/abs/10.1021/jp066268f.

[†] Kua J, Goddard WA III. Chemisorption of Organics on Platinum. 2. Chemisorption of C_2H_x and CH_x on Pt(111). J Phys Chem B 1998 Nov 3;102(47):9492-9500; http://www.wag.caltech.edu/publications/sup/pdf/394.pdf.

[200] Methane adsorbs dissociatively to the Rh(111) surface.[*]

[*] Mavrikakis M, Rempel J, Greeley J, Hansen LB, Norskov JK. Atomic and molecular adsorption on Rh(111). J Chem Phys. 2002 Oct 8;117(14):6737-6744; https://core.ac.uk/download/pdf/13727515.pdf.

[201] Methane dissociatively adsorbs on Ir(111) surface.[*] It may be possible to start with ethylene which deposits on Ir surface as ethylidyne (C-CH_3) at 300 K. Abstraction of the CH_3 by GeRad may be possible because the C-C bond is apparently weak – the hydrocarbon decomposes at 500 K leaving only a C layer on the surface.[†]

[*] e.g., Henkelman G, Jónsson H. Theoretical Calculations of Dissociative Adsorption of CH_4 on an Ir(111) Surface. Phys Rev Lett. 2001 Jan 22;86(4):664-7; http://www.henkelmanlab.org/pubs/henkelman01_664.pdf.

[†] Kostov KL, Marinova TS. Ethylene adsorption on a clear iridium surface. Reaction Kinetics Catalysis Lett. 1986 Mar;32:141-146; https://link.springer.com/article/10.1007/BF02063463.

recombine with another H on the surface, then to leave the surface as H_2 gas while remaining trapped in the chamber. This leaves a CH_3 bound to the Loop 1 carrier surface. The Loop 1 carriers then traverse a series of tunnels tight enough to prevent most stray CH_4 or H_2 molecules from following the carriers through the tunnel. At intervals the tunnels open up into small getter chambers equipped with sorting rotors[202] having binding sites for CH_4 and H_2 to collect and remove any of these molecules that happen to slip through.

Cleared of any bound molecules other than the desired CH_3, the conveyor belt finally emerges into a vacuum where each carrier is brought into firm contact with carriers from another conveyor belt (Loop 5) whose carriers protrude a •GeRad tool. The CH_3 group hops from the Loop 1 carrier onto the •GeRad tool because this transfer is favored energetically, making a CH_3-GeRad intermediate on the Loop 5 carriers. The empty Ge-, Pt-, Rh- or Ir-coated carriers are returned to the starting point, re-entering the methane chamber ready for the next cycle without further processing.

*** Loop 2: Hydrogen abstraction from first methyl.** Each carrier that is attached to the Loop 2 conveyor belt protrudes an HAbst• tool and operates entirely in vacuum. The Loop 2 carriers are brought into firm contact with a CH_3 bound to a CH_3-GeRad intermediate in Loop 5, abstracting one of the H atoms from the bound CH_3 and leaving a •CH_2-GeRad intermediate bound to the carrier of System 5. The spent (hydrogenated) HAbst-H intermediates on the carriers of Loop 2 are brought into contact with a recharge subsystem (Loop 6) whereupon the excess H is removed and disposed of, after which the reclaimed and reactivated HAbst• tools resume the next cycle of Loop 2 operation without further processing.

*** Loop 3: Second methyl feedstock pickup.** This conveyor belt system is exactly the same as Loop 1, and runs parallel to and in synchrony with it. Once the second -CH_3 group has been transferred (see Loop 5), the empty carriers are returned to the starting point, ready for the next cycle without further processing.

*** Loop 4: Hydroxyl feedstock pickup.** The Loop 4 conveyor belt system is almost the same as Loop 1, except that the feedstock attached to the carriers is an -OH group rather than a -CH_3 group (image, right). The bulk input is a chamber containing water (H_2O), which, like the methane, has had one H dissociatively removed, yielding in this case a migrating H and an –OH group bound to the carrier.[203] Once the -OH group has been transferred, the empty carriers are returned to the starting point ready for the next cycle without further processing.

---

[202] Drexler KE. Nanosystems: Molecular Machinery, Manufacturing, and Computation, John Wiley & Sons, New York, 1992, Section 13.2.1(a) “Modulated receptors for selective transport: Basic concepts”; https://www.amazon.com/dp/0471575186/. Freitas RA Jr. Nanomedicine, Volume I: Basic Capabilities, Landes Bioscience, Georgetown, TX, 1999; Section 3.4.2, “Sorting Rotors”; http://www.nanomedicine.com/NMI/3.4.2.htm.

[203] A Cu(110) surface catalyzes water dissociation into H and OH under ambient conditions, and autocatalytic water dissociation is believed to be a general phenomenon on metal surfaces.[*] An $(IrO_2)_n$ (n=1-5) cluster when exposed to one H_2O molecule with 15.1 kcal/mole energy added can be driven uphill to form $IrO_2.H_2O$, which then exoergically transforms to $IrO(OH)_2$ which is downhill by -17.9 kcal/mole.[†] Oxygen-assisted water dissociation reaction (OWD: $H_2O + O \rightarrow 2OH$), based on a tunnel mechanism of H

*** Loop 5: Build ethanol from two methyl groups and one hydroxyl group, then release.** Note that this is the previously-mentioned vacuum-residing conveyor belt system whose carriers initially protrude a •GeRad tool. A molecule of ethanol is assembled on each carrier as the Loop 5 belt encounters, in sequence, carriers from Loop 1, Loop 2, Loop 3, and Loop 4.

Encounter with Loop 1: When brought into contact with a Loop 1 carrier, a CH_3 group transfers from that carrier onto the Loop 5 •GeRad tool, making a CH_3-GeRad intermediate on the Loop 5 carrier. The empty Loop 1 carrier is returned to the starting point, ready for the next cycle without further processing.

Encounter with Loop 2: The CH_3-GeRad intermediate on the Loop 5 carrier is next brought into contact with an HAbst• tool on a Loop 2 carrier, which abstracts one of the H atoms from the bound CH_3 group, leaving a •CH_2-GeRad intermediate on the Loop 5 carrier.

Encounter with Loop 3: The •CH_2-GeRad intermediate on the Loop 5 carrier is next brought into contact with a Loop 3 carrier, whereupon a snap-on reaction occurs because there is an energetic preference for the CH_3 group on the Loop 3 carrier to be bonded to the C atom of the •CH_2-GeRad intermediate on the Loop 5 carrier rather than to the Ge or metal atom holding the CH_3 group onto the Loop 3 carrier. This leaves a CH_3CH_2-GeRad intermediate on the Loop 5 carrier. The empty Loop 3 carrier is returned to the starting point, ready for the next cycle without further processing.

Encounter with Loop 4: The CH_3CH_2–GeRad intermediate on the Loop 5 carrier is then pressed into contact with the OH-metal intermediate on the Loop 4 carrier inside an **ethanol collection chamber**. The hydroxyl group should have some energetic preference to be bonded to the Ge-bonded C atom of the CH_3CH_2–GeRad intermediate rather than to the metal atom holding the OH- group on the Loop 4 carrier,[204] so a metal-Ge bond may form as the -OH group inserts

---

transfer, has activation energies much lower than those of water dissociation on clean metal (Pt, Cu, Ni, Rh) surfaces.[‡] OH groups rest stably on the Rh(111) surface with the H pointing away from the surface.[**]

[*] Andersson K, Ketteler G, Bluhm H, Yamamoto S, Ogasawara H, Pettersson LGM, Salmeron M, Nilsson A. Autocatalytic water dissociation on Cu(110) at near ambient conditions. J Am Chem Soc. 2008 Mar 5;130(9):2793-2797; https://escholarship.org/content/qt0zc1q9rv/qt0zc1q9rv.pdf.

[†] Zhou X, Yang J, Li C. Theoretical study of structure, stability, and the hydrolysis reactions of small iridium oxide nanoclusters. J Phys Chem A. 2012 Oct 11;116(40):9985-9995; https://pubmed.ncbi.nlm.nih.gov/22985267/.

[‡] German ED, Sheintuch M. Oxygen-Assisted Water Dissociation on Metal Surfaces: Kinetics and Quantum Effects. J Phys Chem C. 2011 Apr 29;115(20):10063-10072; https://pubs.acs.org/doi/abs/10.1021/jp200457h.

[**] Mavrikakis M, Rempel J, Greeley J, Hansen LB, Norskov JK. Atomic and molecular adsorption on Rh(111). J Chem Phys. 2002 Oct 8;117(14):6737-6744; https://core.ac.uk/download/pdf/13727515.pdf.

[204] Since metal-oxygen and metal-germanium bond energy data were not readily available, we assumed for the purposes of this calculation that the OH group on Loop 4 is bonded to a GeRad. In this case, the reaction could be plausibly estimated to be exoergic because we are breaking one C-Ge bond (2.47 eV) and one (Loop 4) Ge-O bond (2.81 eV), total +5.28 eV, while creating one (Loop 4-Loop 5) Ge-Ge bond (1.95 eV) and one C-O bond (3.71 eV), total -5.66 eV, therefore the reaction appears energetically favored by **-0.38 eV**. However, this reaction has not been validated using quantum chemistry simulations. Sources:

into the Ge-C bond on the CH_3CH_2–GeRad intermediate on the Loop 5 carrier, creating a CH_3-CH_2-OH molecule of ethanol that is released into the ethanol collection chamber. The Loop 4 and Loop 5 carriers are then pulled apart, breaking the temporary bond between them. This leaves an empty carrier on Loop 4 and a •GeRad tool on Loop 5, both of which are returned to the starting point in their respective loops, ready for the next cycle without further processing.

*** Loop 6: HAbst-H tool recharge.** The recharge subsystem required for Loop 2 may involve two identical tracks and two pairs of specially configured •GeRad tools. In each pair, the first •GeRad tool alternately bonds and unbonds to the distal C atom of the ethynyl C_2 group on an HAbst-H intermediary on Loop 2, a process that can cycle endlessly. The second •GeRad tool of the pair approaches the excess H atom on the HAbst-H intermediary and abstracts it, making an H-GeRad intermediary on a Loop 6 carrier and restoring the active HAbst• tool on a Loop 2 carrier. The second pair of •GeRad tools performs the same operations on a second HAbst-H intermediary on Loop 2. The two H-GeRad intermediaries are then brought into forcible contact while parked inside a separate hydrogen capture chamber, creating a Ge-Ge bond between the two tools and releasing an H_2 gas molecule into the chamber which can be safely exhausted from the system. The two Loop 6 tools are then pulled apart, removed from the H_2 capture chamber, and returned to the starting point ready for the next recharge cycle without further processing. Alternatively, the H-GeRad intermediaries could be re-routed to a reaction sequence for building some molecule other than ethanol in which a hydrogen donation was required.

A similar process may be applied to build any CHO molecule of known structure and elemental composition. Many reaction sequences can be determined in advance and can be hard-coded. Production lines could use switchyards (image, left) to route carriers from one Loop to another Loop on the fly, essentially creating a reprogrammable production network. But in order to be able to handle any known molecule that is composed only of C, H, and O atoms and one or more of the five basic types of organic building blocks mentioned earlier, we will also need automated mechanosynthetic sequence generation to minimize or eliminate the human labor requirement. This seems achievable with future research, given the relative structural simplicity of the molecular targets and the relatively small number of primary tools and core reactions that are likely to be needed (i.e., a relatively small "chemical alphabet" is required) to build organic molecules mechanosynthetically, functional group by functional group. Adding a few more elements such as nitrogen, sulfur, and phosphorus would raise the complexity level and increase the tooltype count – but probably tolerably so, while greatly extending the scope of manufacturable molecules to the full range of biologicals including amino acids, peptides, nucleotides, proteins and DNA.

The energy cost of concentration of compressing mechanosynthetically fabricated molecules into each collection chamber at the intersection of Loops 4 and 5 should be largely recovered when the molecules are later removed for distribution into the human bloodstream.

---

http://www.wiredchemist.com/chemistry/data/bond_energies_lengths.html and Jan Felix Binder, *Electronic and Structural Properties of the Ge/GeO2 Interface through Hybrid Functionals*, PhD Thesis, École Polytechnique Fédérale de Lausanne, 2012, p.30 and Fig. 3.9/p.37 (for estimate of Ge-O bond strength); http://infoscience.epfl.ch/record/176949/files/EPFL_TH5363.pdf.

4.1.2 Quantitative Productivity of Nutrient Synthesis Unit

The 6-loop schema described above appears to fabricate individual molecules of ethanol fairly efficiently using only methane and water as the bulk inputs and generating hydrogen gas as the only waste product. Assuming that each conveyor belt/roller mechanism requires ~1 million carbon atoms,[205] then six of these, along with infrastructure support including ~1 million atoms for the sorting rotor (Section 4.2.1) "getters" plus 5 million atoms for each of 11 chamber/getter boxes with tunnels and equipment housings, sums to 62 million carbon atoms. Adding in motors, controllers, and other hardware, each mechanosynthetic Nanofabricator incorporates perhaps $n_{C\text{-}FS} \sim 100$ million carbon atoms of total mass $M_{FS} = m_C\ n_{C\text{-}FS} = 2 \times 10^{-18}$ kg (for $m_C = 2 \times 10^{-26}$ kg/C atom). Each Nanofabricator may occupy a $(100\ nm)^3$ cube having a volume $V_{FS} \sim 0.001$ micron^3, with about half of this volume occupied by machinery and the rest by empty space (vacuum).

While mechanosynthetic production lines are thought to be operable at MHz frequencies,[206] to keep power consumption low we assume in the present example that each Nanofabricator will be operated at a frequency of only $\nu_{FS} = 0.1$ MHz. This produces $r_{organics} = 10^5$ molecules/sec of organic (ethanol) molecules, representing a production rate of $R_{FS} = r_{organics}\ MW_{organics} / N_A = 7.6 \times 10^{-21}$ kg/sec of ethanol per Nanofabricator, taking molecular weight as $MW_{organics} \sim MW_{ethanol} = 46$ gm/mole, with Avogadro's number $N_A = 6.022 \times 10^{23}$ molecules/mole. Similar production rates should be achievable for other organic molecules in the 100-200 gm/mole size range[207] by adding a few more fabrication loops to Nanofabricator production lines of a size and complexity roughly proportional to the molecular weight of the target molecule.

Table 8 lists all nutrient molecules and ions that must be produced by the **Nutrient Synthesis Unit**, with a complete atom count in **Table 9**. For scaling purposes, we assume that the generic organic Nanofabricators comprising the Nutrient Synthesis Unit must synthesize near-absolute purity organic molecules similar to or slightly larger than ethanol at a target production rate of $R_{NSU} = N_{FS}\ R_{FS} = 6.77 \times 10^{-6}$ kg/sec, comprising 400 gm/day of glucose, 100 gm/day of amino acids, 74.2 gm/day of lipids and 10.8 gm/day of micronutrients, totaling 585 gm/day. This requires $N_{FS} = R_{NSU} / R_{FS} \sim 890$ trillion Nanofabricators having a very modest total volume of $V_{NSU} = N_{FS}\ V_{FS} \sim$ **0.9 cm^3** and mass $M_{NSU} = N_{FS}\ M_{FS} \sim$ **1.8 gm**. The atoms and small molecules that may serve as appropriate feedstock for the Nutrient Synthesis Unit will be provided in the requisite types and amounts by the Waste Recovery Unit, as described in Section 4.2.

---

[205] Drexler KE. Nanosystems: Molecular Machinery, Manufacturing, and Computation, John Wiley & Sons, New York, 1992, Section 13.3.5; https://www.amazon.com/dp/0471575186/.

[206] Drexler KE. Nanosystems: Molecular Machinery, Manufacturing, and Computation, John Wiley & Sons, New York, 1992, Table 14.4; https://www.amazon.com/dp/0471575186/.

[207] The mass-weighted average molecular weight of all daily solid nutrients listed in **Table 8** is (585.1 gm) (6.022 x 10^{23} molecules/mole) / (2.17 x 10^{24} molecules) ~ 162 gm/mole, only a few times larger than the 46 gm/mole molecular weight of ethanol.

Table 8. Estimated synthesis requirements for the Nutrient Synthesis Unit, for a 70 kg male human body at the ~100 watt basal metabolic rate

Molecule or Ion	Formula	gm/day	gm/mole	molecules/day
Glucose	$C_6H_{12}O_6$	400	180	1.34×10^{24}
Alanine	$C_3H_7NO_2$	8.40	89.1	5.68×10^{22}
Arginine	$C_6H_{14}N_4O_2$	9.20	174.2	3.18×10^{22}
Aspartate	$C_4H_7NO_4$	15.05	133.1	6.81×10^{22}
Cysteine	$C_3H_7NO_2S$	0.64	121.2	3.19×10^{21}
Glutamate	$C_5H_9NO_4$	19.10	147.1	7.82×10^{22}
Glycine	$C_2H_5NO_2$	5.00	75.1	4.01×10^{22}
Histidine	$C_6H_9N_3O_2$	1.70	155.2	6.60×10^{21}
Isoleucine	$C_6H_{13}NO_2$	2.30	131.2	1.06×10^{22}
Leucine	$C_6H_{13}NO_2$	5.20	131.2	2.39×10^{22}
Lysine	$C_6H_{14}N_2O_2$	4.70	146.2	1.94×10^{22}
Methionine	$C_5H_{11}NO_2S$	1.66	149.2	6.69×10^{21}
Phenylalanine	$C_9H_{11}NO_2$	2.34	165.2	8.52×10^{21}
Proline	$C_5H_9NO_2$	6.30	115.1	3.30×10^{22}
Serine	$C_3H_7NO_3$	10.75	105.1	6.16×10^{22}
Threonine	$C_4H_9NO_3$	2.40	119.1	1.21×10^{22}
Tryptophan	$C_{11}H_{12}N_2O_2$	0.60	204.2	1.77×10^{21}
Tyrosine	$C_9H_{11}NO_3$	1.76	181.2	5.86×10^{21}
Valine	$C_5H_{11}NO_2$	2.90	117.2	1.49×10^{22}
linoleic acid	$C_{18}H_{32}O_2$	37.1	278.4	8.03×10^{22}
oleic acid	$C_{18}H_{34}O_2$	17.5	282.5	3.73×10^{22}
palmitic acid	$C_{16}H_{32}O_2$	7.0	256.4	1.64×10^{22}
α-linolenic acid	$C_{18}H_{30}O_2$	5.6	280.5	1.20×10^{22}
stearic acid	$C_{18}H_{36}O_2$	2.8	284.5	5.93×10^{21}
phosphatidylcholine	$C_{44}H_{84}NO_8P$	2.97	776	2.30×10^{21}
phosphatidylethanolamine	$C_{41}H_{78}NO_8P$	0.77	768.1	6.04×10^{20}
lysophosphatidylcholine	$C_{10}H_{22}NO_7P$	0.14	299.3	2.82×10^{20}
sphingomyelin	$C_{49}H_{97}N_2O_6P$	0.1	829.3	7.26×10^{19}
lysophosphatidylethanolamine	$C_{23}H_{46}NO_7P$	0.05	479.6	6.28×10^{19}
phosphatidylinositol	$C_{47}H_{83}O_{13}P$	0.17	886.6	1.15×10^{20}
NaOH (for alkaline buffer)	NaOH	0.03	40	4.52×10^{20}
Potassium	K^+	3.4	39.1	5.24×10^{22}
Chloride	Cl^-	2.3	35.5	3.90×10^{22}
Sodium	Na^+	2.3	23	6.02×10^{22}
Calcium	Ca^{2+}	1	40.1	1.50×10^{22}
Phosphorus	equiv. P	0.7	31	1.36×10^{22}
Choline	$C_5H_{14}NO$	0.55	104.2	3.18×10^{21}
Magnesium	Mg^{2+}	0.42	24.3	1.04×10^{22}
Vit. C (ascorbate)	$C_6H_8O_6$	0.09	176.1	3.08×10^{20}
Vit. B3 (niacin)	$C_6H_5NO_2$	0.016	123.1	7.83×10^{19}
Vit. E (α-tocopherol)	$C_{29}H_{50}O_2$	0.015	430.7	2.10×10^{19}
Zinc	Zn^{2+}	0.011	65.4	1.01×10^{20}
Iron	Fe^{3+}	0.001	55.8	1.08×10^{19}
Vit. B5 (pantothenic acid)	$C_9H_{17}NO_5$	0.005	219.2	1.37×10^{19}
Manganese	Mn^{3+}	0.0023	54.9	2.52×10^{19}

Vit. B2 (riboflavin)	$C_{17}H_{20}N_4O_6$	0.0013	376.4	2.08×10^{18}
Vit. B6 (pyridoxine)	$C_8H_{11}NO_3$	0.0013	169.2	4.63×10^{18}
Vit. B1 (thiamin)	$C_{12}H_{17}N_4OS^+$	0.0012	265.4	2.72×10^{18}
Copper	Cu^{2+}	0.0009	63.5	8.54×10^{18}
Vit. A	$C_{20}H_{30}O$	0.0009	286.5	1.89×10^{18}
Vit. B9 (folate)	$C_{19}H_{19}N_7O_6$	0.0004	441.4	5.46×10^{17}
Vit. K	$C_{31}H_{46}O_2$	0.00012	450.7	1.60×10^{17}
Iodine	I^-	0.00015	126.9	7.12×10^{17}
Selenium	equiv. Se	0.000055	79	4.19×10^{17}
Chromium	Cr^{3+}	0.000035	52	4.05×10^{17}
Molybdenum	equiv. Mo	0.000045	95.9	2.83×10^{17}
Vit. B7 (biotin)	$C_{10}H_{16}N_2O_3S$	0.00003	244.3	7.40×10^{16}
Vit. D (cholecalciferol)	$C_{27}H_{44}O$	0.000015	384.6	2.35×10^{16}
Vit. B12 (cobalamin)	$C_{63}H_{88}CoN_{14}O_{14}P$	0.0000024	1355.4	1.07×10^{15}
Subtotals or *(average)*		585.1	(162.4)	2.17×10^{24}
Molecular oxygen	O_2	719	32.0	1.35×10^{25}
Totals or *(average)*		**1304.1**	*(50.0)*	**1.57×10^{25}**

Table 9. Total atom numbers and grams per day for all elements processed by the Nutrient Synthesis Unit

Chemical Element	Total Atoms (atoms/day)	Process Rate (gm/day)	Chemical Element	Total Atoms (atoms/day)	Process Rate (gm/day)
C	1.30×10^{25}	259.48	Zn	1.01×10^{20}	0.01100
H	2.56×10^{25}	42.49	Fe	1.08×10^{19}	0.00100
N	6.19×10^{23}	14.40	Mn	2.52×10^{19}	0.00230
O	2.32×10^{25}	976.85	Cu	8.54×10^{18}	0.00090
S	9.89×10^{21}	0.53	I	7.12×10^{17}	0.00015
K	5.24×10^{22}	3.40	Se	4.19×10^{17}	0.00006
Cl	3.90×10^{22}	2.30	Cr	4.05×10^{17}	0.00004
Na	6.07×10^{22}	2.32	Mo	2.83×10^{17}	0.00005
Ca	1.50×10^{22}	1.00	Co	1.07×10^{15}	0.0000001
P	1.70×10^{22}	0.877			
Mg	1.04×10^{22}	0.42	**Totals**	**7.62×10^{25}**	**1304.1**

To estimate the power consumption for nutrient synthesis via mechanosynthesis within the Nutrient Synthesis Unit, we start with the energy needed to produce nutrient glucose which can be mechanochemically synthesized via the following process:

$$6\ CO_2(g) + 6\ H_2O(l) + 4658\ zJ \rightarrow C_6H_{12}O_6(s) + 6\ O_2(g)$$

where the energy required to drive the reaction forward is $E_{glucose} = 6\ \Delta H_f\ (CO_2) + 6\ \Delta H_f\ (H_2O) - \Delta H_f\ (C_6H_{12}O_6) - \Delta H_f\ (O_2) = 4658$ zJ/molecule of glucose synthesized, taking the standard enthalpies of formation as $\Delta H_f\ (CO_2) = -653.5$ zJ/molecule, $\Delta H_f\ (H_2O) = -474.6$ zJ/molecule, $\Delta H_f\ (C_6H_{12}O_6) = -2110.6$ zJ/molecule, and $\Delta H_f\ (O_2) = 0$ zJ/molecule.[208]

For amino acids, **Table 10** shows the energy requirements for mechanosynthesizing a representative set of amino acids by combining CO_2, H_2O, and urea (CH_4N_2O) as the principal nitrogen source. The mass-requirement-weighted "average" of the 18 amino acids listed in **Table 8** would have a chemical formula of $C_{5.4}H_{9.9}N_{1.4}O_{2.4}$ (~132.7 gm/mole) and inferentially an average energy requirement of $E_{AminoAcid}$ ~ 4500 zJ/molecule of amino acid synthesized.

Table 10. Exemplar energy requirements for synthesizing amino acid molecules, using standard enthalpies of formation

Amino Acid	gm/mole	Posited Mechanosynthetic Reaction	zJ/molecule
Glycine	75.1	$1.5CO_2 + 1.5H_2O + 0.5CH_4N_2O \rightarrow C_2H_5NO_2 + 1.5O_2$	1092
Proline	115.1	$4.5CO_2 + 3.5H_2O + 0.5CH_4N_2O \rightarrow C_5H_9NO_2 + 5.5O_2$	3940
Valine	117.2	$4.5CO_2 + 4.5H_2O + 0.5CH_4N_2O \rightarrow C_5H_{11}NO_2 + 6.0O_2$	4350
Tyrosine	181.2	$8.5CO_2 + 4.5H_2O + 0.5CH_4N_2O \rightarrow C_9H_{11}NO_3 + 9.5O_2$	6828
"Average"	~132.7	$(\sim C_{5.4}H_{9.9}N_{1.4}O_{2.4})$	~4500

All the major lipids listed in **Table 8** are similar in molecular weight but the largest by mass requirement is linoleic acid ($C_{18}H_{32}O_2$, 278.4 gm/mole, 37.1 gm/day, $\Delta H_f = -634.7$ kJ/mole),[209] which could be mechanosynthesized using only CO_2 and H_2O according to the chemical reaction: $18\ CO_2 + 16\ H_2O + 18{,}300\ zJ \rightarrow C_{18}H_{32}O_2 + 25\ O_2$, which suggests using E_{lipid} ~ 18,300 zJ/molecule of lipid synthesized.

Using the molecules/day requirements from **Table 8**, the minimum power requirement for all nutrient synthesis, ignoring the micronutrients, is $P_{nutrients} \sim N_{glu}\ E_{glucose} + N_{AA}\ E_{AminoAcid} + N_{lip}\ E_{lipid} = 130$ watts, taking $N_{glu} = 1.34 \times 10^{24}$ glucose molecules/day, $N_{AA} = 4.83 \times 10^{23}$ amino acid

---

[208] https://en.wikipedia.org/wiki/Standard_enthalpy_of_formation.

[209] "9,12-Octadecadienoic acid (Z,Z)-", NIST Chemistry WebBook, SRD 69; https://webbook.nist.gov/cgi/cbook.cgi?ID=C60333&Mask=2.

molecules/day, and N_{lip} = 1.55 x 10^{23} lipid molecules/day. Assuming an aggressively high energy efficiency of chemical processing via mechanosynthesis of ε_{MS} ~ 80%,[210] as might be appropriate for a mill-style[211] production line, then the power requirement for synthesizing all the nutrients is $P_{NSU} \sim P_{nutrients} / \varepsilon_{MS}$ = **162 watts**.

Note that in all mechanosynthetic reactions listed above, pure oxygen (O_2) is produced as the sole nutrient byproduct and can be withdrawn in pure form and passed to the Blood Extraction Subunit (Section 4.2.2) to enable CO_2 extraction and re-oxygenation of renal venous blood, without that blood having to pass through the lungs for reoxygenation in the natural manner. Since most oxygen is being recycled, this implies that the user should be able to survive for extended periods of time while breathing extremely oxygen-poor air (e.g., 1% O_2 content or less).

4.1.3 Comparison to Biological Human Liver

It is of interest to compare the performance of the Nutrient Synthesis Unit described above to the performance of the human liver,[212] which is the natural biological organ most directly responsible for synthesizing carbohydrates, proteins, and lipids in the human body. For a 70 kg male human, a 1.5 kg liver includes M_{hepato} ~ 1.2 kg of hepatocytes[213] of volume V_{hepato} ~ 1.14 L,[214] the main synthetic cells actively performing carbohydrate, protein, and lipid synthesis. The daily synthetic output consists of ~200 gm/day (range 180-220 gm/day) of glucose via gluconeogenesis and glycogenolysis),[215] total *de novo* protein synthesis of ~52 gm/day[216] (of which serum albumin accounts for 12-15 gm/day,[217] plus 2-4 gm/day for fibrinogen, a major clotting factor), and ~80

---

[210] For comparison, in eukaryotic aerobic respiration the yield is 30-32 ATP molecules per molecule of glucose,[*] the energy content of 1 ATP hydrolysis (ΔG under physiological conditions) is ~57 kJ/mole or 94.7 zJ/molecule,[†] and the energy content of complete glucose oxidation is 4658 zJ/molecule, so the energy efficiency of ATP synthesis inside cells is (30-32) (94.7)/(4658) ~ 61-65%.
[*] https://en.wikipedia.org/wiki/Cellular_respiration#Efficiency_of_ATP_production.
[†] https://en.wikipedia.org/wiki/Adenosine_triphosphate#Reactive_aspects.

[211] Drexler KE. Nanosystems: Molecular Machinery, Manufacturing, and Computation, John Wiley & Sons, New York, 1992, Section 14.4.2, "Products, building blocks, and assembly sequences"; https://www.amazon.com/dp/0471575186/.

[212] https://en.wikipedia.org/wiki/Liver#Metabolism.
[213] https://en.wikipedia.org/wiki/Hepatocyte.

[214] Overmoyer BA, McLaren CE, Brittenham GM. Uniformity of liver density and nonheme (storage) iron distribution. Arch Pathol Lab Med. 1987 Jun;111(6):549-54; https://pubmed.ncbi.nlm.nih.gov/3579513/.

[215] https://www.sciencedirect.com/topics/biochemistry-genetics-and-molecular-biology/glycogen-liver-level.

[216] Barle H, Nyberg B, Essén P, Andersson K, McNurlan MA, Wernerman J, Garlick PJ. The synthesis rates of total liver protein and plasma albumin determined simultaneously in vivo in humans. Hepatology. 1997 Jan;25(1):154-8; https://aasldpubs.onlinelibrary.wiley.com/doi/pdf/10.1002/hep.510250128.

[217] Moman RN, Gupta N, Varacallo MA. Physiology, Albumin. StatPearls [Internet], 26 Dec 2022; https://www.ncbi.nlm.nih.gov/books/NBK459198/.

gm/day of total VLDL-triglyceride secretion[218] from both endogenous and remnant-derived fatty acids, but of which only ~8 gm/day is derived from *de novo* lipogenesis,[219] for a total *de novo* product output of $\mathbf{m_{synthL} \sim 260\ gm/day}$. The energy expenditure to perform these synthetic tasks can be estimated using the standard biochemical costs, e.g., ~57 kJ/mol ATP,[220] gluconeogenesis ~6 ATP/glucose molecule, protein polymerization ~4 ATP/amino acid, and palmitate synthesis ~7 ATP + 14 NADPH (~220 kJ/mole for NADPH),[221] as summarized in **Table 11** below, giving a total energy expenditure of P_{synthL} ~ 6.9 W (~596 kJ/day) for *de novo* chemical synthesis in the liver.

Table 11. Liver energy expenditure for *de novo* synthetic tasks for a 70 kg male human body at the ~100 watt basal metabolic rate

Synthetic Process	Quantity per Day	Energy Cost per Unit	Daily Energy	Power Equivalent
Gluconeogenesis	1.11 mole glucose (200 gm)	6 ATP x 57 kJ/mole = 342 kJ/mole	380 kJ/day	4.4 W
Protein synthesis	0.473 mole amino acids	4 ATP x 57 kJ/mole = 228 kJ/mole	108 kJ/day	1.25 W
De novo lipogenesis	0.031 mole palmitate (8 gm)	7 ATP x 57 kJ/mole + 14 NADPH x 220 kJ/mole = 3479 kJ/mole	108 kJ/day	1.25 W
Total (P_{synthL})			**596 kJ/day**	**6.9 W**

Of course, liver hepatocytes are also responsible for non-synthetic tasks such as the breakdown[222] of hormones and peptides, conjugation of bilirubin for excretion in bile, ammonia disposal (via urea cycle enzymes in mitochondria and cytosol), and detoxification and elimination of other

---

[218] Sørensen LP, Andersen IR, Søndergaard E, Gormsen LC, Schmitz O, Christiansen JS, Nielsen S. Basal and insulin mediated VLDL-triglyceride kinetics in type 2 diabetic men. Diabetes. 2011 Jan;60(1):88-96; https://pmc.ncbi.nlm.nih.gov/articles/PMC3012201/pdf.

[219] Rosqvist F, McNeil CA, Pramfalk C, Parry SA, Low WS, Cornfield T, Fielding BA, Hodson L. Fasting hepatic de novo lipogenesis is not reliably assessed using circulating fatty acid markers. Am J Clin Nutr. 2019 Feb 1;109(2):260-268; https://pmc.ncbi.nlm.nih.gov/articles/PMC6367991/pdf.

[220] https://en.wikipedia.org/wiki/Adenosine_triphosphate#Reactive_aspects.

[221] Manoj KM, Manekkathodi A. Light's interaction with pigments in chloroplasts: The murburn perspective. J Photochem Photobiol. 2021 Mar; 5:100015; https://www.sciencedirect.com/science/article/pii/S2666469020300154.

[222] https://en.wikipedia.org/wiki/Liver#Breakdown.

waste products.[223] The liver draws P_{liver} ~ 17 W (~17%) of basal metabolic energy,[224] so the power demand for all non-synthetic tasks is $P_{nonsynthL} \sim P_{liver} - P_{synthL}$ = 10.1 W. From this we can crudely estimate that the liver mass devoted to the synthesis of carbohydrates, proteins, and lipids is $M_{synthL} \sim (P_{synthL} / P_{liver}) M_{hepato}$ = 487 gm (V_{synthL} ~ 463 cm^3) while the liver mass engaged primarily in breaking down hormones, ammonia, toxins, and other maintenance tasks, i.e., non-synthetic activities, is $M_{synthL} \sim (P_{nonsynthL} / P_{liver}) M_{hepato}$ = 713 gm (V_{synthL} ~ 677 cm^3).

From these estimates we can conclude that the Nutrient Synthesis Unit, as described above but augmented with tenfold redundancy in all nanomechanical components (Section 4.3.1), has a $(P_{NSU} M_{synthL} / M_{NSU} P_{synthL}) \sim$ **440 times higher power density** but only $(R_{NSU} P_{synthL} / P_{NSU} m_{synthL}) \sim$ **12% of the energy efficiency**[225] (i.e., power consumed per kg/day of output) of the biological human liver, but is $(R_{NSU} M_{synthL} / M_{NSU} m_{synthL}) \sim$ **60 times more productive per unit mass** (i.e., kg/day of output per kg of factory) and $(R_{NSU} V_{synthL} / V_{NSU} m_{synthL}) \sim$ **170 times more productive per unit volume** (i.e., kg/day of output per cm^3 of factory) than the synthesis-directed components of the biological human liver.

---

[223] Chiang J. Liver physiology: Metabolism and detoxification. In: McManus LM, Mitchell RN, eds. Pathophysiology of Human Diseases, Elsevier, Jul 2014, pp. 1770-1782; https://www.researchgate.net/publication/271910276_Liver_Physiology_MetaboLism_and_Detoxification.

[224] Löffler MC, Betz MJ, Blondin DP, Augustin R, Sharma AK, Tseng YH, Scheele C, Zimdahl H, Mark M, Hennige AM, Wolfrum C, Langhans W, Hamilton BS, Neubauer H. Challenges in tackling energy expenditure as obesity therapy: From preclinical models to clinical application. Mol Metab. 2021 Sep;51:101237; https://pmc.ncbi.nlm.nih.gov/articles/PMC8122111/.

[225] Our initial design might be suboptimal in energy efficiency. Future analysis and redesign of the Nutrient Synthesis Unit may allow us to equal or even exceed biological organ metabolic efficiencies.

4.2 Waste Recovery Unit (WRU)

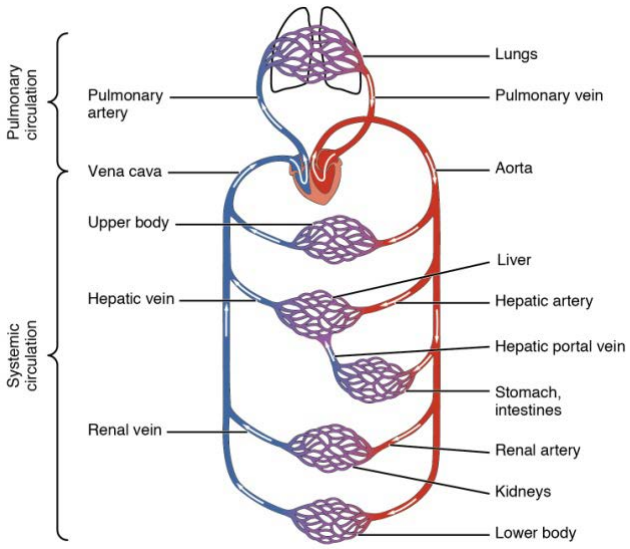

All nutrient and waste molecules are transported through the bloodstream (image, right).[226] In the case of nutrients, these molecules circulate until they are withdrawn by the tissue as needed to maintain local metabolism. Therefore, to provide all the nutritional needs of the human body it should suffice for the Nutrient Synthesis Unit to maintain proper bloodstream concentrations of each nutrient molecule. These nutrients could be injected into the bloodstream at any convenient location within the general circulation.[227]

However, in the case of waste molecules it would not be sufficient to simply extract them from the bloodstream. Certain body organs perform the function of quickly extracting waste molecules from the bloodstream, concentrating them, and then excreting them from the body. Any molecules that are excreted from the body will avoid recapture via bloodstream extraction and would need to be provided to the person as supplemental nutrition, a circumstance that we wish to minimize.

As previously noted in Section 3, the principal excretory pathways in the human body are the kidney and bladder (urine), the lungs (CO_2 exhalation), the intestinal tract (feces), and the skin (perspiration). Maximizing the practical recovery of waste molecules requires two distinct subsystems comprising the Waste Recovery Unit: (1) a **Urine Extraction Subunit** (Section 4.2.1) positioned near the bladder, equipped with molecular pumps able to extract essential waste molecules directly from urine; and (2) a **Blood Extraction Subunit** (Section 4.2.2) positioned near the proximal end of the renal veins as they exit the kidneys, to facilitate the extraction of carbon dioxide before it can be excreted from the body via exhalation in the lungs. These two subunits should ensure essentially complete recovery from the urine and blood of all waste molecules not excreted in feces or skin.

The ~0.4% of all waste atoms that are not recoverable from feces or skin loss must be provided by other means, as discussed in Section 4.2.3.

---

[226] https://en.wikipedia.org/wiki/Circulatory_system#Structure.

[227] Injecting 585.1 gm/day (**Table 8**) ~ 585.1 cm^3/day (assuming ~water density) ~ **0.41 cm^3/min** into the ~5400 cm^3/min of total human blood flow seems tolerable and well within the standard guidelines for intravenous parenteral feeding of 25-40 mL/kg/day = **1.2-1.9 cm^3/min** for a resting 70 kg male; https://www.ashp.org/-/media/assets/pharmacy-practice/resource-centers/Clinical-Pharmacy-Resources/Nutrition-Support/2016-MCM/MCM16-335-Strategies-for-Successful-Parenteral-nutrition.pdf.

4.2.1 Urine Extraction Subunit (UES)

The nanorobotic Urine Extraction Subunit (UES) is positioned above the bladder (image, right),[228] and includes a set of molecular pumps that could be positioned inside the bladder storage volume that can extract all essential waste molecules directly from the urine. However, we prefer installing the pumps inside the ureters near the top which allows the metabolic organ to be positioned conveniently closer to the kidneys (image, left), probably in the retroperitoneal space. **Table 12** lists the 26 molecules/ions and quantities that this Subunit would need to extract. In possible implementations, the Subunit would be mounted above the external bladder wall with a probe penetrating a ureter wall, passing into the interior volume, with an arboreal tip structure that guarantees full physical access to the fluid content regardless of the bladder's state of fullness or the person's postural state relative to the local gravity field.[229] After chemically processing the 8 organic molecules that are larger than urea (~2.9 gm/day or ~3.7% of the total; **Table 12**) into simpler molecules suitable for use as feedstock, these final molecular products of the UES are transported via a physical connection to the Nutrient Synthesis Unit.

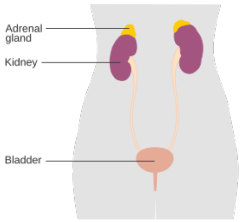

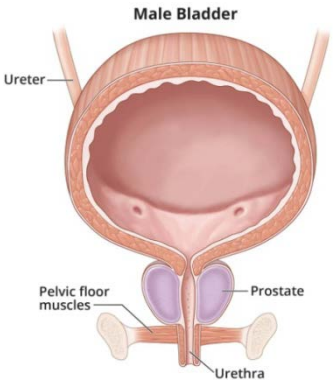

Small molecules can be selectively removed from urine using molecular pumps called sorting rotors,[230] classically illustrated (image, left) as a disk about 10 nm in diameter and about 3 nm thick having 12 binding site "pockets" along the rim that are exposed alternately to the source fluid at left and the receiving chamber at right by the clockwise axial rotation of the disk. Each pocket selectively binds a specific molecule when exposed to the source fluid at left. The rotor turns clockwise, moving the pocket containing the bound molecule through the

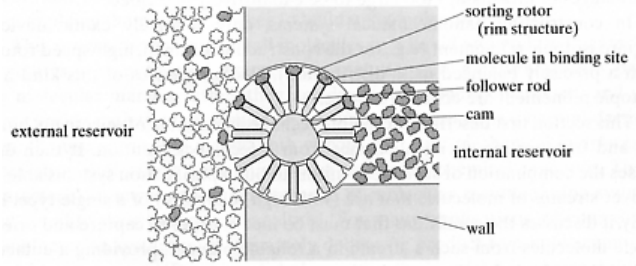

---

[228] https://www.niddk.nih.gov/health-information/urologic-diseases/bladder-control-problems/symptoms-causes.

[229] It might be useful to consider actively controlling the internal urethral sphincter muscle (https://en.wikipedia.org/wiki/Urethral_sphincters) or provide supplemental mechanical gating to the internal urethral opening to prevent unintended voluntary or involuntary drainage of urine from the body before valuable waste molecules can be fully extracted.

[230] Drexler KE. Nanosystems: Molecular Machinery, Manufacturing, and Computation. John Wiley & Sons, New York, 1992, Section 13.2, "Sorting and Ordering Molecules"; https://www.amazon.com/dp/0471575186/. Freitas RA Jr. Nanomedicine, Volume I: Basic Capabilities. Landes Bioscience, Georgetown, TX, 1999, Section 3.4.2, "Sorting Rotors"; http://www.nanomedicine.com/NMI/3.4.2.htm.

wall from left to right. Once the binding site has rotated far enough to expose it to the receiving chamber at right, the bound molecules are forcibly ejected by rods (e.g., polyynes) thrust outward by the cam surface.

Table 12. Estimated recyclable waste molecules and ions excreted in urine for a 70 kg male human body at the ~100 watt basal metabolic rate

Waste Molecule	Formula	gm/day	gm/mole	molecules/day
Urea	H_2NCONH_2	27.58	60.1	2.76×10^{23}
Creatinine	$C_4H_7N_3O$	1.6	113.1	8.52×10^{21}
Uric acid	$C_5H_4N_4O_3$	0.315	168.1	1.13×10^{21}
Hippuric acid	$C_9H_9NO_3$	0.700	179.2	2.35×10^{21}
Sulfate anion	SO_4^{2-}	1.5279	96.1	9.57×10^{21}
Ammonium ion	NH_4^+	0.540	18.0	1.81×10^{22}
Phosphate ion	as $H_2PO_4^-$	2.47	97.0	1.53×10^{22}
Urobilinogen	$C_{33}H_{44}N_4O_6$	0.004	592.7	4.06×10^{18}
Cholic acid	$C_{24}H_{40}O_5$	0.0002	408.6	2.95×10^{17}
Cheno-/deoxycholic acid	$C_{24}H_{40}O_4$	0.0003	392.6	4.60×10^{17}
Cholesterol	$C_{27}H_{46}O$	0.001	385.7	1.56×10^{18}
Sodium	Na^+	2.058	23.0	5.39×10^{22}
Potassium	K^+	3.283	39.1	5.06×10^{22}
Chloride	Cl^-	1.900	35.5	3.22×10^{22}
Iodide	I^-	0.00013	126.9	6.17×10^{17}
Calcium	Ca^{2+}	0.860	40.1	1.29×10^{22}
Magnesium	Mg^{2+}	0.386	24.3	9.57×10^{21}
Zinc	Zn^{2+}	0.01025	65.4	9.44×10^{19}
Iron	Fe^{3+}	0.00007	55.8	7.55×10^{17}
Manganese	Mn^{3+}	0.00002	54.9	2.19×10^{17}
Copper	Cu^{2+}	0.00010	63.5	9.48×10^{17}
Selenium	SeO_3^{2-}	0.0000275	79.0	2.10×10^{17}
Chromium	Cr^{3+}	0.000028	52.0	3.24×10^{17}
Molybdenum	MoO_4^{2-}	0.000034	95.9	2.14×10^{17}
Cobalt (as cobalamin)	$C_{63}H_{88}CoN_{14}O_{14}P$	0.0000002	1355.4	8.89×10^{13}
Subtotals		43.24		4.91×10^{23}
Miscwastium (99.7% of total)	$C_{19}H_{15}O_{10}$	17.85	405.0	2.67×10^{22}
Totals		**61.08**		**5.17×10^{23}**

Molecular sorting rotors can be designed from ~10^5 atoms (including housing and pro rata share of the drive system), measuring roughly 7 nm x 14 nm x 14 nm in size (volume V_{rot} ~ 1372 nm^3) with a mass of $M_{rot} = 2 \times 10^{-21}$ kg and a working-face area of A_{rot} = 7 nm x 14 nm = 98 nm^2. For

a fluid environment having the approximate viscosity of water (~10^{-3} kg/m-sec at 20 ^{o}C) on both sides of the wall, the sorting rotor described and operated as above has an estimated continuous drag power loss of $P_{drag} \sim 10^{-16}$ W (~0.0001 pW) against the fluid while transporting ~10^{6} molecules/sec,[231] or ~0.1 zJ/molecule transported.

Rotors turn at ~86,000 rev/sec with a conservative rim speed of 2.7 mm/sec, sorting small molecules at a rate of $r_{max} \sim 10^{6}$ molecules/rotor-sec with laminar flow, assuming 99% occupancy of the binding sites at this rotor speed which can occur at aqueous molecular concentrations of $c_{max} \sim 10^{-1}$ molecules/nm^3 or higher.[232] Target molecules are continuously extracted at about the same rate as they are passing into the bladder, but to continuously draw down the urine concentrations to $f_{conc} \sim 1\%$ of the unextracted natural concentration (i.e., $c_{initial}/c_{final} \sim f_{conc}^{-1} \sim 100$, implying 99% complete solute extraction) would require a thermodynamic extraction energy of $\Delta G \sim k_B T \ln(c_{initial}/c_{final}) \sim 2 \times 10^{-20}$ J/molecule, taking T ~ 310 K (37 °C, or human body temperature) and $k_B = 1.381 \times 10^{-23}$ J/K (Boltzmann constant), so each rotor would need $P_{rot} = r_{max} \Delta G \sim$ **0.02 pW** to operate continuously at the ~86,000 rev/sec spin rate. However, because target molecules are continuously extracted, the average urine concentration ratio is only $c_{initial}/c_{final} \sim 21.5$ for 99% solute extraction,[233] giving a revised $\Delta G \sim k_B T \ln(c_{initial}/c_{final}) \sim 1.3 \times 10^{-20}$ J/molecule and $P_{rot} = r_{max} \Delta G \sim$ **0.013 pW**.

Solute extraction energy can be further reduced by passing the entire urine stream through an in-ureter nanopore filter with pore diameter 0.28-0.34 nm. This is sufficient to pass H_2O rapidly while excluding ions such as Na^+ (hydrated) and larger-diameter organic molecules.[234] In one representative scenario, the solute concentration is allowed to rise by 10-fold in the feed stream giving an lower average $f_{conc}^{-1} \sim 3.91$,[235] which reduces the sortation energy to $\Delta G \sim k_B T \ln(f_{conc}^{-1}) \sim 5.8 \times 10^{-21}$ J/molecule and $P_{rot} = r_{max} \Delta G \sim$ **0.0058 pW**. Pore membrane area $A_{membrane} \geq n_{x,pores} A_{pore} V_{wasteM} / r_{poreM} \sim 0.6$ mm^2, well within the 3-13 mm^2 cross-sectional area (2-4 mm diameter) of the kidney ureters which the nanopore membrane would span, taking solute

---

[231] Drexler KE. Nanosystems: Molecular Machinery, Manufacturing, and Computation. John Wiley & Sons, New York, 1992, Section 13.2.1(e), "Modulated Receptors for Selective Transport: Energy dissipation"; https://www.amazon.com/dp/0471575186/.

[232] Drexler KE. Nanosystems: Molecular Machinery, Manufacturing, and Computation. John Wiley & Sons, New York, 1992, Section 13.2.1(a), "Modulated Receptors for Selective Transport: Basic Concepts"; https://www.amazon.com/dp/0471575186/.

[233] For an exponentially declining solute concentration $C(t) = C_0 \exp(-kt)$ where $C_0 =$ **100** and $C(t_1) = 1$, the average concentration over the interval t = 0 to $t = t_1$ is $C_{avg} = (100 / t_1) [(1 - \exp(-kt_1)) / k] = 99/\ln(100) =$ **21.5**, where $t_1 = \ln(100) / k$ because $C(t_1) = 100 \exp(-kt_1) = 1$.

[234] Pore design may require charge decoration (for ion rejection) at pore entrances, hydrophilic lining to promote water flux, and hydrogen bonding fields or conformational selectivity to disrupt transit by the smallest target organic molecules such as urea. Surfaces must also resist clogging from organic/inorganic buildup over long runtimes, and continuous flow systems generally need fluidic control to prevent pressure buildup or bubble formation. Such precise pore and filter system design is beyond the scope of the present work.

[235] For an exponentially declining solute concentration with $C_0 =$ **10** and $C(t_1) = 1$, $C_{avg} = 9/\ln(10) =$ **3.91**.

molecule filtration requirement V_{wasteM} = 5.17 x 10^{23} molecules/day = 5.98 x 10^{18} molecules/sec (**Table 12**), pore transit rate r_{poreM} ~ 10^9 molecules/pore-sec,[236] pore module area A_{pore} = 10 nm^2 and L_{pore} ~ 100 nm thick, and pore redundancy $n_{x,pores}$ = 10. The entire nanopore system has negligible volume ($A_{membrane}$ L_{pore} ~ 60,000 μm^3) and mass (~0.2 ng), and consumes no power.

The sorting rate declines approximately linearly with the concentration $c_{molecule}$ of the molecule to be sorted, or r_{sort} ~ $c_{molecule}$ r_{max} / c_{max} molecules/rotor-sec. Extracting each target molecule at the $n_{molecules}$ (molecules/day) rate tabulated in the rightmost column of **Table 12** requires N_{rotors} = $n_{molecules}$ / r_{sort} sorting rotors, each with binding sites engineered for optimal affinity for the particular target molecule.[237] Since the lowest solute concentration is $c_{molecule}$ = f_{conc} $n_{molecules}$ /

---

[236] Experimental and simulation studies of human aquaporin AQP1 report that it conducts water at approximately 3 x 10^9 molecules/sec-monomer.[*] Short (~1-10 nm) hydrophobic CNTs with diameters ~3 Å have been simulated and observed to conduct water with fluxes of ~10^9 water molecule/sec-channel.[†]

[*] Kozono D, Yasui M, King LS, Agre P. Aquaporin water channels: atomic structure molecular dynamics meet clinical medicine. J Clin Invest. 2002 Jun;109(11):1395-9; https://pmc.ncbi.nlm.nih.gov/articles/PMC151002/.

[†] Moskowitz I, Snyder MA, Mittal J. Water transport through functionalized nanotubes with tunable hydrophobicity. J Chem Phys. 2014 Nov 14;141(18):18C532; https://arxiv.org/abs/1503.03707.

[237] **Binding site design** is a major topic that is outside the scope of this document. Previous work by this author has discussed binding site design[A] for a variety of small molecules including **O_2** (oxygen),[B] **N_2** (nitrogen),[B] **CO** (carbon monoxide),[B] **CO_2** (carbon dioxide),[C] **H_2O** (water),[BD] **NH_3** (ammonia),[B] **CH_4** (methane),[BD] **C_2H_2** (acetylene),[B] **CH_3OH** (methanol),[D] **C_2H_5OH** (ethanol),[BD] **C_2H_6OS** (dimethyl sulfoxide),[B] **$C_2H_6O_2$** (ethylene glycol),[B] **$C_3H_8O_3$** (glycerol),[B] **$C_6H_{12}O_6$** (glucose),[B] and **$C_nH_{2n+z}O_2$** (naphthenic acids).[E] The design,[F] simulation[G] and fabrication[H] of artificial binding sites for more complex molecules has long been an active field of research.

[A] Freitas RA Jr. Nanomedicine, Volume I: Basic Capabilities, Landes Bioscience, Georgetown, TX, 1999; Section 3.5.7, "Receptor Configurations"; 7http://www.nanomedicine.com/NMI/3.5.7.htm.

[B] Freitas RA Jr. Cryostasis Revival: The Recovery of Cryonics Patients through Nanomedicine. Alcor Life Extension Foundation, Scottsdale AZ, 2022; Section H.2, "Binding Sites for Other Simple Molecules"; https://www.alcor.org/cryostasis-revival/.

[C] Freitas RA Jr. The Nanofactory Solution to Global Climate Change: Atmospheric Carbon Capture. IMM Report No. 45, December 2015; Section 4.2, "Binding Site Design for Carbon Dioxide"; http://www.imm.org/Reports/rep045.pdf.

[D] Freitas RA Jr. The Whiskey Machine: Nanofactory-Based Replication of Fine Spirits and Other Alcohol-Based Beverages. IMM Report No. 47, May 2016; Section 5.3.3, "Receptor-Based Purification of Ethanol and Water"; http://www.imm.org/Reports/rep047.pdf.

[E] Freitas RA Jr. Nanofactory-Based Environmental Remediation: Cleanup of Polluted Oil Sands Tailings Pond Water in Alberta, Canada. IMM Report No. 51, 10 April 2023; Section 4.3, "Binding Site Design for Naphthenic Acids"; http://www.imm.org/Reports/rep051.pdf.

[F] e.g., Chaves EJF, Coêlho DF, Cruz CHB, Moreira EG, Simões JCM, Nascimento-Filho MJ, Lins RD. Structure-based computational design of antibody mimetics: challenges and perspectives. FEBS Open Bio. 2025 Feb;15(2):223-235; https://pmc.ncbi.nlm.nih.gov/articles/PMC11788748/.

[G] e.g., Rohs R, Bloch I, Sklenar H, Shakked Z. Molecular flexibility in ab initio drug docking to DNA: binding-site and binding-mode transitions in all-atom Monte Carlo simulations. Nucleic Acids Res. 2005 Dec 13;33(22):7048-57; https://pmc.ncbi.nlm.nih.gov/articles/PMC1312361/. Bielska W, Jaszczyszyn I, Dudzic P, Janusz B, Chomicz D, Wrobel S, Greiff V, Feehan R, Adolf-Bryfogle J, Krawczyk K. Applying computational protein design to therapeutic antibody discovery - current state and perspectives. Front Immunol. 2025 May 22;16:1571371; https://pmc.ncbi.nlm.nih.gov/articles/PMC12137305/.

V_{urine}, where average urine production of a 70 kg adult male is V_{urine} ~ 1.4 liters/day,[238] then the number of sorting rotors needed for each target molecule is independent of target molecule concentration and is given by $N_{rotors} = c_{max}\ V_{urine} / f_{conc}\ r_{max} = 1.62 \times 10^{14}$ rotors. For $N_{molecules}$ = 26 target molecules or ions, the total rotor count to extract all required urine-borne molecules[239] is $N_{urinerotors} = N_{molecules}\ N_{rotors} = 4.21 \times 10^{15}$ sorting rotors of total mass $M_{urinerotors} = M_{rot}\ N_{urinerotors} = 8.42 \times 10^{-6}$ kg ~ **10 mg**, volume $V_{urinerotors} = V_{rot}\ N_{urinerotors} = 5.78 \times 10^{-9}$ m^3 ~ **10 mm^3**, and continuous power consumption $P_{urinerotors} = P_{rot}\ N_{urinerotors}$ ~ **24 W** for the entire population of bladder- or ureter-resident sorting rotors in the Urine Extraction Subunit.

We must also extract $n_{H2O} \sim 1.37 \times 10^{20}$ molecules/sec of water (~355 gm/day; **Table 5**) to enable the Nutrient Synthesis Unit to reconstitute all necessary glucose, amino acids, and lipid nutrients (Section 4.1.2), requiring $N_{H2Orotors} \sim n_{H2O} / r_{max} = 1.37 \times 10^{14}$ additional water rotors (as the high concentration of water in urine guarantees maximum sorting speed) having mass $M_{H2Orotors} = M_{rot}\ N_{H2Orotors} = 2.74 \times 10^{-7}$ kg ~ **0.3 mg**, volume $V_{H2Orotors} = V_{rot}\ N_{H2Orotors} = 1.88 \times 10^{-10}$ m^3 ~ **0.2 mm^3**, and continuous power consumption $P_{H2Orotors} \sim P_{drag}\ N_{H2Orotors}$ ~ **0.01 W** because $c_{initial}/c_{final}$ ~ 1 implies ΔG ~ 0 J/molecule in this case. This leaves ~1 liter/day of urine output, well above the accepted pathological levels of 0.08-0.4 liters/day in oliguria[240] and <0.08 liters/day in anuria.

The presence of such a small volume of nanomechanical sorting rotors, even allowing for a substantial mass of supportive structures, should be nonintrusive to the interior volume of the ureters, or even to the male bladder which can typically hold up to 700 cm^3 of urine (though the urge to urinate usually starts when the bladder is filled to about 150-250 cm^3).[241]

[H] e.g., Bracci L, Lozzi L, Pini A, Lelli B, Falciani C, Niccolai N, Bernini A, Spreafico A, Soldani P, Neri P. A branched peptide mimotope of the nicotinic receptor binding site is a potent synthetic antidote against the snake neurotoxin alpha-bungarotoxin. Biochemistry. 2002 Aug 13;41(32):10194-9; http://www.kingsnake.com/aho/pdf/menu6/bracci2002.pdf. Subat M, Borovik AS, König B. Synthetic creatinine receptor: imprinting of a Lewis acidic zinc(II)cyclen binding site to shape its molecular recognition selectivity. J Am Chem Soc. 2004 Mar 17;126(10):3185-90; https://pubmed.ncbi.nlm.nih.gov/15012148/. Franke R, Hirsch T, Overwin H, Eichler J. Synthetic mimetics of the CD4 binding site of HIV-1 gp120 for the design of immunogens. Angew Chem Int Ed Engl. 2007;46(8):1253-5; https://onlinelibrary.wiley.com/doi/10.1002/anie.200603274. Mohsenzadeh E, Ratautaite V, Brazys E, Ramanavicius S, Zukauskas S, Plausinaitis D, Ramanavicius A. Design of molecularly imprinted polymers (MIP) using computational methods: A review of strategies and approaches. WIREs Computat Molec Sci. 2024 May/Jun; 14(3):e1713; https://wires.onlinelibrary.wiley.com/doi/abs/10.1002/wcms.1713.

[238] https://en.wikipedia.org/wiki/Urine#Quantity.

[239] For computational convenience, we assume that 99.7% of miscwastium waste molecules are recoverable from the urine. Extracting some or all miscwastium molecules from the blood instead of the urine should not significantly alter the overall conclusions of the present design analysis.

[240] https://en.wikipedia.org/wiki/Oliguria.

[241] In brief: How does the urinary system work? Institute for Quality and Efficiency in Health Care (IQWiG), Cologne, Germany, InformedHealth.org [Internet], 29 Mar 2022; https://www.ncbi.nlm.nih.gov/books/NBK279384/.

A mechanical transport system for conveying nanorobotic cargo containers at v_{tube} ~ 0.4 mm/sec through a w_{tube} ~ 3.5 mm wide tube has a materials transfer rate of $V_{transfer}$ ~ **4.9 mm^3/sec**, accommodating the ~**4.8 mm^3/sec** containerized urinary solid waste flow volume requirement of V_{Uwaste} ~ 61.64 cm^3/day = **0.7 mm^3/sec** (assuming urinary waste mass rate ~61.64 gm/day at ~water density) plus another 355 gm/day ~ **4.1 mm^3/sec** for water molecule transport to the NSU. Transport would occur through a transfer tube of maximum length L_{tube} ~ 15 cm[242] (i.e., reaching from the ureter interior through the ureter wall to the Urine Extraction Subunit located external to the bladder) with tube transit time of $t_{tube} = L_{tube} / v_{tube}$ ~ 375 sec and a total tube volume of $V_{tube} = w_{tube}^2 L_{tube}$ ~ **1.8 cm^3** and mass M_{tube} ~ **0.3 gm**. One estimate of the drag power for containerized transport of molecules using pallets sliding along tracks at 0.4 mm/sec is P_{pallet} ~ 4 x 10^{-23} W/molecule,[243] giving a total transport power of $P_{transport} = (t_{tube}\ n_{molecules} / t_{day})\ P_{pallet}$ = **2.1 W**, for t_{day} = 86,400 sec/day and $n_{molecules}$ ~ 5.19 x 10^{23} waste molecules/day (**Table 12**) + 1.18 x 10^{25} molecules/sec of water (~355 gm/day; **Table 5**) = 1.23 x 10^{25} molecules/sec.

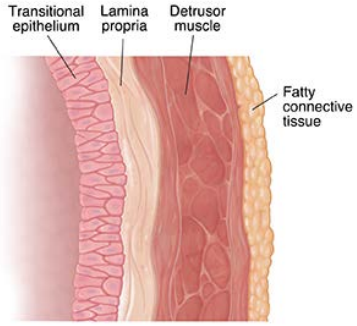

A transport system plumbing employing bladder- or ureter-resident molecular pumps might penetrate the four primary layers of the ~3.4 mm thick bladder wall,[244] tissue which includes (image,[245] right): (1) the **urothelium** or transitional epithelium (the layer of urothelial cells lining the inside of the kidneys, ureters, bladder, and urethra), (2) the **lamina propria (**a type of connective tissue), (3) the **detrusor muscle** or muscularis propria (an outer layer of thick smooth muscle tissue), and (4) the **fatty connective tissue** (covering the outside of the bladder and separating it from other organs). A similar arrangement can be used for a pumping apparatus that must penetrate the ureter walls which consist of the urothelium surrounded by the lamina propria, two muscular layers, and an adventitia (image, left).[246] Long-term biocompatibility can be enhanced by employing a lipophilic coating on the exterior of the transepithelial-penetrating nanorobotic transport system to ensure a tight seal.[247] Penetrating members should employ a

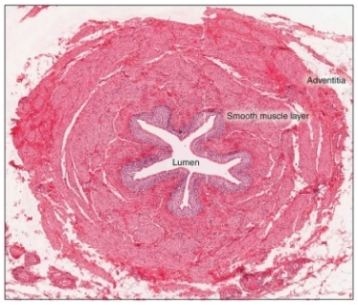

---

[242] At full capacity the human bladder measures ~13 cm long and ~8 cm wide; https://www.sciencedirect.com/topics/medicine-and-dentistry/bladder.

[243] Freitas RA Jr. Nanomedicine, Volume I: Basic Capabilities, Landes Bioscience, Georgetown, TX, 1999; Section 3.4.3, "Internal Transport Streams"; 7http://www.nanomedicine.com/NMI/3.4.3.htm.

[244] Hakenberg OW, Linne C, Manseck A, Wirth MP. Bladder wall thickness in normal adults and men with mild lower urinary tract symptoms and benign prostatic enlargement. Neurourol Urodyn. 2000;19(5):585-93; https://pubmed.ncbi.nlm.nih.gov/11002301/.

[245] https://www.saintlukeskc.org/health-library/anatomy-bladder#.
[246] https://en.wikipedia.org/wiki/Ureter#Microanatomy.

[247] Freitas RA Jr. Nanomedicine, Volume IIA: Biocompatibility, Landes Bioscience, Georgetown, TX, 2003; Section 15.5.2.1, "Transepithelial Penetration"; http://www.nanomedicine.com/NMIIA/15.5.2.1.htm.

mechanically compliant jacket having properties similar to extracellular matrix and should possess a structural elasticity or mechanical compliance equivalent to the underlying tissue to which attachment must be secured to avoid ulcerative pathologies.[248]

Once transported to the Urine Extraction Subunit, a few of the waste molecules must be broken down into simpler molecules suitable for use as feedstock by the Nutrient Synthesis Unit (NSU). This requires synthetic nanomachinery whose operating parameters are assumed similar to those of the previously described chemical Nanofabricators (Section 4.1.1). Note that the energy for breaking down the waste molecules CO_2, H_2O, and urea (CH_4N_2O) to build nutrient molecules in the Nutrient Synthesis Unit is already included in the NSU size and energy estimates (Section 4.1.2). So the only significant chemical processing that must be performed in the Urine Extraction Subunit is the conversion of ~2.895 gm/day of creatinine ($C_4H_7N_3O$), uric acid ($C_5H_4N_4O_3$), hippuric acid ($C_9H_9NO_3$), and urobilinogen ($C_{33}H_{44}N_4O_6$) – the only four significant non-urea urine excreta by mass rate – into urea for use in the NSU. Using the mechanodecomposition reactions outlined in **Table 13** and the mass rates compiled in **Table 12**, the total power requirement is roughly: P_{urineN} ~ (creatinine [(8.52 x 10^{21} molecules/day) (2300 zJ/molecule)] + uric acid [1.13 x 10^{21} molecules/day) (1090 zJ/molecule)] + hippuric acid [(2.35 x 10^{21} molecules/day) (6480 zJ/molecule)] + urobilinogen [(2.84 x 10^{20} molecules/day) (28,100 zJ/molecule)]) / ε_{MS} ~ **1 W**, taking ε_{MS} ~ 80% as before. Processing these ~1.23 x 10^{22} extra molecules (comprising 2.22 x 10^{23} product atoms/day)[249] should require an additional ~5.5 trillion Nanofabricators of volume ~**5.7 mm^3** and mass ~**0.01 gm**.

Table 13. Energy requirements for synthesizing urea from four nitrogen-rich urinary waste molecules, using standard enthalpies of formation[250]

N Source	gm/mole	Posited Mechanosynthetic Reaction	zJ/molecule
Creatinine	113.1	$2C_4H_7N_3O + 6O_2 \rightarrow 3\mathbf{CH_4N_2O} + 5CO_2 + H_2O$	2300
Uric acid	168.1	$2C_5H_4N_4O_3 + 3O_2 + 4H_2O \rightarrow 4\mathbf{CH_4N_2O} + 6CO_2$	1090
Hippuric acid	179.2	$2C_9H_9NO_3 + 18O_2 \rightarrow \mathbf{CH_4N_2O} + 17CO_2 + 7H_2O$	6480
Urobilinogen	592.7	$C_{33}H_{44}N_4O_6 + 38O_2 \rightarrow 2\mathbf{CH_4N_2O} + 31CO_2 + 18H_2O$	28,100

[248] Freitas RA Jr. Nanomedicine, Volume IIA: Biocompatibility, Landes Bioscience, Georgetown, TX, 2003; Section 15.5.3.4.1, "Nanorobotic Ulcerative Vasculopathy"; http://www.nanomedicine.com/NMIIA/15.5.3.4.1.htm.

[249] Creatinine [(8.52 x 10^{21} molecules/day) (15 atoms/molecule)] + uric acid [1.13 x 10^{21} molecules/day) (16 atoms/molecule)] + hippuric acid [(2.35 x 10^{21} molecules/day) (22 atoms/molecule)] + urobilinogen [(2.84 x 10^{20} molecules/day) (87 atoms/molecule)] = 2.22 x 10^{23} atoms.

[250] Use:ΔH_f (creatinine) = -239.93 kJ/mole (https://webbook.nist.gov/cgi/cbook.cgi?ID=C60275&Mask=2), ΔH_f (uric acid) = -618.81 kJ/mole (https://webbook.nist.gov/cgi/cbook.cgi?ID=C69932&Mask=4EF&Units=SI), ΔH_f (hippuric acid) = -609.53 kJ/mole (https://www.chemeo.com/cid/22-610-9/Hippuric-acid), and ΔH_f (urobilinogen) ~ -1095 kJ/mole (est. from NIST's internally compiled SRD-69 data and the DIPPR® Project 801 compilation).

Thus the Urine Extraction Subunit (UES) has an active nanodevice mass of M_{UES} ~ 0.013 gm (rotors) + 0.3 gm (transport) + 0.01 gm (nanofabricators) = **0.323 gm**, volume V_{UES} ~ 0.012 cm^3 (rotors) + 1.8 cm^3 (transport) + 0.0057 cm^3 (nanofabricators) = **1.8177 cm^3**, and power consumption P_{UES} ~ 24 W (rotors) + 2.1 W (transport) + 1 W (nanofabricators) = **27.1 W**, with a mass processing rate of R_{UES} ~ **61.08 gm/day**.

How does the performance of the Urine Extraction Subunit compare to the filtration performance of the human kidney, the biological organ most responsible for filtering the same chemicals out of the human bloodstream? In humans, the kidneys are a paired set of blood-filtering organs,[251] each producing ~90 L/day of ultrafiltrate, most of which is reabsorbed. Filtration takes place in the renal cortex which comprises ~73% of kidney volume.[252] For a 70 kg adult male human, each 150 gm kidney includes M_{cortex} ~ **110 gm** of cortex of volume V_{cortex} ~ **104 cm^3**, taking density ρ_{kidney} ~ 1.0597 gm/cm^3.[253] To compare the kidney to the Urine Extraction Subunit, we're interested only in the amount of solute excreted from, not the total volume of fluid processed by, the biological organ. Each kidney removes – and initially presents to the tubules – approximately 800-1000 gm/day of small-molecule solutes from the blood, but most is reabsorbed and returned to the circulation, with ~61.64 gm/day excreted into the urine from both kidneys (**Table 12**), or m_{solute} ~ **30.82 gm/day** for each kidney. The two kidneys consume ~9 W of power at the basal metabolic rate,[254] so the power draw for the renal cortex of a single kidney is P_{cortex} ~ (0.5) (73%) (9 W) = **3.3 W**.

From these estimates we can conclude that the Urine Extraction Subunit, as described above but augmented with tenfold redundancy in all nanomechanical components (Section 4.3.1), has a (P_{UES} M_{cortex} / M_{UES} P_{cortex}) ~ **750 times higher power density** but only (R_{UES} P_{cortex} / P_{UES} m_{solute}) ~ **24% of the energy efficiency** (i.e., power consumed per kg/day of output) of the biological human liver, but is (R_{UES} M_{cortex} / M_{UES} m_{solute}) ~ **180 times more productive per unit mass** (i.e., kg/day of output per kg of factory) and (R_{UES} V_{cortex} / V_{UES} m_{solute}) ~ **34 times more productive per unit volume** (i.e., kg/day of output per cm^3 of factory) than the synthesis-directed components of the biological human liver.

4.2.2 Blood Extraction Subunit (BES)

The nanorobotic Blood Extraction Subunit (BES) is positioned to allow access to the proximal ends of the two renal veins as they exit the kidneys, primarily to facilitate the extraction of carbon dioxide (CO_2) waste molecules before they can be excreted from the body via exhalation in the lungs. The proposed BES may be viewed as an extension of current design concepts for implantable artificial kidneys (typically including miniaturized hemofilters, sorbent-based

---

[251] https://en.wikipedia.org/wiki/Kidney.

[252] Hommos MS, Glassock RJ, Rule AD. Structural and Functional Changes in Human Kidneys with Healthy Aging. J Am Soc Nephrol. 2017 Oct;28(10):2838-2844; https://pmc.ncbi.nlm.nih.gov/articles/PMC5619977/.

[253] https://radiology-universe.org/calculator/kidney-depth-correction/.

[254] https://courses.lumenlearning.com/suny-physics/chapter/7-8-work-energy-and-power-in-humans/.

dialysate regeneration, and cell-based bioreactors) that are regarded as the next step beyond wearable devices,[255] with enumerated technological challenges such as membrane efficiency, package size, and immunoprotection.[256] The first miniaturized capillary filters specifically aimed at the implantable artificial kidney context were tested *in vitro* and in animal preparations to assess filtration rates and hemocompatibility in 1989.[257] More recently, silicon nanopore membrane hemofilter cartridges were anastomosed to the vasculature of Class A dogs showing proof-of-concept for chronic implantation,[258] and a silicon-nanopore-membrane bioreactor (containing human renal epithelial cells) was implanted in pigs for seven days, demonstrating viability and functionality under physiological flow without systemic anticoagulation.[259]

The principal task of the BES is to extract CO_2 from the blood. Carbon dioxide is produced in all aerobic cells throughout the body as the end-product of the citric acid or "Krebs" cycle in the mitochondria, with a smaller contribution from cytosolic reactions. During oxidation of carbohydrates, fats, and proteins, carbon atoms are fully oxidized and released as CO_2, which diffuses out of the mitochondrial matrix into the cytosol and then across the cell membrane into interstitial fluid.[260] Once in the extracellular fluid, CO_2 enters the circulation and in the normal course is carried from tissues to the lungs by three main mechanisms:[261]

(1) **Bicarbonate (HCO_3^-),** ~70-80% of the total. Carbon dioxide dissolves into the blood plasma and enters red blood cells (RBC), where carbonic anhydrase enzyme[262] catalyzes its hydration to carbonic acid which then rapidly dissociates to form bicarbonate ions (HCO_3^-) and a hydrogen ion (H^+) according to $CO_2 + H_2O \rightarrow H_2CO_3 \rightarrow H^+ + HCO_3^-$ (aka. "bicarbonate"). More CO_2 then passively diffuses into the cell in response to the decrease in pCO_2, the intracellular partial pressure of carbon dioxide. While cell membranes are generally impermeable to charged ions like H^+ and HCO_3^-, RBCs can exchange bicarbonate for chloride using the

---

[255] Fissell WH, Roy S. The implantable artificial kidney. Semin Dial. 2009 Nov-Dec;22(6):665-70; https://pubmed.ncbi.nlm.nih.gov/20017839/.

[256] Salani M, Roy S, Fissell WH 4th. Innovations in Wearable and Implantable Artificial Kidneys. Am J Kidney Dis. 2018 Nov;72(5):745-751; https://pubmed.ncbi.nlm.nih.gov/30146422/.

[257] Dörp E, Wüstenberg PW, Klinkmann H, Ivanovich P, Trekel S. Optimization of hemofilters for the development of implantable artificial kidneys. Artif Organs. 1989 Jun;13(3):241-6; https://pubmed.ncbi.nlm.nih.gov/2764764/.

[258] Kensinger C, Karp S, Kant R, Chui BW, Goldman K, Yeager T, Gould ER, Buck A, Laneve DC, Groszek JJ, Roy S, Fissell WH. First Implantation of Silicon Nanopore Membrane Hemofilters. ASAIO J. 2016 Jul-Aug;62(4):491-5; https://pmc.ncbi.nlm.nih.gov/articles/PMC4983406/.

[259] Kim EJ, Chen C, Gologorsky R, Santandreu A, Torres A, Wright N, Goodin MS, Moyer J, Chui BW, Blaha C, Brakeman P, Vartanian S, Tang Q, David Humes H, Fissell WH, Roy S. Feasibility of an implantable bioreactor for renal cell therapy using silicon nanopore membranes. Nat Commun. 2023 Aug 29;14(1):4890; https://pmc.ncbi.nlm.nih.gov/articles/PMC10465514/.

[260] Doyle J, Cooper JS. Physiology, Carbon Dioxide Transport. StatPearls [Internet], 4 Jul 2023; https://www.ncbi.nlm.nih.gov/books/NBK532988/.

[261] https://en.wikipedia.org/wiki/Carbon_dioxide#Transport_in_the_blood.
[262] https://en.wikipedia.org/wiki/Carbonic_anhydrase.

transmembrane anion exchanger protein Band 3[263] which allows blood chloride to enter the cell from blood plasma and the HCO_3^- to exit the cell and enter the plasma, a phenomenon known as the "chloride shift".[264] This allows the bicarbonate anion to travel dissolved in plasma, while filling the RBC with excess chloride ion. The plasma of venous blood returning to the lungs carries a higher HCO_3^- concentration and a lower Cl^- concentration than the plasma in arterial blood, and vice versa inside the venous RBCs.

As venous blood is pumped through the heart and pulmonary artery and enters the pulmonary (alveolar) capillaries of the lungs, the external pO_2 rises and pCO_2 falls, forcing release of CO_2 from hemoglobin during RBC oxygenation due to the Haldane effect.[265] This releases hydrogen ions from hemoglobin, increasing free H^+ concentration within RBCs and shifting the equilibrium back towards CO_2 and water formation from bicarbonate. The subsequent decrease in intracellular bicarbonate concentration reverses the earlier chloride-bicarbonate exchange, with bicarbonate moving into the cell from the plasma in exchange for chloride moving out of the RBC into the plasma.[266] The reverse movement of bicarbonate via the Band 3 exchanger allows carbonic anhydrase to convert HCO_3^- back into CO_2. As soon as CO_2 is generated inside the RBCs, its partial pressure (pCO_2) inside the capillary blood (~46 mmHg in mixed-venous blood),[267] which remains higher than the alveolar pCO_2 (~40 mmHg), creates a gradient that drives the CO_2 to diffuse from RBCs into plasma, and thence across the thin 0.2-0.6 μm capillary endothelial and alveolar epithelial layers into the alveolar gas where CO_2 is removed by exhalation during normal ventilation, thus maintaining the low alveolar pCO_2 that keeps the reaction going in the [bicarbonate + $H^+ \rightarrow CO_2 + H_2O$] direction.

(2) **Carbaminohemoglobin,** ~10-15% of the total. RBCs also contain ~35% by weight of a reversible oxygen-binding protein called hemoglobin.[268] CO_2 in blood plasma reversibly binds to hemoglobin's terminal amine groups, forming carbaminohemoglobin. This CO_2 is normally released in the lungs when hemoglobin is re-oxygenated. The amount of carbaminohemoglobin formed is inversely proportional to the amount of oxygen attached to hemoglobin – at lower oxygen saturation, more carbaminohemoglobin is formed.[269] As with bicarbonate, CO_2 is driven out of carbaminohemoglobin in the presence of excess oxygen.

(3) **Dissolved carbon dioxide,** ~5-10% of the total. A small portion of CO_2 remains physically dissolved in plasma, ranging from 3.3-8.3 x 10^{-5} gm/cm^3 in blood plasma,[270] directly following its partial-pressure gradient. Offloading dissolved CO_2 from blood plasma requires lowering the external pCO_2, creating a diffusion-limited gradient.

---

[263] https://en.wikipedia.org/wiki/Band_3_anion_transport_protein.
[264] https://en.wikipedia.org/wiki/Chloride_shift.
[265] https://en.wikipedia.org/wiki/Haldane_effect.
[266] https://en.wikipedia.org/wiki/Chloride_shift#Mechanism.
[267] https://en.wikipedia.org/wiki/Carbon_dioxide#Content.
[268] https://en.wikipedia.org/wiki/Hemoglobin.
[269] https://en.wikipedia.org/wiki/Haldane_effect.

[270] Freitas RA Jr. "Appendix B. Concentrations of Human Blood Components", Nanomedicine, Volume I: Basic Capabilities, Landes Bioscience, Georgetown, TX, 1999, pp. 387-392; http://www.nanomedicine.com/NMI/AppendixB.htm.

We can envision a **Blood Extraction Subunit** that receives the entire venous outflow from the two renal veins (the full venous output from both kidneys), routes it through a vascular tree into an artificial nanomechanical capillary bed or "nanofilter",[271] then returns the blood to the renal veins whereupon it resumes its normal journey to the inferior vena cava,[272] the right atrium of the heart, and onward to the lungs. During this process the renal blood flow, representing $f_{renal} \sim 20\%$ by volume[273] of the entire circulation of $\nu_{blood} \sim 5400$ cm^3/min, has 99% of its stored CO_2 removed with its red cells fully reoxygenated using O_2 generated by the Nutrient Synthesis Unit (Section 4.1.2), supplemented from a small refillable onboard pressure tank[274] containing compressed O_2 if necessary – the BES essentially acting as a mini blood oxygenator.[275] A description of exactly how blood moves through the nanofilter is an important design detail but is beyond the scope of this document and must be left to future work.

As RBCs containing CO_2-laden **carbaminohemoglobin** pass through the nanofilter, exposing them to elevated pO_2 will prompt the spontaneous release of most of the CO_2, due to the Haldane effect. Maintaining a pCO_2 of 40 mmHg or less prevents the CO_2 from re-binding. Using the simplifying assumption that the fraction of carbamino-bound CO_2 released tracks approximately with O_2-saturation (i.e., that binding of each O_2 molecule ejects one CO_2 carbamate, and that free CO_2 in the gas phase at $pCO_2 \leq 40$ mmHg does not appreciably re-bind), then the oxy-hemoglobin dissociation curve[276] predicts that a pO_2 = **150 mmHg** would offload $f_{carb} \sim 99\%$ of the CO_2 for $pCO_2 \sim 40$ mmHg (normal physiological conditions).[277] Under typical alveolar conditions ($pCO_2 \leq 40$ mmHg), the rate-limiting step for carbamino-CO_2 off-loading is the red-cell anion exchange (the "Hamburger shift") coupled to O_2 binding. Experimental studies in adult human RBCs at 37 °C show that 99% CO_2 equilibration is reached within a nanofilter capillary transit time of $t_{carb} \sim$ **0.7 sec**.[278]

Regarding the extraction of CO_2 from the **bicarbonate** in venous RBCs, the fraction of CO_2 released under the Haldane effect also tracks directly with hemoglobin's O_2-saturation, thus also requires ~**150 mmHg O_2** at $pCO_2 \sim 40$ mmHg. The rate-limiting chloride shift has an

---

[271] https://en.wikipedia.org/wiki/Hemofiltration.
[272] https://en.wikipedia.org/wiki/Inferior_vena_cava.
[273] https://en.wikipedia.org/wiki/Renal_circulation.

[274] The energy used to compress NSU-produced O_2 for high-pressure tank storage can in principle be mostly recovered when the O_2 molecules are withdrawn from the tank, so the power consumption for tank operation can be minimal in a properly designed system.

[275] https://en.wikipedia.org/wiki/Oxygenator.
[276] https://en.wikipedia.org/wiki/Oxygen%E2%80%93hemoglobin_dissociation_curve.

[277] From the Hill equation,* fractional release $S = (pO_2^n) / (pO_2^n + P_{50}^n) = 0.99$, therefore $pO_2 \sim 150$ mmHg, taking $P_{50} = 26.6$ mmHg, Hill $n \sim 2.7$; https://en.wikipedia.org/wiki/Hill_equation_%28biochemistry%29.
* Hill AV. The possible effects of the aggregation of the molecules of haemoglobin on its dissociation curves. J Physiol. 1910; 40 Suppl. iv-vii.)

[278] https://bionumbers.hms.harvard.edu/bionumber.aspx?id=110883&s=n&v=9.

approximate 50% equilibration (half-time) of 0.138 sec under physiological conditions.[279] Treating that step as a first-order process (time constant $\tau_{bicarb} \sim t_{1/2} / \ln(2) \sim 0.2$ sec), the time to remove a fraction f_{bicarb} of the bicarbonate-derived CO_2 is $t_{bicarb} = t(f_{bicarb}) = -\tau_{bicarb} \ln(1 - f_{bicarb}) \sim$ **0.9 sec**, taking $f_{bicarb} = 0.99$.

Regarding the extraction of the remaining 5-10% of CO_2 that is **dissolved in blood plasma**, solvation is governed by Henry's law and in equilibrium exerts a partial pressure equal to the blood's pCO_2 of ~46 mmHg (range 41-51 mmHg) in mixed venous blood.[280] De-gassing a given fraction of the dissolved CO_2 requires lowering the external pCO_2 to below the internal pCO_2 until the desired proportion diffuses out, hence 99% removal would require lowering the external pCO_2 to $\leq$ 1% of the venous pCO_2, or (0.01) (46 mmHg) ~ **0.46 mmHg CO_2**. The degassing process depends solely on the CO_2 partial-pressure gradient, so the external pO_2 has no effect on the off-loading of the dissolved fraction. Unfortunately, reducing pCO_2 from the normal physiological level of ~40 mmHg down to ~0.46 mmHg would seriously disturb the acid-base homeostasis of the blood (normally maintained by the lungs and the kidneys),[281] leading to respiratory alkalosis, cessation of voluntary respiration,[282] and other common symptoms of hypocapnia,[283] so for simplicity we will forgo any attempt to retrieve this last remnant of CO_2 from the blood.[284] Leaving pCO_2 close to 40 mmHg maintains the respiratory drive.[285]

What are some likely specifications for the nanofilter component of the Blood Extraction Subunit? We will assume our resting 70 kg male produces $R_{CO2} \sim 884$ gm/day of CO_2 waste at the basal metabolic rate (**Table 5**), or $r_{CO2} = 1.40 \times 10^{20}$ molecules/sec of CO_2 that the nanofilter

---

[279] Hemingway A, Hemingway CJ, Roughton FJ. The rate of the chloride shift of respiration studied with a rapid filtration method. Respir Physiol. 1970 Jul;10(1):1-9; https://www.sciencedirect.com/science/article/abs/pii/0034568770900216.

[280] https://en.wikipedia.org/wiki/Carbon_dioxide#Content.
[281] https://en.wikipedia.org/wiki/Acid-base_homeostasis.

[282] Dempsey JA, Smith CA, Przybylowski T, Chenuel B, Xie A, Nakayama H, Skatrud JB. The ventilatory responsiveness to CO(2) below eupnoea as a determinant of ventilatory stability in sleep. J Physiol. 2004 Oct 1;560(Pt 1):1-11; https://pmc.ncbi.nlm.nih.gov/articles/PMC1665213/.

[283] https://en.wikipedia.org/wiki/Hypocapnia#Effects.

[284] If necessary, the 1% of the target carbamino and bicarbonate CO_2 mass that we fail to extract (because $f_{carb} = f_{bicarb} = 0.99$) and the 5-10% of target solvated CO_2 mass that we're neglecting could be fully recovered by increasing the notional target by 6-11% (e.g., to ~960 gm/day of CO_2 instead of 884 gm/day), increasing all nanofilter size and power estimates by 6-11%, because the original target requires extracting only ~53% of available venous CO_2 and because hyperventilation can safely drive arterial pCO_2 as low as 30-35 mmHg without permanent ill effect (making still more CO_2 safely available for extraction).[*]
[*] Zhang Z, Guo Q, Wang E. Hyperventilation in neurological patients: from physiology to outcome evidence. Curr Opin Anaesthesiol. 2019 Oct;32(5):568-573; https://pmc.ncbi.nlm.nih.gov/articles/PMC6735527/. See also: Sharma S, Hashmi MF. Hypocarbia. StatPearls [Internet], 19 Feb 2023; https://www.ncbi.nlm.nih.gov/books/NBK493167/.

[285] Kurian T, Paramez AR, Thomas M, Mampilly EM, Thelac P. Central Sleep Apnea. Pulmon. 2022 May-Aug; 24(2):59-62; https://journals.lww.com/pulmon/fulltext/2022/05000/central_sleep_apnea.2.aspx.

must remove. For clarity, this is roughly the experimentally measured rate at which CO_2 is removed from the blood passing through the human lungs and is subsequently exhaled.[286] If not removed, these molecules would add a concentration of $c_{initial} \sim r_{CO2} / \nu_{nanofilter} = 7.78 \times 10^{-3}$ molecules/nm^3 (~53% of the normal physiological concentration[287] of 1.48×10^{-2} molecules/nm^3). These must be drawn down to a concentration of $c_{final} = 1.25 \times 10^{-3}$ molecules/nm^3 to achieve the 40 mmHg CO_2 target. For sorting rotors, the thermodynamic extraction energy is $\Delta G \sim k_B T \ln(c_{initial}/c_{final}) \sim 7.8 \times 10^{-21}$ J/molecule, giving a continuous total rotor power demand of $P_{cap} = r_{CO2} \Delta G \sim$ **1.1 W**. The rotor sorting rate for CO_2 is $r_{sort} \sim c_{avg} r_{max} / c_{max} \sim 31{,}000$ molecules/rotor-sec, taking geometric average CO_2 concentration $c_{avg} \sim 3.1 \times 10^{-3}$ molecules/nm^3, which would imply a need for $N_{bloodrotors} = r_{CO2} / r_{sort} \sim 4.5 \times 10^{15}$ rotors with a total capillary-facing area of $A_{rotors} = A_{rot} N_{rotors} =$ **0.4 m^2** and a total rotor volume $V_{rotors} = V_{rot} N_{rotors} =$ **6 mm^3** and mass $M_{rotors} = M_{rot} N_{rotors} =$ **9 mg**.

The blood flow through the nanofilter is $\nu_{nanofilter} = f_{renal} \nu_{blood} \sim 18$ cm^3/sec. Assuming nanofilter capillaries of width $w_{cap} \sim 15$ μm, length $L_{cap} \sim 1$ cm, and a blood residence time $t_{cap} \sim 5$ sec (>> t_{carb}, t_{bicarb}), then the nanofilter consists of $N_{cap} = t_{cap} \nu_{nanofilter} / w_{cap}^2 L_{cap} = 40$ million capillaries of total volume $V_{cap} = w_{cap}^2 L_{cap} N_{cap} \sim 90$ cm^3 and surface area $A_{cap} = 4 w_{cap} L_{cap} N_{cap} \sim$ **24 m^2** (>> A_{rotors}). Each gas-permeable capillary is surrounded by an $x_{jacket} = 1$ μm thick jacket pressurized to 120 mmHg with O_2 sourced from the NSU and an optional small storage tank, increasing total capillary volume from $V_{cap} \sim 90$ cm^3 to $V_{cap+jacket} = (w_{cap} + x_{jacket})^2 L_{cap} N_{cap} \sim 100$ cm^3. Biological capillaries represent ~49% of the total vascular volume in the human kidney[288] and ~60% in the liver,[289] which suggests that a nanofilter with comparable "plumbing"

---

[286] In a study of 20 healthy volunteers (mean weight 73.6 ± 16.3 kg), resting CO_2 production (VCO_2) experimentally measured by breath-by-breath indirect calorimetry was 221.3 ± 57.2 mL CO_2/min,[*] or $(VCO_2)(N_A)$ / (22.4 L/mole at STP) ~ 0.7-1.3 x 10^{20} molecules/sec of CO_2.
[*] Popp CJ, Tisch JJ, Sakarcan KE, Bridges WC, Jesch ED. Approximate Time to Steady-state Resting Energy Expenditure Using Indirect Calorimetry in Young, Healthy Adults. Front Nutr. 2016 Nov 3;3:49; https://pmc.ncbi.nlm.nih.gov/articles/PMC5093115/.

[287] The concentration of CO_2 in venous whole blood[*] is 9.8-11.8 x 10^{-4} gm/cm^3 ~ 1.48 x 10^{-2} molecules/nm^3 (range 1.34-1.62 x 10^{-2} molecules/nm^3).
[*] Freitas RA Jr. "Appendix B. Concentrations of Human Blood Components", Nanomedicine, Volume I: Basic Capabilities, Landes Bioscience, Georgetown, TX, 1999, pp. 387-392; http://www.nanomedicine.com/NMI/AppendixB.htm.

[288] Kidney capillary volume ~ tuft volume of glomerular capillaries + peritubular capillaries ~ (4.21 x 10^6 μm^3/glomerulus)[*] (10^6 glomeruli/kidney) + (105.8 cm^3 cortical volume)[†] (12% peritubular capillary volume fraction)[‡] ~ 16.9 cm^3; kidney intravascular blood volume (including arteries, arterioles, capillaries, venules, and veins)[**] ~ 34.8 cm^3; 16.9 cm^3 / 34.8 cm^3 = 48.6%.
[*] https://www.researchgate.net/scientific-contributions/JM-Macleod-26270998.
[†] Muto NS, Kamishima T, Harris AA, Kato F, Onodera Y, Terae S, Shirato H. Renal cortical volume measured using automatic contouring software for computed tomography and its relationship with BMI, age and renal function. Eur J Radiol. 2011 Apr;78(1):151-6; https://pubmed.ncbi.nlm.nih.gov/19914788/.
[‡] Freitas F, Attwell D. Pericyte-mediated constriction of renal capillaries evokes no-reflow and kidney injury following ischaemia. Elife. 2022 Mar 14;11:e74211; https://pmc.ncbi.nlm.nih.gov/articles/PMC8947765/.
[**] Effros RM, Lowenstein J, Baldwin DS, Chinard FP. Vascular and extravascular volumes of the kidney of man. Circ Res. 1967 Feb;20(2):162-73; https://www.ahajournals.org/doi/reader/10.1161/01.RES.20.2.162.

geometry should have a total volume of $V_{nanofilter} \sim V_{cap+jacket} / f_{cap} \sim$ **180 cm^3**, taking capillary fraction $f_{cap} \sim 55\%$, with a mass of $M_{nanofilter} \sim$ **180 gm**, assuming ~water density of the device.

The nanofilter also provides the means for injecting $N_{nutrients} \sim 1.57 \times 10^{25}$ molecules/day or $R_{nutrientsV} \sim 10.8$ mm^3/sec of mechanosynthetically fabricated nutrient molecules[290] back into the bloodstream, from the Nutrient Synthesis Unit. A mechanical transport system of similar design to the one described in Section 4.2.1 for urine waste can transport this nutrient flow requirement with a tube volume of $(R_{nutrientsV} / V_{transfer}) V_{tube} \sim$ **4.0 cm^3**, mass $(R_{nutrientsV} / V_{transfer}) M_{tube} \sim$ **0.7 gm**, and transport power $(R_{nutrientsV} / V_{transfer}) V_{tube} \sim$ **4.6 W**. These molecules are then conveyed into the bloodstream using $N_{nutrientrotors} \sim N_{nutrients} / t_{day}\ r_{max} \sim 1.82 \times 10^{14}$ bloodstream-interfacing sorting rotors of mass $M_{rot}\ N_{nutrientrotors} \sim$ **0.4 mg** and volume $V_{rot}\ N_{nutrientrotors} \sim$ **0.25 mm^3**, with negligible power use because the molecules are being transferred from a region of high concentration to a region of low concentration. Note that returning fully oxygenated blood through the pulmonary artery should not elicit hypoxic pulmonary vasoconstriction (HPV)[291] which is inhibited by normal or high alveolar PO_2 – alveolar hyperoxia actually produces a mild vasodilatory effect in pulmonary vessels,[292] not constriction – and clinical cardiopulmonary bypass (CPB) experience confirms that pulmonary artery perfusion with oxygenated blood is well-tolerated and often protective of lung function.[293]

How does the performance of the Blood Extraction Subunit compare to the CO_2-extraction performance of the lungs? Together, the two human lungs[294] of volume $V_{lungs} \sim$ **6000 cm^3** (and mass $M_{lungs} \sim$ **1.3 kg**)[295] can process $\nu_{lungblood} \sim 7200$ L/day = **83 cm^3/sec** of whole blood given the resting cardiac output of ~5 L/min,[296] for an average 70 kg human male at rest. The power

---

[289] Richard Bowen, "Physiology of the Hepatic Vascular System," VIVO Pathophysiology, Colorado State University, 2002; https://vivo.colostate.edu/hbooks/pathphys/digestion/liver/bloodsys.html.

[290] $R_{nutrientsM} \sim 0.0151$ gm/sec (~1304.1 gm/day; **Table 8**) or $R_{nutrientsV} \sim R_{nutrientsM} / \rho_{nutrients} \sim 0.0108$ cm^3/sec, assuming average nutrient density $\rho_{nutrients} \sim \rho_{lost16} \sim 1.40$ gm/cm^3 (**Section 4.2.3 (3)**).

[291] Farrell S, Curley GF. Respiration: ventilation. Anesthesia Inten Care Med. 2021 Mar; 22(3):179-184; https://www.sciencedirect.com/science/article/abs/pii/S1472029921000126.

[292] https://en.wikipedia.org/wiki/Oxygen_therapy#Pulmonary_vasodilation.

[293] Santini F, Onorati F, Telesca M, Patelli F, Berton G, Franchi G, Faggian G, Mazzucco A. Pulsatile pulmonary perfusion with oxygenated blood ameliorates pulmonary hemodynamic and respiratory indices in low-risk coronary artery bypass patients. Eur J Cardiothorac Surg. 2011 Oct;40(4):794-803.; https://academic.oup.com/ejcts/article/40/4/794/447627. Buggeskov KB, Sundskard MM, Jonassen T, Andersen LW, Secher NH, Ravn HB, Steinbrüchel DA, Jakobsen JC, Wetterslev J. Pulmonary artery perfusion versus no pulmonary perfusion during cardiopulmonary bypass in patients with COPD: a randomised clinical trial. BMJ Open Respir Res. 2016 Sep 6;3(1):e000146; https://pmc.ncbi.nlm.nih.gov/articles/PMC5020677/.

[294] https://en.wikipedia.org/wiki/Lung_volumes_and_capacities.
[295] https://en.wikipedia.org/wiki/Lung.
[296] https://en.wikipedia.org/wiki/Cardiac_output.

consumption of the lungs is P_{lungs} ~ **5.7 W**, which includes ~5 W for the work of breathing[297] and ~0.7 W for lung cell metabolism.[298]

From these estimates we can conclude that the Blood Extraction Subunit, as described above but augmented with tenfold redundancy in all nanomechanical components (Section 4.3.1), has a (P_{cap} V_{lungs} / $V_{nanofilter}$ P_{lungs}) ~ **6.4 times higher power density** and ($\nu_{nanofilter}$ P_{lungs} / P_{cap} $\nu_{lungblood}$) ~ **110% of the energy efficiency** (i.e., power consumed per cm^3/sec of output) of the biological human lungs, and only ($\nu_{nanofilter}$ M_{lungs} / $M_{nanofilter}$ $\nu_{lungblood}$) ~ **1.6 times more productive per unit mass** (i.e., cm^3/sec of output per kg of device) and ($\nu_{nanofilter}$ V_{lungs} / $V_{nanofilter}$ $\nu_{lungblood}$) ~ **7.2 times more productive per unit volume** (i.e., cm^3/sec of output per cm^3 of device) than the biological human lungs.

4.2.3 Supplemental Nutrient Atoms

After most of the waste molecules have been recovered from urine by the Urine Extraction Subunit and from blood by the Blood Extraction Subunit, a small remnant of waste molecules may be permanently lost from the body via other avenues. **Table 14** summarizes the estimated mass flow of waste molecules that are excreted intestinally (feces) and dermally (sweat) and thus would evade recapture by the two previously described nanorobotic processing subunits. These estimates include the f_{conc} ~ 1% of urinary waste molecules that will not be captured by the UES sorting rotors (Section 4.2.1) and thus will be lost to micturition.

---

[297] In a normal resting state the work of breathing constitutes about 5% of the total body oxygen consumption (https://en.wikipedia.org/wiki/Work_of_breathing), or ~5 W for a ~100 W person.

[298] "Residual organs" like lungs have a specific resting metabolic rate of ~11.6 kcal/kg/day,* or ~0.73 W assuming ~1.3 kg of lung tissue in a 70 kg human male.

* Wang Z, Ying Z, Bosy-Westphal A, Zhang J, Schautz B, Later W, Heymsfield SB, Müller MJ. Specific metabolic rates of major organs and tissues across adulthood: evaluation by mechanistic model of resting energy expenditure. Am J Clin Nutr. 2010 Dec;92(6):1369-77; https://pmc.ncbi.nlm.nih.gov/articles/PMC2980962/.

Table 14. Estimated "lost" waste molecules and ions excreted in feces and sweat for a 70 kg male human body at the ~100 watt basal metabolic rate, i.e., "supplemental nutrition"

Waste Molecule	Formula	gm/day	gm/mole	molecules/day
Urea	H_2NCONH_2	0.7758	60.1	7.77×10^{21}
Creatinine	$C_4H_7N_3O$	0.0204	113.1	1.09×10^{20}
Uric acid	$C_5H_4N_4O_3$	0.16195	168.1	5.80×10^{20}
Hippuric acid	$C_9H_9NO_3$	0.1572	179.2	5.28×10^{20}
Sulfate anion	SO_4^{2-}	0.064879	96.1	4.07×10^{20}
Ammonium ion	NH_4^+	0.0721	18.0	2.41×10^{21}
Phosphate ion	equiv. P	0.1124	31.0	2.18×10^{21}
Bilirubin	$C_{33}H_{36}N_4O_6$	0.280	584.7	2.88×10^{20}
Cholic acid	$C_{24}H_{40}O_5$	0.200	408.6	2.95×10^{20}
Cheno-/deoxycholic acid	$C_{24}H_{40}O_5$	0.300	392.6	4.60×10^{20}
Cholesterol	$C_{27}H_{46}O$	1.000	385.7	1.56×10^{21}
Sodium	Na^+	0.27358	23.0	7.16×10^{21}
Potassium	K^+	0.14983	39.1	2.31×10^{21}
Chloride	Cl^-	0.419	35.5	7.11×10^{21}
Iodide	I^-	0.0000213	126.9	1.01×10^{17}
Calcium	Ca^{2+}	0.1486	40.1	2.23×10^{21}
Magnesium	Mg^{2+}	0.03786	24.3	9.38×10^{20}
Zinc	Zn^{2+}	0.0008525	65.4	7.85×10^{18}
Iron	Fe^{3+}	0.0009307	55.8	1.00×10^{19}
Manganese	Mn^{3+}	0.0022802	54.9	2.50×10^{19}
Copper	Cu^{2+}	0.000801	63.5	7.60×10^{18}
Selenium	SeO_3^{2-}	0.00002778	79.0	2.12×10^{17}
Chromium	Cr^{3+}	0.00000728	52.0	8.43×10^{16}
Molybdenum	MoO_4^{2-}	0.00001134	95.9	7.12×10^{16}
Cobalt (as cobalamin)	$C_{63}H_{88}CoN_{14}O_{14}P$	0.000002202	1355.4	9.78×10^{14}
0.3% of Miscwastium	$\sim C_{19}H_{15}O_{10}$	0.1785	403.0	2.67×10^{20}
Totals		**4.36**		**3.67×10^{22}**

Table 15 gives the estimated total atom numbers and grams per day for all "lost" waste molecules listed in **Table 14** that might have to be provided as supplemental nutrition to allow a human equipped with a metabolic organ to be completely self-sufficient in the absence of conventional food input. The potentially "lost" atoms for these key 20 chemical elements represent a relatively small ~0.3% of all waste product mass and ~0.4% of all waste product atoms.

Table 15. Nominal atom counts and grams per day for all "lost" waste molecules and ions					
Chemical Element	**Total Atoms (atoms/day)**	**Process Rate (gm/day)**	**Chemical Element**	**Total Atoms (atoms/day)**	**Process Rate (gm/day)**
C	9.06×10^{22}	1.81	Zn	7.85×10^{18}	0.00085
H	1.65×10^{23}	0.27	Fe	1.00×10^{19}	0.00093
N	2.23×10^{22}	0.52	Mn	2.50×10^{19}	0.00228
O	2.21×10^{22}	0.59	Cu	7.60×10^{18}	0.00080
S	4.07×10^{20}	0.022	I	1.01×10^{17}	0.000021
K	2.31×10^{21}	0.15	Se	2.12×10^{17}	0.000028
Cl	7.11×10^{21}	0.42	Cr	8.43×10^{16}	0.000007
Na	7.16×10^{21}	0.27	Mo	7.12×10^{16}	0.000011
Ca	2.23×10^{21}	0.15	Co	9.78×10^{14}	0.0000001
P	2.18×10^{21}	0.11			
Mg	9.38×10^{20}	0.038	**Totals**	**3.22×10^{23}**	**4.36**

Given the desire to enable the metabolic organ-equipped person to become as nutritionally independent as possible, at least four possible mitigation strategies for generating or supplying these supplemental atoms to the Nutrient Synthesis Unit have been identified, enabling the user's nutritional needs to be fully met by the device:

(1) **Enhanced bloodstream withdrawals: C, H, and O**. Obtaining the missing 1.81 gm/day of **carbon** (**Table 15**) requires extracting an additional (1.81 gm/day C) (44 gm/mole CO_2) / (12 gm/mole C) = **6.64 gm/day of CO_2** waste from the bloodstream – an additional 0.75% above the 884 gm/day already being extracted by the Blood Extraction Subunit (Section 4.2.2). This could be accomplished by increasing the CO_2 rotor count in the Blood Extraction Subunit from $N_{rotors} \sim 4.50 \times 10^{15}$ rotors to just 4.53×10^{15} CO_2 rotors, or by dropping the blood pCO_2 from 40 mmHg to perhaps 38 mmHg to increase extraction of plasma-dissolved CO_2,[299] with any extra carbon supplied from atmospheric sources and an altered respiratory gas mix in the lungs. Obtaining the missing 0.27 gm/day of **hydrogen** only requires extracting an additional (0.27 gm/day H) (18 gm/mole H_2O) / (2) (1 gm/mole H) = **2.43 gm/day of H_2O** from the bloodstream – an additional 0.68% above the 355 gm/day already being extracted by the Urine Extraction Subunit (Section 4.2.1) – which can be accomplished by increasing the H_2O rotor count from $N_{H2Orotors} \sim 1.37 \times 10^{14}$ rotors to just 1.38×10^{15} water rotors in the UES. The 0.69 gm/day shortfall of **oxygen** is fully covered by the above two supplemental extractions which together generate 6.99 gm/day of oxygen,[300] a 6.30 gm/day O_2 surplus.

---

[299] Whole blood holds ~10^{-3} gm/cm^3 CO_2 x 5400 cm^3 whole blood ~ 5.4 gm CO_2 at any given time, of which 5-10% or 0.27-0.54 gm is dissolved in plasma water.

[300] (1.81 gm/day C) (32 gm/mole O_2) / (12 gm/mole C) = 4.83 gm/day of O_2 and (2.43 gm/day H_2O) (16 gm/mole O) / (18 gm/mole H_2O) = 2.16 gm/day of O_2; 4.83 gm/day + 2.16 gm/day = 6.99 gm/day of O_2.

(2) **Atmospheric sourcing: N**. Atmospheric nitrogen (~78% N_2 in air) is present in the lungs and dissolves in whole blood in constant equilibrium with the air at a normal concentration of $c_{N2} \sim 8.2 \times 10^{-6}$ gm/cm^3.[301] The Blood Extraction Subunit could extract the missing $f_{N2}\ c_{N2}\ \nu_{nanofilter}$ = 0.52 gm/day of **nitrogen** (**Table 15**) using a small number of sorting rotors that need only remove $f_{N2} \sim 4\%$ of the N_2 present in the blood, taking $\nu_{nanofilter} \sim 18$ cm^3/sec (Section 4.2.2). There are no other elements in deficit supply that are practical to source from the atmosphere.

(3) **Storage or Periodic Resupply**. Eliminating all CHON shortages leaves $m_{lost16} \sim 1.17$ gm/day of "lost" atoms that we need to resupply, or a volume of $V_{lost16} = m_{lost16} / \rho_{lost16} \sim 0.84$ cm^3/day of nutritional supplement assuming efficient storage and a process-mass-weighted average pure-element density of $\rho_{lost16} \sim 1.40$ gm/cm^3 for the remaining 16 chemical elements. This supplement could be provided by orally swallowing a comfortably-sized single daily 1.5 cm x 0.75 cm pill, or by receiving a daily 0.84 cm^3 injection or infusion of the supplement, preferably via a permanently-implanted dermal nanorobotic intravenous injection port that might already be commonplace among future human populations to allow quick administration of medical nanorobots. (Metered dose inhalers that typically provide up to ~20 mm^3/dose of aerosolized liquid medication are impractical because too many doses would be required.) *In situ* long-term storage is another possibility, requiring a ~25 cm^3 tank (~ping pong ball size) for a 1-month supply of nutritional supplement or a $V_{tank} \sim$ **300 cm^3** tank (~size of 12 oz soda can or a human heart) for a 1-year supply, of mass $M_{tank} = V_{tank}\ \rho_{lost16} \sim$ **420 gm**.

(4) **Bone resorption: Ca, P, and Mg**. The skeleton of a 70 kg human male has a mass of ~9.2 kg and includes ~1000 gm of Ca, 380 gm of P, and 35 gm of Mg.[302] When dietary intake is insufficient, the body compensates by mobilizing these elements from bone, which serves as a natural *in situ* mineral reservoir. The process is physiologically regulated and occurs through bone resorption, primarily mediated by osteoclasts and controlled by hormonal signaling. The principal hormone that triggers and increases bone resorption is parathyroid hormone (PTH). Normal bloodstream levels of PTH are 10-65 pg/cm^3, but when PTH exceeds 65-70 pg/cm^3 on a sustained basis (e.g., released into the bloodstream by the Blood Extraction Subunit), bone resorption may occur[303] in the amounts of ~0.5 gm/day of Ca^{2+},[304] ~0.2 gm/day of PO_4^{3-},[305] and

---

[301] Freitas RA Jr. "Appendix B. Concentrations of Human Blood Components", Nanomedicine, Volume I: Basic Capabilities, Landes Bioscience, Georgetown, TX, 1999, pp. 387-392; http://www.nanomedicine.com/NMI/AppendixB.htm.

[302] Ciosek Ż, Kot K, Kosik-Bogacka D, Łanocha-Arendarczyk N, Rotter I. The Effects of Calcium, Magnesium, Phosphorus, Fluoride, and Lead on Bone Tissue. Biomolecules. 2021 Mar 28;11(4):506; https://pmc.ncbi.nlm.nih.gov/articles/PMC8066206/.

[303] Frolik CA, Black EC, Cain RL, Satterwhite JH, Brown-Augsburger PL, Sato M, Hock JM. Anabolic and catabolic bone effects of human parathyroid hormone (1-34) are predicted by duration of hormone exposure. Bone. 2003 Sep;33(3):372-9; https://pubmed.ncbi.nlm.nih.gov/13678779/.

[304] Goltzman D. Approach to Hypercalcemia. Endotext [Internet], 17 Apr 2023; https://www.ncbi.nlm.nih.gov/books/NBK279129/.

[305] Goretti Penido M, Alon US. Phosphate homeostasis and its role in bone health. Pediatr Nephrol. 2012 Nov;27(11):2039-2048; https://pmc.ncbi.nlm.nih.gov/articles/PMC3461213/.

0.01-0.04 gm/day of Mg^{2+},[306] about enough to cover the apparent shortfalls of these 3 elements listed in **Table 15**. Assuming at most a ~10% loss of bone mass might be tolerable,[307] the bone mineral reservoir could temporarily supply the mineral supplement for up to ~670 days (Ca), ~350 days (P), and ~90 days (Mg). Unfortunately there are no similar conveniently large reservoirs of Na, K, Cl or S in the body to draw upon.

4.3 Summary of Artificial Metabolic Organ Structure and Operation

4.3.1 Reliability and Redundancy

Permanently implanted nanorobotic systems that are incapable of self-repair (unlike biological systems) must be biocompatible[308] and extremely reliable unless some means for full replacement or *in situ* repair is provided.[309] To accomplish high reliability, the author's previous medical nanorobot designs including respirocytes,[310] vasculocytes,[311] vasculoid,[312] microbivores,[313] and

---

[306] Rude RK, Gruber HE. Magnesium deficiency and osteoporosis: animal and human observations. J Nutr Biochem. 2004 Dec;15(12):710-6; https://pubmed.ncbi.nlm.nih.gov/15607643/.

[307] https://www.osteoporosis.foundation/facts-statistics/epidemiology-of-osteoporosis-and-fragility-fractures.

[308] Freitas RA Jr. Nanomedicine, Volume IIA: Biocompatibility. Landes Bioscience, Georgetown, TX, 2003; http://www.nanomedicine.com/NMIIA.htm.

[309] Providing a dermal port that allows direct physical access to the implanted device would make this possible if the layout explicitly incorporates at least partial repairability (e.g., access channels, plug-in modules, etc) as a major design criterion.

[310] Freitas RA Jr. Exploratory design in medical nanotechnology: a mechanical artificial red cell. Artif Cells Blood Substit Immobil Biotechnol. 1998 Jul;26(4):411-30; https://www.tandfonline.com/doi/pdf/10.3109/10731199809117682. A longer version of this paper appears at: https://web.archive.org/web/20100420085137/http://www.foresight.org/Nanomedicine/Respirocytes.html.

[311] Freitas RA Jr. Chapter 23. Comprehensive Nanorobotic Control of Human Morbidity and Aging, Section 6.2.3 "Heart and Vascular Disease". In: Fahy GM, West MD, Coles LS, Harris SB, eds, The Future of Aging: Pathways to Human Life Extension, Springer, New York, 2010, pp. 685-805; http://www.nanomedicine.com/Papers/Aging.pdf.

[312] Freitas RA Jr., Phoenix CJ. Vasculoid: A personal nanomedical appliance to replace human blood. J Evol Technol. 2002 Apr;11:1-139; http://www.jetpress.org/volume11/vasculoid.pdf.

[313] Freitas RA Jr. Microbivores: Artificial mechanical phagocytes using digest and discharge protocol. J Evol Technol 2005;14:1-52; http://www.jetpress.org/volume14/freitas.html.

chromallocytes[314] have all incorporated the general principle of **10-fold redundancy** among all major nanoscale mechanical components.

If we accept Drexler's assertion that systematic failure rates for nanomachines are dominated by radiation damage effects,[315] then we can apply his nanomachine radiation damage model to a system comprising N_c components each of which is composed of n redundant parts. In this case, the probability P_{op} that the system remains operational after $t_{lifetime}$ (yr) is $P_{op} = \exp(-N_c (1 - p_{op})^n)$ and the annual probability of failure is $(1 - P_{op})$, where the probability that an individual part remains operational is $p_{op} \sim \exp(-10^{15} D_{rad} m_{part})$, m_{part} is the mass of the part in kg, and $D_{rad} \sim 0.5 t_{lifetime}$ is the radiation dose (in rads) for normal background radiation in the terrestrial environment.

For the **Nutrient Synthesis Unit** (Section 4.1.2) with $N_c = N_{FS} \sim 890$ trillion Nanofabricators. Assuming each Nanofabricator includes ~1000 nanoparts each of mass $m_{part} = M_{FS} / 1000 = 2 \times 10^{-21}$ kg, the annual probability of failure is $(1 - P_{op}) \sim$ **10^{-2}/yr** for n = 3 and ~**10^{-14}/yr** for n = 5. For the **Urinary Extraction Subunit** (Section 4.2.1) with $N_c = N_{urinerotors} + N_{H2Orotors} \sim 4.35 \times 10^{15}$ sorting rotors, and assuming each rotor includes ~10 nanoparts each of mass $m_{part} = M_{rotor} / 10 = 2 \times 10^{-22}$ kg, then the annual probability of failure is $(1 - P_{op}) \sim$ **10^{-5}/yr** for n = 3, ~**10^{-19}/yr** for n = 5. The probability is about the same for the **Blood Extraction Subunit** (Section 4.2.2) which has almost the same $N_c = N_{rotors} \sim 4.5 \times 10^{15}$ sorting rotors. Specifying n = 10 fold redundancy instead of 5-fold should provide a significant extra margin of reliability. Note that including this additional nanomachinery increases device mass and volume but does not affect power usage, since a redundant component only receives power when it is replacing another similar component that has failed and lost power. It does not seem unreasonable to expect that systems involving ~10^{15} nanomachines, including mechanosynthetic tooltips and related components, can be designed and reliably operated. Even by the late 1990s, Texas Instruments had experimentally demonstrated successful operation of simple micromachines for >10^{18} mechanical cycles without failure.[316]

Many other factors may affect system reliability. For example, sorting rotors operating in a messy protein-rich liquid environment such as whole blood must be designed to withstand clogging and fouling by bloodborne adhesive molecules (Section 4.3.7). Software and control system reliability can also be enhanced by redundancy, with the five onboard Space Shuttle computers[317] providing a well-known classic example. A more complete analysis of the reliability of the metabolic organ must await development of future specific system designs.

---

[314] Freitas RA Jr. The ideal gene delivery vector: Chromallocytes, cell repair nanorobots for chromosome replacement therapy. J Evol Technol 2007;16:1-97; http://jetpress.org/v16/freitas.pdf.

[315] Drexler KE. Nanosystems: Molecular Machinery, Manufacturing, and Computation. John Wiley & Sons, New York, 1992; Section 6.7.2, "System lifetimes"; https://www.amazon.com/dp/0471575186/

[316] Douglass M, Sontheimer A. DLP-device-to-product transition: Defining customer satisfaction deliverables. TI Technical Journal 1998 Jul-Sep; 128-136; http://www.dlp.com/dlp/resources/whitepapers/pdf/titj14.pdf.

[317] Sklaroff JR. Redundancy management technique for Space Shuttle computers. IBM J Res Develop. 1976 Jan; 20:20-28; http://www.research.ibm.com/journal/rd/201/ibmrd2001E.pdf.

Reliability considerations suggest that all nanomechanical components employed in the metabolic organ should be grouped into physical modules or cartridges that permit convenient exchange of new units for failed units via minor surgery and easy access to installed systems. The immense redundancy (trillions of nanodevices) means the AMO can tolerate the random failure of millions of units without performance loss, and faulty components could be cleared or replaced during scheduled maintenance or periodic servicing of the implant.

4.3.2 Computational Requirements

To control the metabolic organ, the single largest computational requirement will be to operate 890 trillion (Section 4.1.2) and 5.5 trillion (Section 4.2.1) mill-style[318] nanofabricators, totaling $N_{nanofabs} \sim 8.955 \times 10^{14}$ nanofabricators, that assemble target nutrient molecules one by one via mechanosynthetic processes. These nanofabricators process a total of 7.62×10^{25} atoms/day in the Nutrient Synthesis Unit (**Table 9**) and 2.22×10^{23} atoms/day in the Urine Extraction Subunit (Section 4.2.1), or $N_{NanofabAtoms} = 7.6422 \times 10^{25}$ atoms/day ~ 8.85×10^{20} atoms/sec.

Mechanosynthetic systems that employ individual **manipulator arms** to pick and place feedstock atoms or molecules to ~20 pm accuracy over tooltip path lengths of ~20 nm can be computationally extremely expensive, requiring $n_{steps} \sim (2)\ (20\ nm) / (20\ pm) \sim 2000$ steps per round-trip motion,[319] $n_{motions} \sim 6$ round trip motions per atom placed,[320] and at least $i_{step} \sim 1$ bit per step, or $I_{atom\text{-}Manip} \sim n_{steps}\ n_{motions}\ i_{step} \sim$ **12,000 bits/atom** placed if no clever shortcuts are employed. By contrast, a mechanosynthetic **mill system** to produce a particular molecule may consist of a number of interlocking short production lines or "loops". The control system need only switch a particular loop on or off, requiring 1 bit of information per loop. The mechanosynthetic mill system illustrated in Section 4.1.1 consists of 6 loops that continuously synthesize ethanol, a 9-atom molecule, which implies $I_{atom\text{-}Mill} \sim$ (1 bit/loop) (6 loops/ 9 atoms) ~ **1 bit/atom**. Assuming roughly linear scaling of the number of production loops with target molecule size, then processing $N_{NanofabAtoms}$ requires $I_{NanofabAtoms} = I_{atom\text{-}Mill}\ N_{NanofabAtoms} \sim$ **8.85×10^{20} bits/sec** of computation by the control system. Taking the experimentally-confirmed[321]

---

[318] Drexler KE. Nanosystems: Molecular Machinery, Manufacturing, and Computation, John Wiley & Sons, New York, 1992, Section 14.4.2, "Products, building blocks, and assembly sequences"; https://www.amazon.com/dp/0471575186/.

[319] Freitas RA Jr., Merkle RC. A Nanofactory Roadmap: Research Proposal for a Comprehensive Diamondoid Nanofactory Development Program. IMM Report No. 58, 2008/2025; Section 3.4.1.4, "Manipulator Speed and NFW Productivity"; http://www.imm.org/Reports/rep058.pdf.

[320] Freitas RA Jr., Merkle RC. A Nanofactory Roadmap: Research Proposal for a Comprehensive Diamondoid Nanofactory Development Program. IMM Report No. 58, 2008/2025; Section 3.2.1.7, "Operation of the MFW"; http://www.imm.org/Reports/rep058.pdf.

[321] Bérut A, Arakelyan A, Petrosyan A, Ciliberto S, Dillenschneider R, Lutz E. Experimental verification of Landauer's principle linking information and thermodynamics. Nature. 2012 Mar 7;483(7388):187-189; https://www.nature.com/articles/nature10872.

classical Landauer limit[322] for non-reversible computational energy dissipation of $E_{Landauer310K}$ = $k_B T \ln(2)$ J/bit ~ 2.97 x 10^{-21} J/bit at T = 310 K (human body temperature) with Boltzmann's constant k_B = 1.381 x 10^{-23} J/K, and assuming an ε ~ 50% energy efficiency for nanocomputer systems, the computational power draw is $P_{NanofabAtoms} = E_{Landauer310K}\ I_{NanofabAtoms} / \varepsilon$ ~ **5.2 W**. Given a specific data processing power of U_{nano} ~ 10^{30} bit/sec-m^3 for advanced diamondoid mechanical nanocomputers,[323] then the volume of nanocomputers needed to control all nanofabricators in the metabolic organ is $V_{NanofabAtoms} = I_{NanofabAtoms} / U_{nano}$ ~ **0.9 mm^3** with a mass of ~**2 mg** assuming devices with ~60% of crystalline diamond density.

Another major subsystem that must be properly controlled is the population of sorting rotors $N_{AllRotors} = N_{urinerotors}$ (Section 4.2.1) + $N_{H2Orotors}$ (Section 4.2.1) + $N_{bloodrotors}$ (Section 4.2.2) + $N_{nutrientrotors}$ (Section 4.2.2) ~ 9 x 10^{15} sorting rotors. These molecular pumps are tasked with absorbing or releasing at most $n_{moltypes}$ ~ 100 different molecules, including CO_2, H_2O, O_2, the 60 nutrient molecules and ions listed in **Table 8**, the 25 waste molecules and ions listed in **Table 12**, and perhaps 1-2 dozen of the currently undetermined molecular components comprising miscwastium (Section 3.8). Most of the time, most of the rotors should be switched on and running at constant speed, but it may be desirable to adjust rotor motion in response to sensor data, e.g., slowing down or switching off some rotors when sensors determine storage has reached capacity for particular molecules. Even if the metabolic organ has $n_{Msensor}$ = 1000 nanosensors for every target molecule and every nanosensor provides i_{read} = 10 bits of data at each reading, a nanocomputer capable of processing only $n_{moltypes}\ n_{Msensor}\ i_{read} / t_{response}$ ~ 10^6 bits/sec could allow continuously altering rotor status with a $t_{response}$ ~ 1 sec response time. Rotor control has low computational intensity because all sorting rotors of a given type can simultaneously receive the same command and be controlled together in groups, possibly averaging $N_{AllRotors} / n_{moltypes}$ ~ 9 x 10^{13} rotors/group in size.

A master automation control system will also be needed to control all processes taking place inside the metabolic organ, including component failure monitoring. A comprehensive analysis is difficult without a detailed system design and thus is outside the scope of this paper, but we can consider the computational requirements for running some of the biggest and most complex factories in the world. For example, the Volkswagen Wolfsburg Automotive Plant covers 6.5 km^2 of land area with ~5000 robots and has an estimated aggregate data processing rate of ~10^9 bits/sec which would imply an annual data archive footprint of ~3 x 10^{16} bits.[324] The TSMC

---

[322] Landauer R. Irreversibility and heat generation in the computing process. IBM J Res Devel. 1961;5:183-191; http://fab.cba.mit.edu/classes/MAS.862/notes/computation/Landauer-1961.pdf. Bennett C, Landauer R. The fundamental physical limits of computation. Sci Am. 1985 Jul;253(1):48-57; http://web.eecs.umich.edu/~taustin/EECS598-HIC/public/Physical-Limits.pdf.

[323] Assuming 1 GHz operation of a $(400\ nm)^3$ CPU,[*] and using 64-bit words: (64 bits/operation) (10^9 operations/sec) / $(400\ nm)^3$ = 1 x 10^{30} bits/sec-m^3.

[*] Drexler KE. Nanosystems: Molecular Machinery, Manufacturing, and Computation, John Wiley & Sons, New York, 1992, Chapter 12, "Nanomechanical Computational Systems"; https://www.amazon.com/dp/0471575186/.

[324] On its private 5G campus network at Wolfsburg, the system achieves "data transmission rates in the gigabit range"; https://www.volkswagen-newsroom.com/en/press-releases/volkswagen-tests-5g-for-production-on-its-way-to-smart-factories-7570.

Leading-Edge Semiconductor Fab processes an estimated 5 x 10^9 bits/sec, implying an annual data archive footprint of ~2 x 10^{17} bits.[325] Ocado Group's Customer Fulfillment Center in Andover UK, the world's most advanced automated warehouse, has 4000 robots which generate 3.7 x 10^8 bit/sec of telemetry[326] and receive ~8.2 x 10^7 bits/sec of commands,[327] for a total computational load of ~4.5 x 10^8 bits/sec, with ~3 x 10^{13} bits of RAM[328] and an inferred annual data archive footprint of ~1 x 10^{16} bits. Individual complex machines have much lower requirements. For example, the Boeing 777 passenger aircraft employs ~ 6 x 10^6 bit/sec of sustained flight-control throughput,[329] with ~4 x 10^9 bits of non-volatile hard data storage (mostly in the cockpit voice recorder) and an Airplane Information Management System requiring ~4 x 10^8 bits for the software.[330]

Assuming $I_{ProcessControl}$ ~ 10^{10} bits/sec processing requirement and $i_{ProcessControl}$ ~ 10^{17} bits of onboard memory, the control computer for the metabolic organ might have a volume of $V_{OrganControl} = I_{ProcessControl} / U_{nano}$ ~ **0.01 µm^3** with a mass of ~**0.02 pg** assuming ~60% diamond density, a power draw of $P_{ProcessControl} = E_{Landauer310K}\ I_{ProcessControl} / \varepsilon$ ~ **60 pW**, plus $i_{ProcessControl} / i_{nano}$ ~ **10 mm^3** and 0.6 $\rho_{diamond}\ i_{ProcessControl} / i_{nano}$ ~ **20 mg** of memory assuming a storage density of i_{nano} ~ 10^{25} bits/m^3 with a t_{nano} = 10^{10} bit/sec data access speed, taking $\rho_{diamond}$ = 3510 gm/cm^3.

The control computer will need appropriate sensors and systems to detect when the user has partaken of regular solid food, and to determine the digestive and metabolic consequences of that action, so that the recycling activities of the metabolic organ can be adjusted to accommodate the supplementary nutritional materials.

One major technical challenge will be to ensure real-time control – for example, the blood extraction rotors might need rapid feedback loops to maintain proper blood gas levels. Latency and reliability in the control network (likely a hierarchical design with local autonomy at the

---

[325] Modern fabs instrument every tool with hundreds of sensors. One report notes a single fab tracking over 500 variables in real time, producing >50 TB of sensor data per day; https://www.softwebsolutions.com/resources/data-analytics-in-semiconductor.html.

[326] https://www.techmonitor.ai/digital-economy/ocado-technology-robot-hive-innovation.

[327] The AI 'air traffic' control system orchestrates the movement of the 4000-robot fleet, communicating with each robot 10 times/sec, a total traffic of 82 Mbits/sec assuming 256 bits/message; https://www.ocadogroup.com/solutions/our-technology.

[328] Assuming Ocado's control stack runs on Kubernetes clusters and simulation servers, a representative cluster might be 50 nodes x 64 GB RAM = 3.2TB of RAM ~ 2.56 x 10^{13} bits.

[329] For the Boeing 777 primary flight-control system itself, all of the pilot-input, autopilot, air-data/inertial-reference and actuator-feedback traffic flows over three fully-redundant ARINC 629 buses, each operating at 2 Mbit/sec, for a total of 6 Mbit/sec; https://en.wikipedia.org/wiki/ARINC_629.

[330] Vittorio Cortellessa, Bojan Cukic, Diego Del Gobbo, Ali Mili, Marcello Napolitano, Mark Shereshevsky, Harjinder Sandhu, "Certifying Adaptive Flight Control Software," 2005; https://web.archive.org/web/20061212093006/http://www.isacc.com/presentations/3c-bc.pdf. See also: http://archive.adaic.com/projects/atwork/boeing.html.

nanodevice level and supervisory control higher up) will be vital. Latency in response to changes in metabolic demand should be low – there are ~1.8 gm of Nanofabricators in the NSU that are always on (Section 4.1.2), and another ~0.3 gm can be powered up for each ~100 W of additional activity metabolism demand (**Table 19**) on a timescale of order $r_{organics}^{-1}$ ~ 10 μsec (Section 4.1.2). The AMO works in concert with residual human metabolic reserves. For instance, if the AMO falls behind, the body can temporarily mobilize glycogen; conversely, if the AMO oversupplies, the body can store a bit as fat or glycogen. The AMO must be able to appropriately manage nutrient levels without causing pathologies like hyperglycemia and ketoacidosis. For example, existing artificial pancreas systems employ control systems that use glucose sensors and pump insulin accordingly.[331]

The sheer number of nanomachine components implies that the system must be largely autonomous or pre-programmed at the nano-level, which highlights a risk: the design may rely on hard-wired behavior for many components, reducing flexibility in response to unforeseen conditions. In practice, one might need the device to adapt or even shut down sections if something goes wrong (e.g., if a portion of the nanofilter clogs, the system should detect and isolate it). The feasibility of error detection at the nanoscale and fail-safes is a key engineering concern, and future design efforts must take account of the possibility of unforeseen emergent problems.

Designers must also address the control logic that interfaces with the body's own homeostasis, ensuring consistent operation in dynamic conditions. For example, the metabolic organ will likely employ sensors for blood glucose, amino acids, and other nutrient levels to adjust its output dynamically, otherwise it could overshoot (making too much of something) or undershoot production. The device could take cues from the body to modulate its activity, such as hormonal signals like insulin or direct sensing of blood metabolite concentrations. Rather than simply running open-loop at a fixed 100 W output, this would allow the device to mimic how a biological pancreas or liver responds to metabolic state, replicating not just the raw throughput but also the regulatory behaviors of the natural organs. The master control system would dynamically adjust NSU and WRU outputs – for instance, if the user suddenly starts running, the device must quickly increase glucose recycling from CO_2 to supply muscles, and the BES must ramp up CO_2 capture accordingly. The device would sense rising CO_2 in venous blood and automatically increase NSU activity to convert it back to glucose, the internal CO_2 → glucose recycler adjusting to metabolic rate. This helps to ensure that the device can handle changing metabolic demands and maintain homeostasis, not just steady-state output. In sum, multiple sensors feed data into the AMO's control algorithms, allowing it to dynamically adjust the output of the nutrient synthesis unit to match the user's current metabolic demand. This feedback control prevents over- or under-supply of nutrients, maintaining homeostasis akin to natural metabolic regulation.

---

[331] Ming W, Guo X, Zhang G, Liu Y, Wang Y, Zhang H, Liang H, Yang Y. Recent advances in the precision control strategy of artificial pancreas. Med Biol Eng Comput. 2024 Jun;62(6):1615-1638; https://pubmed.ncbi.nlm.nih.gov/38418768/.

4.3.3 Power Unit

With the Nutrient Synthesis Unit (Section 4.1) and the Waste Recovery Unit (Section 4.2) already described, it remains only to discuss the energy source for the metabolic organ that will power the mechanosynthetic and transport processes throughout the organ. From **Table 16**, the Power Unit must supply a continuous P_{MetOrg} ~ 200 W of power for ~1 day, or ~**17.3 MJ** of energy. It seems prudent to draw power from an energy storage buffer or battery system (Section 4.3.3.1) whose output can be carefully regulated to match organ energy demand to the available energy sources (Section 4.3.3.2).

4.3.3.1 Flywheel Battery

According to a recent survey[332] of the energy densities of possible energy storage systems, the two systems with the highest energy densities that are fully reversible (i.e., conveniently regulated, discharged, and recharged at will) and thus might be most appropriate for implanted macroscale nanorobotic systems are nonambient chemical combustion and flywheel systems.

Nonambient chemical combustion refers to the combustion of chemical fuels with an oxidant in which both fuel and oxidant are contained entirely within the energy storage system, with no material inputs provided from the environment.[333] The assumption is that the reaction products of combustion are retained, and that the original reactants can be recovered, either by mechanosynthetic or conventional chemical retrosynthetic methods, with the application of externally supplied energy. The range of energy densities for such systems is a respectable **2.7-47.8 MJ/L**. Unfortunately the highest densities are achieved by extremely exotic fuel/oxidant systems, such as $Be+O_8$ (47.8 MJ/L), $Be+F_2$ (41.7 MJ/L), and $Al+O_8$ (39.0 MJ/L). Among the more mundane systems which include no toxic chemicals such as beryllium or fluorine are MgO_2+Al (36.6 MJ/L), Al+$LiClO_4$ (32.1 MJ/L), Al+$N(NO_2)_3$ [trinitramide] (32.0 MJ/L), Al+O_2 (27.0 MJ/L), Al+CO_2 (17.4 MJ/L), $C_{10}H_{16}$ [adamantane]+O_2 (11.6 MJ/L), or C_2H_2 [acetylene]+O_2 (11.1 MJ/L), but many of these require elevated combustion temperatures or very highly compressed oxygen to achieve the indicated energy density. Another disadvantage of such chemical systems is that they commonly release energy mostly in the form of heat, which must subsequently be converted to mechanical energy via thermodynamically inefficient pressurized pistons or other similarly inconvenient means.

The best solution for a metabolic organ appears to be the **flywheel battery**,[334] because the mechanical flywheel is the most energy-dense storage configuration for rotational energy.[335] The

---

[332] Freitas RA Jr. Energy Density. IMM Report No. 50, 25 June 2019; Figure 16, "Energy Density of Energy Storage Modalities"; http://www.imm.org/Reports/rep050.pdf.

[333] Freitas RA Jr. Energy Density. IMM Report No. 50, 25 June 2019; Section 4.2.2, "Nanoambient Chemical Combustion" and Table 28; http://www.imm.org/Reports/rep050.pdf.

[334] Freitas RA Jr. Energy Density. IMM Report No. 50, 25 June 2019; Section 5.3.2, "Rotational Motion"; http://www.imm.org/Reports/rep050.pdf.

[335] https://en.wikipedia.org/wiki/Flywheel_energy_storage.

maximum rotational energy that can be stored in a spinning mechanical flywheel depends on the physical properties of the flywheel material and the shape of the flywheel, with a maximum energy density of ~90 MJ/L achieved using a constant-stress solid disk geometry[336] (image right) made of atomically-precise single-crystal diamond.

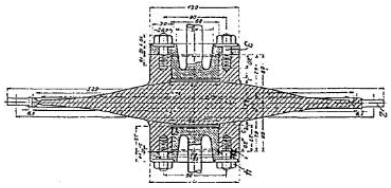

In principle, flywheels can be rapidly charged and discharged, providing high peak on-demand power delivered mechanically through the rotor shaft. However, large frictional energy losses may occur in the bearings that support the spinning disk, an effect that becomes increasingly severe in flywheels reduced to micron size or smaller. For example, one published calculation[337] estimates that a diamond flywheel disk measuring 1 µm in diameter and 1.3 µm in height, riding on a well-designed 100 nm diameter flawless diamond bearing, may lose half of its energy due to friction in the bearings with a half-life $\tau_{1/2}$ ~ 20 sec.

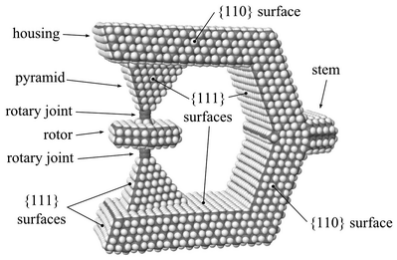

This source of energy loss can be greatly decreased if the bearing is reduced in size to a single atom. Recent computational work[338] analyzed the frictional losses in a spinning diamond rotor supported by an acetylenic (-C≡C-) rotary joint (image, left) in which each face of the disk is bonded to the larger diamond housing through a single C-C bond. An acetylenic-mounted diamond flywheel with a serviceable energy half-life of $\tau_{1/2} \geq 10^5$ sec (~1 day) requires using a rotor of size $R_{disk} \geq 230$ nm. (Larger rotors leak energy through the acetylenic rotary joint even more slowly.) Rotor rotational frequency is ~ 7.0 GHz for a ~230 nm disk spun up to the maximum rotational energy density of E_D = **90 MJ/L** for flawless single-crystal diamond.

Assuming a design with ε ~ 40% volumetric efficiency, the volume of a battery consisting of closely packed diamond flywheels capable of delivering a full day of stored mechanical energy for a metabolic organ operating at the basal metabolic rate is $V_{flybatt} \sim P_{MetOrg}\ t_{day} / \varepsilon\ E_D \sim$ **480 cm^3** of mass $M_{flybatt} \sim \rho_{diamond}\ V_{flybatt}$ = **1680 gm**, implying a total of $N_{flybatt} \sim V_{flybatt} / \pi\ R_{disk}^2\ h_{disk} \sim 2.9 \times 10^{16}$ flywheels each of mass $m_{disk} \sim M_{flybatt} / N_{flybatt} \sim 5.8 \times 10^{-17}$ kg, assuming a constant-stress disk of radius R_{disk} = 230 nm with a maximum thickness of h_{disk} = 100 nm and disk volume ~6.9×10^6 nm^3. The baseline flywheel battery thus holds $E_{flybatt} \sim P_{MetOrg}\ t_{day} \sim$ **17.3 MJ**. Future design efforts and simulations should address remaining issues such as unwanted multiscale vibrational modes and resonances, and gyroscopic force management (e.g., flywheels with opposite rotations can be paired to eliminate unwanted gyroscopic effects).

---

[336] Genta G. Some considerations on the constant stress disc profile. Meccanica 1989 Dec;24(4):235-248; https://link.springer.com/article/10.1007/BF01556455.

[337] Freitas RA Jr. Nanomedicine, Volume I: Basic Capabilities, Landes Bioscience, Georgetown TX, 1999, Sec. 6.2.2.2 "Flywheels"; http://www.nanomedicine.com/NMI/6.2.2.2.htm#p7.

[338] Hogg T, Moses M, Allis D. Evaluating the friction in rotary joints in molecular machines. Mol Syst Des Eng. 2017;2:235-252; http://pubs.rsc.org/en/content/articlehtml/2017/me/c7me00021a.

Solid diamond disks should remain functional even after radiation damage inflicts a few defects so no redundancy has been added for these "bulk" components, but if the performance of the flywheels depends on the successful functioning of ~1000 nm^3 (~3.5 x 10^{-21} kg) energy coupling nanodevices of multiplicity n associated with each flywheel, then the annual probability of failure is $(1 - P_{op}) \sim$ **10^{-1}/yr** for n = 3 and ~**10^{-13}/yr** for n = 5 using the estimation method described in Section 4.3.1; using n =10 still only occupies ~0.1% of the available space.

4.3.3.2 Wall Current

The flywheel battery (Section 4.3.3.1) must be recharged from an appropriate external energy source. The simplest and most convenient energy source[339] is **wall-plug electricity** (image, right), wherein the user recharges for $t_{recharge}$ = 5 hours a day while asleep in bed. Recharging the flywheel battery requires transferring $E_{flybatt} \sim P_{MetOrg}\ t_{day}$ = 17.3 MJ of energy through an electric cord that is plugged into a wall socket in the bedroom and connects to a transdermal port linked to the metabolic organ located inside the user's abdomen. Electricity flows in at the standard line voltage of $e_{recharge}$ = 110 volts, drawing $i_{recharge} = E_{flybatt} / t_{recharge}\ e_{recharge} \sim$ 8.7 amps of electrical current which supplies power to the metabolic organ at the rate of $e_{recharge}\ i_{recharge} \sim$ 960 W, or about half the power of a commonplace hair dryer or floor heater appliance. Waste heat generated overnight during the recharge cycle can be conducted away by sleeping on a waterbed or by other convenient means. At the average U.S. residential power cost of $e_\$$ = $0.1745/kW-hr = 4.85 x 10^{-8} $/J in Apr 2025,[340] the cost for a day's recharge is about $E_{flybatt}\ e_\$ \sim$ **$0.84/day**, or ~25 times cheaper than the estimated **$21/day** per capita food expenditure of the average U.S. resident in 2023.[341] (And electricity prices are likely to be ~100 times cheaper per kilowatt-hour[342] than today, in a future nanotech-rich world capable of building and deploying metabolic organs.)

---

[339] One early proposal* to use radionuclide (α-emitter) batteries in medical nanorobots is infeasible in the present application due to the excessive amount of shielding required, but might become feasible in situations where biological tissue is rendered radiation-tolerant, e.g., when implanted with a large permanent population of radiation-repair nanorobots continuously patrolling the human body.
* Freitas RA Jr. Nanomedicine, Volume I: Basic Capabilities, Landes Bioscience, Georgetown TX, 1999, Sec. 6.3.7.1, "Radionuclides"; http://www.nanomedicine.com/NMI/6.3.7.1.htm#p7.

[340] "Table 5.3 Average Price of Electricity to Ultimate Customers", Electric Power Monthly, Apr 2025; https://www.eia.gov/electricity/monthly/epm_table_grapher.php?t=table_5_03.

[341] Zeballos E, Rivera-Cintron D, Sinclair W. Per capita food spending in the United States reached an all-time high in 2023. USDA Economic Research Service, 2024; https://www.ers.usda.gov/data-products/chart-gallery/chart-detail?chartId=110110.

[342] Freitas RA Jr. Cryostasis Revival: The Recovery of Cryonics Patients through Nanomedicine. Alcor Life Extension Foundation, Scottsdale AZ, 2022; Appendix G, "Historical and Future Commercial Electricity Prices"; https://www.alcor.org/cryostasis-revival/. Freitas RA Jr. Economic Impact of the Personal Nanofactory. Nanotechnology Perceptions: A Review of Ultraprecision Engineering and Nanotechnology 2006 May;2:111-126; http://www.rfreitas.com/Nano/NoninflationaryPN.pdf.

In this scenario, the user must recharge their metabolic organ daily, like a cell phone, electric vehicle, or other battery powered appliance that is in heavy regular use. If the user fails to recharge, their metabolic organ shuts down until power is restored. In most circumstances, this will be merely an annoyance, not a medical crisis. In survival training,[343] according to the well-known Rule of Threes,[344] adult males can survive ~3 minutes without breathable air, ~3 days without water, and ~**3 weeks without food**. Alternatively, the user could just resume eating normal food to satisfy all nutritional needs until it becomes convenient to recharge the flywheel battery.

4.3.4 Metabolic Organ Mass, Volume, and Power Estimates

Table 16 summarizes all the components of the baseline metabolic organ, along with the estimated mass, volume, and continuous power consumption. Note that the number, mass and volume of all nanocomponents except the flywheels have been increased 10-fold to serve as redundant backups in case of individual nanocomponent failure (consistent with the conclusions of Section 4.3.1), but the power draw remains the same because these extra components consume no power until they are switched on, replacing another component that is no longer drawing power.

The anticipated power draw of ~200 W for the metabolic organ is comparable to a previously published estimate of ~175 W needed to power a "head caddy" device that could provide and recycle all nutrients necessary to keep an isolated human cephalon alive.[345]

---

[343] https://en.wikipedia.org/wiki/Survival_skills.
[344] https://en.wikipedia.org/wiki/Rule_of_threes_(survival).

[345] Freitas RA Jr. Cryostasis Revival: The Recovery of Cryonics Patients through Nanomedicine. Alcor Life Extension Foundation, Scottsdale AZ, 2022; Section 6.1.3, "Head Caddy or Biocompatible Artificial Body"; https://www.alcor.org/cryostasis-revival/.

Table 16. Mass, volume, and power estimates for the baseline metabolic organ

System or Subsystem	Mass (gm)	Volume (cm^3)	Power (W)
Nutrient Synthesis Unit			
890 trillion Nanofabricators (x10)	18	9	162
Nutrient Molecule Transport System (x10)	7	40	4.6
Nutrient Distribution Sorting Rotors (x10)	0.004	0.003	~0
Waste Recovery Unit			
Urine Extraction Subunit			
Nanofilter Concentrator (x10)	~0	~0	0
Waste Sorting Rotors (x10)	0.1	0.1	24
Water Sorting Rotors (x10)	0.003	0.002	0.01
Molecule Transport System (x10)	3	18	2.1
5.5 trillion Nanofabricators (x10)	0.1	0.057	1
Blood Extraction Subunit			
CO_2 Sorting Rotors (x10)	0.09	0.06	1.1
Nanofilter Capillaries & Plumbing	180	180	0
Nutrient Storage Tank (loaded, ~1 yr supply)	420	300	~0
Onboard Nanocomputers			
Nanofabricator Computers (x10)	0.02	0.01	5.2
Process Control Computers and Memory (x10)	0.2	0.1	~0
Support infrastructure (housing, bracing, wires, etc.)	11.483	22.67	~0
Subtotals	640	578	200
Power Unit			
Flywheel Battery	1680	480	0
Wall Current Infrastructure	80	50	0
Totals	**2400**	**1100**	**200**

4.3.5 Thermoregulation Issues

Thermoregulation is the ability of an organism to keep its body temperature within certain boundaries, even when the external temperature is very different.[346] Humans have been able to adapt to a great diversity of climates, including hot humid and hot arid, using four avenues of heat loss: convection, conduction, radiation, and evaporation.[347]

Natural human body heat is generated mostly in the deep organs, especially the liver, brain, and heart, and in contraction of skeletal muscles. The entire body normally produces P_{BMR} ~ 100 W at the resting basal metabolic rate and can create over ~1000 W during brief periods of extreme physical activity. The presence of a functioning metabolic organ in the torso of a human user will add P_{MetOrg} ~ 200 W of waste heat to the central core, significantly increasing the workload on the human thermoregulatory system.

With no mitigations, the body will normally respond as soon as the hypothalamus detects a rise in core body temperature, activating two primary cooling mechanisms: (1) cutaneous vasodilation, in which blood is redirected to the skin surface to enhance conductive, convective, and radiative heat loss; and (2) eccrine sweating, in which fluid (mostly water) is secreted to remove heat via evaporation, <0.1 L/hr under the basal conditions. Evaporating sweat requires E_s ~ 2.43 MJ/kg of water at body temperature,[348] so to dissipate the extra 200 W the body would have to evaporate $R_{sweat} \sim (P_{BMR} + P_{MetOrg}) / E_s \sim 0.12$ gm/sec ~ 0.45 L/hr. While an adult can sweat as much as 2-4 L/hr under extreme conditions,[349] maintaining 0.45 L/hr indefinitely might (1) risk dehydration or require excessive water consumption to offset ~11 L/day of water loss; (2) impose cardiovascular strain, including elevated heart rate and blood flow demands; and (3) risk Na^+/K^+ electrolyte imbalances, imposing greater demands on the nutrient supplement tank (Section 4.2.3(3)). If sweat evaporation is impaired due to high humidity or impermeable clothing, core temperature could climb toward dangerous hyperthermia.

What are the comfortable human limits to sustainable heat dissipation? Doubly-labeled-water studies show that in well-fed untrained individuals, the ratio of total daily energy expenditure to basal metabolic rate (BMR) rarely exceeds 2.2-2.5 over the long term,[350] or P_{max} ~ 220-250 W. Thus the upper bound of metabolic organ waste heat production that can be comfortably sustained indefinitely without net loss of body mass or chronic energy deficit in the absence of any

---

[346] https://en.wikipedia.org/wiki/Thermoregulation.
[347] https://en.wikipedia.org/wiki/Human_thermoregulation.

[348] Baker LB. Physiology of sweat gland function: The roles of sweating and sweat composition in human health. Temperature (Austin). 2019 Jul 17;6(3):211-259; https://pmc.ncbi.nlm.nih.gov/articles/PMC6773238/.

[349] https://en.wikipedia.org/wiki/Perspiration.

[350] Westerterp KR. Limits to sustainable human metabolic rate. J Exp Biol. 2001 Sep;204(Pt 18):3183-7; https://pubmed.ncbi.nlm.nih.gov/11581332/. Westerterp KR. Physical activity and physical activity induced energy expenditure in humans: measurement, determinants, and effects. Front Physiol. 2013 Apr 26;4:90; https://pmc.ncbi.nlm.nih.gov/articles/PMC3636460/.

mitigations is $P_{max} - P_{BMR} \sim 150$ W, with cutaneous vasodilation and radiation/convection carrying off 30-50 W and the remainder of excess heat offloaded via eccrine sweating.

At 200 W, our metabolic organ is uncomfortably warm by ~50 W.[351] Several mitigation strategies have been identified, including:

(1) **BMR Reduction**. The most promising method for dealing with the excess heat is to reduce the user's basal metabolic rate from $P_{BMR} \sim 100$ W down to $P_{BMR50} \sim 50$ W ($= P_{setpoint} + P_{Na+/K+} + P_{T3/T4}$; see below). This may be accomplished using three specific interventions in combination:

(A) **Reduce Hypothalamic Setpoint**. A reduction in BMR of 5.2% per °C was observed in lightly sedated, non-shivering adults between 37 °C and 33 °C,[352] so if the core body temperature can be safely reduced by ~2 °C then this reduction would lower BMR by 10.4%, or $P_{setpoint} \sim$ **10 W**. This cooling-induced drop in BMR occurs regardless of calorie food intake because it reflects the temperature-sensitivity of core biochemical processes, not the thermic effect of food.[353] CHA (N6-cyclohexyladenosine) and similarly acting A_1R agonists and "torpor" agents can be given systemically and will cross into the CNS to reset the hypothalamic thermostat. From mouse data, 0.1 mg/kg CHA, given intraperitoneally, produces a –3.4 ± 0.16 °C drop in core temperature within 30 min and lasts several hours,[354] so a 4.2 mg dose of CHA should depress core temperature by ~2 °C in a 70 kg adult human male. An intravenous infusion of 4.2 mg every few hours (~34 mg/day), manufactured in the Nutrient Synthesis Unit (Section 4.1) and transported to the nanofilter in the Blood Extraction Subunit (Section 4.2.2) for

---

[351] The estimated power demand for the metabolic organ assumes that nutrient synthesis (**Section 4.1.2**) can be accomplished mechanosynthetically with an energy efficiency of ~80%. This seems feasible for a mill-style system but might be technically aggressive, given the estimates in previous works of ~50% efficiency for manipulator-style mechanosynthesis. If the technical goal of 80% cannot be reached, then the amount of excess heat generated by the metabolic organ would be somewhat higher, requiring additional attention to thermoregulatory mitigations.

[352] Flickinger KL, Weissman A, Elmer J, Coppler PJ, Guyette FX, Repine MJ, Dezfulian C, Hopkins D, Frisch A, Doshi AA, Rittenberger JC, Callaway CW. Metabolic Manipulation and Therapeutic Hypothermia. Ther Hypothermia Temp Manag. 2024 Mar;14(1):46-51; https://pubmed.ncbi.nlm.nih.gov/37405749/.

[353] Westerterp KR. Diet induced thermogenesis. Nutr Metab (Lond). 2004 Aug 18;1(1):5; https://pmc.ncbi.nlm.nih.gov/articles/PMC524030/.

[354] Johansson B, Halldner L, Dunwiddie TV, Masino SA, Poelchen W, Giménez-Llort L, Escorihuela RM, Fernández-Teruel A, Wiesenfeld-Hallin Z, Xu XJ, Hårdemark A, Betsholtz C, Herlenius E, Fredholm BB. Hyperalgesia, anxiety, and decreased hypoxic neuroprotection in mice lacking the adenosine A1 receptor. Proc Natl Acad Sci U S A. 2001 Jul 31;98(16):9407-12; https://pmc.ncbi.nlm.nih.gov/articles/PMC55434/.

infusion into the venous blood flow, should suffice to hold the reduced setpoint indefinitely.[355]

(B) **Na^+/K^+-ATPase Down-Regulation**. The Na^+/K^+ pump is one of the largest consumers of ATP in cells and is estimated to use ~20 % of whole-body resting energy expenditure.[356] The BMR can be cut by $P_{Na+/K+}$ ~ **10 W** if its expression or activity can safely be cut by 50% (more aggressive knockdown risks membrane-potential collapse), possibly using AAv9-delivered shRNA against ATP1A1 in an intravenous dose of ~7 x 10^{14} vector genomes in a 70 kg man to produce 40-70% mRNA knockdown by 4-6 weeks post-injection,[357] resulting in ~50% reduction in ATP1A1 transcript and protein levels and a ~10 W decrease in basal heat production. (AAV9-CRISPR/Cas9-mediated allele disruption might also be employed.)[358] Down-regulating Na^+/K^+-ATPase expression reduces a fixed, obligatory component of resting ATP turnover, one that is independent of nutritional intake or core temperature. An experimental mouse study with a 30% knock-down saw no loss of running performance, even under maximal treadmill tests.[359] Halving Na^+/K^+-ATPase expression would reduce the maximum exercise power that the person can generate, but there should still be plenty of headroom in total capacity – a user who was sprinting might notice a slight drop in top speed or sprint duration, but not an inability to run. A potential user of the metabolic organ would schedule this whole-body genetic modification procedure prior to being outfitted with the device.

(C) **Thyroid Hormone Reduction**. Triiodothyronine (T_3) and thyroxine (T_4) are the master regulators of the "obligatory" heat increment that makes up BMR. Reducing circulating T_3/T_4 levels lowers the rate at which virtually every cell consumes

---

[355] Human use must be considered hypothetical because CHA has not yet been tested for systemic hypothermia in people. Rodent pharmacokinetics and CNS penetration will differ, so any first-in-human protocol would need careful PK/PD studies and safety monitoring.

[356] Suhail M. Na, K-ATPase: Ubiquitous Multifunctional Transmembrane Protein and its Relevance to Various Pathophysiological Conditions. J Clin Med Res. 2010 Feb;2(1):1-17; https://pmc.ncbi.nlm.nih.gov/articles/PMC3299169/.

[357] Foust KD, Salazar DL, Likhite S, Ferraiuolo L, Ditsworth D, Ilieva H, Meyer K, Schmelzer L, Braun L, Cleveland DW, Kaspar BK. Therapeutic AAV9-mediated suppression of mutant SOD1 slows disease progression and extends survival in models of inherited ALS. Mol Ther. 2013 Dec;21(12):2148-59; https://pmc.ncbi.nlm.nih.gov/articles/PMC3863799/.

[358] Yang Y, Wang L, Bell P, McMenamin D, He Z, White J, Yu H, Xu C, Morizono H, Musunuru K, Batshaw ML, Wilson JM. A dual AAV system enables the Cas9-mediated correction of a metabolic liver disease in newborn mice. Nat Biotechnol. 2016 Mar;34(3):334-8; https://pmc.ncbi.nlm.nih.gov/articles/PMC4786489/.

[359] Kutz LC, Mukherji ST, Wang X, Bryant A, Larre I, Heiny JA, Lingrel JB, Pierre SV, Xie Z. Isoform-specific role of Na/K-ATPase α1 in skeletal muscle. Am J Physiol Endocrinol Metab. 2018 Jun 1;314(6):E620-E629; https://pmc.ncbi.nlm.nih.gov/articles/PMC6032065/.

O_2 and generates ATP, and thus heat and BMR,[360] with mild hypothyroidism lowering BMR by 10-20% and complete thyroid removal cutting BMR by 40-45%. Achieving and maintaining a 30% BMR reduction of $P_{T3/T4}$ ~ **30 W** may require lowering blood concentration of free T_3 from its normal level of 3.25 pg/ml to 2.28 pg/ml and free T_4 from 1.30 ng/dL to 0.91 ng/dL (to prevent compensatory T_3 generation), the lowest levels that may avoid overt hypothyroid-related clinical symptoms,[361] assuming a linear dose-response over the upper 70-100% of thyroid levels as supported by observed correlations between free T_3 and RMR in euthyroid adults.[362] A small number of sorting rotors in the Blood Extraction Subunit (Section 4.2.2) could perform and maintain these reductions indefinitely, extracting the molecules from the venous blood and passing them to the nanofabricators in the Urine Extraction Subunit (Section 4.2.1) for molecular recycling.

All three of these interventions target independent components of the BMR, and their effects sum linearly because they operate via distinct mechanisms – thermostat reset, ion-pump load, and hormone-driven mitochondrial activity – and none depend on dietary intake, because the basal (non-thermic) portion of human metabolism remains affected whether the user consumes a normal ~2000 kcal/day diet or no food at all.

(2) **Refrigerative Apparel**. The user could wear a cooling device disguised as an article of clothing like a cooling shirt, jacket, or a sash wrapped around the midriff. An efficient macroscopic cooling system can be based on the forced convection of liquids such as encapsulated submicron ice particles (with surface structures that prevent aggregation) suspended in a low-viscosity, low-melting-point carrier such as pentane (a light hydrocarbon), circulated through a fractal pipe network, can absorb E_{cool} ~ 1.2 x 10^8 J/m^3 of waste heat, taking advantage of the large phase transition energy of water.[363] A fluid circulation time of $t_{cirrculate}$ ~ 10 sec implies the cooling garment would only need a modest P_{BMR50} $t_{circulate}$ / E_{cool} ~ 4.2 cm^3 of circulating coolant fluid. A thermal radiator able to emit P_{BMR50} ~ 50 W of waste heat via radiative cooling using a ΔT ~ 20 K temperature differential compared to the environment and an emissivity $\varepsilon_{clothing}$ ~ 0.65 typical of clothing[364] has a surface area of $A_{radiator}$ ~ P_{BMR50} / σ $\varepsilon_{clothing}$

---

[360] McCullagh EP. Some clinical considerations of basal metabolism. Cleveland Clin Quart. 1938:108-116; https://cdn.mdedge.com/files/s3fs-public/issues/articles/media_f1fb093_ccq5_2-0108.pdf. Kumar K, Dubey HP, Prasad D. Thyroid Dysfunction Impact on Basal Metabolic Rate: A Retrospective Cross-Sectional Study. Intl J Curr Pharma Rev Res. 2025;17(3):1523-1528; http://impactfactor.org/PDF/IJCPR/17/IJCPR,Vol17,Issue3,Article257.pdf.

[361] https://en.wikipedia.org/wiki/Hypothyroidism#Signs_and_symptoms.

[362] Samuels MH, Kolobova I, Antosik M, Niederhausen M, Purnell JQ, Schuff KG. Thyroid Function Variation in the Normal Range, Energy Expenditure, and Body Composition in L-T4-Treated Subjects. J Clin Endocrinol Metab. 2017 Jul 1;102(7):2533-2542; https://pmc.ncbi.nlm.nih.gov/articles/PMC5505196/.

[363] Drexler KE. Nanosystems: Molecular Machinery, Manufacturing, and Computation, John Wiley & Sons, New York, 1992; Section 11.5, "Convective cooling systems"; https://www.amazon.com/dp/0471575186/.

[364] The thermal emissivity is ~0.68 for cotton fabrics, ~0.73 for wool fabrics, and 0.52-0.82 for a range of different clothing fabrics. Zhang H, Hu TL, Zhang JC. Surface emissivity of fabric in the 8-14 μm waveband. J Textile Institute 2009 Jan; 100(1):90-94; https://www.researchgate.net/profile/Hui-Zhang-

$((T_{room} + \Delta T)^4 - T_{room}^4) \sim$ **0.6 m²**, where $\sigma = 5.67 \times 10^{-8}$ W/m²-K⁴ (Stefan-Boltzmann constant), when the apparel is worn in a room at $T_{room} \sim 300$ K. Since the user may begin to overheat if separated from the refrigerative apparel, the metabolic organ would need (1) external temperature sensors to detect this condition, and (2) control subroutines to throttle back metabolic activity during such an event.[365]

(3) **Drink ice-water**. The user could dissipate heat by drinking cold or slush-ice water. Drinking a liter of ice-cold (0 °C) liquid water and heating it up to human body temperature (37 °C) can dissipate (4186 J/L-°C) (37 °C) ~ 0.155 MJ/L, and a liter of frozen water-ice slush at (0 °C) can dissipate 0.334 MJ + 0.155 MJ ~ 0.489 MJ. Unloading the extra **50 W** would require drinking an extra ~1.2 L/hr of the cold water or ~**0.4 L/hr of the ice slush**. Sports science studies found that it is safe to consume up to 1.1-1.8 L/hr of water-ice slush with no thermal or gastrointestinal complications.[366] Reported risks if these safe limits are exceeded include cold-induced esophageal dysfunction,[367] vagally mediated cardiac arrhythmias (e.g., AFib),[368] GI discomfort,[369] and potential systemic hypothermia.

(4) **Reduced Run Rate**. The metabolic organ operates in tandem with normal digestive and excretory processes, not as a replacement for those processes. The proposed artificial organ has been scaled to provide nutrient recycling sufficient to support a 100 W metabolic demand,

---

339/publication/233074273_Surface_emissivity_of_fabric_in_the_8-14_m_m_waveband/links/5701ecf308aea6b7746a81f4/Surface-emissivity-of-fabric-in-the-8-14-m-m-waveband.pdf.

[365] A radiator system directly implanted or embedded in the $A_{skin} \sim 2$ m² of human skin would require covering $A_{radiator} / A_{skin} \sim 30\%$ of the human body.

[366] Choo HC, Peiffer JJ, Lopes-Silva JP, Mesquita RNO, Amano T, Kondo N, Abbiss CR. Effect of ice slushy ingestion and cold water immersion on thermoregulatory behavior. PLoS One. 2019 Feb 27;14(2):e0212966; https://pmc.ncbi.nlm.nih.gov/articles/PMC6392407/. Morito A, Inami T, Hirata A, Yamada S, Shimomasuda M, Haramoto M, Kato K, Tahara S, Oguma Y, Ishida H, Kohtake N. Ice slurry ingestion improves physical performance during high-intensity intermittent exercise in a hot environment. PLoS One. 2022 Sep 15;17(9):e0274584; https://pmc.ncbi.nlm.nih.gov/articles/PMC9477354/.

[367] Meyer GW, Castell DO. Human esophageal response during chest pain induced by swallowing cold liquids. JAMA. 1981 Nov 6;246(18):2057-9; https://pubmed.ncbi.nlm.nih.gov/7288992/.

[368] Siddanagoudra SP, Arjunwadekar P. Effect of ice water ingestion on cardiac autonomic reactivity in healthy subjects. Natl J Physiol Pharm Pharmacol. 2017; 7(12):1309-1312; https://www.njppp.com/fulltext/28-1498113184.pdf. Lien IC, Vinson DR, Ramalingam ND, Nicole Tran H, Liu TI. A Case Report of Cold Drinks and Food as a Trigger of Paroxysmal Atrial Fibrillation. Perm J. 2022 Dec 19;26(4):110-113; https://pmc.ncbi.nlm.nih.gov/articles/PMC9761284/.

[369] Stevens CJ, Dascombe B, Boyko A, Sculley D, Callister R. Ice slurry ingestion during cycling improves Olympic distance triathlon performance in the heat. J Sports Sci. 2013;31(12):1271-9; https://pubmed.ncbi.nlm.nih.gov/23506436/. Bongers CC, Hopman MT, Eijsvogels TM. Cooling interventions for athletes: An overview of effectiveness, physiological mechanisms, and practical considerations. Temperature (Austin). 2017 Jan 3;4(1):60-78; https://pmc.ncbi.nlm.nih.gov/articles/PMC5356217/.

requiring a metabolic organ that draws 200 W of power. If operated at a 75% run rate (~150 W) to offset the excess 50 W of heat and minimize thermoregulatory issues, the metabolic organ would still supply ~75 W of nutritional power instead of 100 W, which equates to ~1500 kcal/day or 75% of daily nutritional requirements. This would allow the user to survive on 75% less nutritional intake – that is, on just ~25% (~500 kcal/day) of the normal food intake. This percentage drops to ~22% (~440 kcal/day) when we acknowledge that the whole-body BMR rate decreases to ~85% during sleep as compared to quiet wakefulness.[370]

4.3.6 Gastrointestinal and Appetite Regulation Issues

There are a number of alimentary system pathologies (**Table 17**) that must be addressed if the metabolic organ is employed to displace all food consumption, resulting in virtually no bulk transport through the stomach and intestines. Even in the no-food scenario, there is no evidence that the stomach "digests itself" during exclusive Total Parenteral Nutrition (TPN). Gastric acid and pepsinogen secretion decline (i.e., less gastrin release), but the mucosal barrier remains intact, and responsiveness to food returns on resumption of enteral intake. TPN induces a shift to "fasting" migrating motor complexes that continue clearing secretions, but intestinal walls do not adhere in the absence of bulk flow – no adhesion pathology has been reported solely from lack of luminal contents.

However, some gastrointestinal mucosal atrophy and functional changes have been reported. In animal models (neonatal piglets), transition from enteral to exclusive TPN causes a rapid (< 8 hr) drop in jejunal blood flow (–30%), followed by significant reductions in jejunal weight and villus height by 24 hr, and suppression of crypt cell proliferation with increased apoptosis by 48 hr.[371] In critically-ill humans (enteral fasting), duodenal biopsies show significant decreases in villus height and crypt depth, plus abnormal lactulose-mannitol permeability, after a mean 7.8 days of no enteral feeds.[372] Three weeks of exclusive TPN on healthy volunteers reduces total mucosal thickness by ~20% (risking constipation), nearly doubles intestinal permeability, and cuts epithelial cell number by ~10% (all reversible within 5 days of resuming enteral feeding).[373] (GLP-2[374] and IGF-I[375] show promise in preclinical models for attenuating mucosal atrophy.)

---

[370] Sharma S, Kavuru M. Sleep and metabolism: an overview. Int J Endocrinol. 2010;2010:270832; https://pmc.ncbi.nlm.nih.gov/articles/PMC2929498/.

[371] Niinikoski H, Stoll B, Guan X, Kansagra K, Lambert BD, Stephens J, Hartmann B, Holst JJ, Burrin DG. Onset of small intestinal atrophy is associated with reduced intestinal blood flow in TPN-fed neonatal piglets. J Nutr. 2004 Jun;134(6):1467-74; https://www.sciencedirect.com/science/article/pii/S0022316623028225.

[372] Hernandez G, Velasco N, Wainstein C, Castillo L, Bugedo G, Maiz A, Lopez F, Guzman S, Vargas C. Gut mucosal atrophy after a short enteral fasting period in critically ill patients. J Crit Care. 1999 Jun;14(2):73-7; https://pubmed.ncbi.nlm.nih.gov/10382787/.

[373] Tappenden KA. Mechanisms of enteral nutrient-enhanced intestinal adaptation. Gastroenterology. 2006 Feb;130(2 Suppl 1):S93-9; https://www.gastrojournal.org/article/S0016-5085%2805%2902431-5/pdf.

[374] Lovshin J, Drucker DJ. New frontiers in the biology of GLP-2. Regul Pept. 2000 Jun 30;90(1-3):27-32 ; https://pubmed.ncbi.nlm.nih.gov/10828489/. Lei Q, Bi J, Wang X, Jiang T, Wu C, Tian F, Gao X, Wan X,

And brush border enzymes such as duodenal sucrase, maltase, lactase, and other hydrolases drop by 40-83%, even without gross histologic changes, after 21 days of TPN.[376]

Table 17. Timeline of key gastrointestinal pathologies under exclusive TPN

Pathology	Approximate Onset
Jejunal blood flow reduction	< 8 hrs (animal)
Villus atrophy (small intestine)	~24 hrs (animal); ~8 days (humans)
Increased permeability and bacterial translocation	~8 days fasting (critically ill)
Mucosal thickness ↓20%	~3 weeks (healthy volunteers)
Brush-border enzyme activity ↓70-80%	~3 weeks (adults)
Gallbladder sludge	~3 weeks (6%), ~13 weeks (100%)
Cholestasis/hepatic steatosis	weeks to months

None of these pathologies produces physical discomfort, and all are quickly reversible upon resumption of food intake. The normal range of healthy male fecal output is 72-470 gm/day (avg. 104 gm/day), with only ~1% of men (and 17% of women) passing <50 gm/day,[377] so ingesting ~350 gm/week of solid food should fully preserve normal gut motility, enzymatic activity, barrier function, and colonic health, since the onset of pathologies is very slow, measured in weeks. However, with a metabolic organ in operation and zero food intake, total fecal generation will be less than ~4 gm/day (**Table 14**), or about one bowel movement per month. More research is needed to determine if the materials comprising the 4 gm/day residuum will flow easily through the bowel or may desiccate and compactify, risking constipation. If this risk is realized, it may be necessary to add a separate flow pathway from the metabolic organ to the gut (e.g., a biliary anastomosis) from which ~17 gm/day of polyethylene glycol (an osmotic agent) or glycerol (a

---

Zheng H. GLP-2 Prevents Intestinal Mucosal Atrophy and Improves Tissue Antioxidant Capacity in a Mouse Model of Total Parenteral Nutrition. Nutrients. 2016 Jan 9;8(1):33; https://pmc.ncbi.nlm.nih.gov/articles/PMC4728647/.

[375] Murali SG, Nelson DW, Draxler AK, Liu X, Ney DM. Insulin-like growth factor-I (IGF-I) attenuates jejunal atrophy in association with increased expression of IGF-I binding protein-5 in parenterally fed mice. J Nutr. 2005 Nov;135(11):2553-9; https://www.sciencedirect.com/science/article/pii/S0022316622104633.

[376] Guedon C, Schmitz J, Lerebours E, Metayer J, Audran E, Hemet J, Colin R. Decreased brush border hydrolase activities without gross morphologic changes in human intestinal mucosa after prolonged total parenteral nutrition of adults. Gastroenterology. 1986 Feb;90(2):373-8; https://pubmed.ncbi.nlm.nih.gov/3079717/.

[377] Cummings JH, Bingham SA, Heaton KW, Eastwood MA. Fecal weight, colon cancer risk, and dietary intake of nonstarch polysaccharides (dietary fiber). Gastroenterology. 1992 Dec;103(6):1783-9; https://pubmed.ncbi.nlm.nih.gov/1333426/.

stimulant laxative),[378] synthesized in the NSU, can be directed into the gut lumen to provide symptomatic relief.

TPN, by bypassing the gut lumen, also disrupts the normal trophic and metabolic interactions between dietary substrates and resident microbes, leading to significant and reproducible alterations in gut microbiota – reducing overall diversity, depleting key commensal taxa, and potentially permitting expansion of potential pathogens.[379] These effects have been observed in rats[380] after ~2 weeks of TPN and in humans[381] after ~4 weeks of TPN, and might occur in AMO users who choose to eat no food for extended periods of time unless the AMO design is augmented to allow nutrient injection into the bile duct or other channels that empty directly into the intestinal tract.

Fortunately, gut refloration is fairly straightforward[382] and non-urgent because the NSU can synthesize any vitamins that would otherwise be produced by missing gut flora. Even after weeks to months of exclusive TPN – with minimal or no bulk flow through the bowel – the appendix's protected biofilm likely preserves sufficient microbial diversity.[383] The appendiceal biofilm remains intact during inflammation or luminal starvation, and commensal bacteria can be released

---

[378] American Gastroenterological Association; Bharucha AE, Dorn SD, Lembo A, Pressman A. American Gastroenterological Association medical position statement on constipation. Gastroenterology. 2013 Jan;144(1):211-7; https://www.gastrojournal.org/article/S0016-5085(12)01545-4/fulltext.

[379] Demehri FR, Barrett M, Teitelbaum DH. Changes to the Intestinal Microbiome With Parenteral Nutrition: Review of a Murine Model and Potential Clinical Implications. Nutr Clin Pract. 2015 Dec;30(6):798-806; https://deepblue.lib.umich.edu/bitstream/handle/2027.42/142098/ncp0798.pdf. Dahlgren AF, Pan A, Lam V, Gouthro KC, Simpson PM, Salzman NH, Nghiem-Rao TH. Longitudinal changes in the gut microbiome of infants on total parenteral nutrition. Pediatr Res. 2019 Jul;86(1):107-114 ; https://pmc.ncbi.nlm.nih.gov/articles/PMC6594895/. Cerdó T, García-Santos JA, Rodríguez-Pöhnlein A, García-Ricobaraza M, Nieto-Ruíz A, G Bermúdez M, Campoy C. Impact of Total Parenteral Nutrition on Gut Microbiota in Pediatric Population Suffering Intestinal Disorders. Nutrients. 2022 Nov 6;14(21):4691; https://pmc.ncbi.nlm.nih.gov/articles/PMC9658482/.

[380] Hodin CM, Visschers RG, Rensen SS, Boonen B, Olde Damink SW, Lenaerts K, Buurman WA. Total parenteral nutrition induces a shift in the Firmicutes to Bacteroidetes ratio in association with Paneth cell activation in rats. J Nutr. 2012 Dec;142(12):2141-7; https://core.ac.uk/download/pdf/231393832.pdf.

[381] Dahlgren AF, Pan A, Lam V, Gouthro KC, Simpson PM, Salzman NH, Nghiem-Rao TH. Longitudinal changes in the gut microbiome of infants on total parenteral nutrition. Pediatr Res. 2019 Jul;86(1):107-114; https://pmc.ncbi.nlm.nih.gov/articles/PMC6594895/.

[382] Dixit K, Chaudhari D, Dhotre D, Shouche Y, Saroj S. Restoration of dysbiotic human gut microbiome for homeostasis. Life Sci. 2021 Aug 1;278:119622; https://pubmed.ncbi.nlm.nih.gov/34015282/. Acevedo-Román A, Pagán-Zayas N, Velázquez-Rivera LI, Torres-Ventura AC, Godoy-Vitorino F. Insights into Gut Dysbiosis: Inflammatory Diseases, Obesity, and Restoration Approaches. Int J Mol Sci. 2024 Sep 8;25(17):9715; https://pmc.ncbi.nlm.nih.gov/articles/PMC11396321/.

[383] Randal Bollinger R, Barbas AS, Bush EL, Lin SS, Parker W. Biofilms in the large bowel suggest an apparent function of the human vermiform appendix. J Theor Biol. 2007 Dec 21;249(4):826-31; https://pubmed.ncbi.nlm.nih.gov/17936308/.

from the appendix to re-establish a healthy microbiota after gut disturbances.[384] Upon resumption of enteral feeding (and luminal nutrient flow), microbes released from this reservoir should accelerate gut refloration, much as they do after diarrheal illnesses or antibiotic courses.

There are also a few hepatobiliary and barrier complications. In particular, 6% of TPN patients develop gallbladder stasis and biliary sludge by 3 weeks, rising to 100% by 13 weeks, although the sludge typically resolves within 4 weeks of refeeding.[385] Cholestatic liver disease and steatosis are common with long-term TPN (weeks to months), especially under continuous infusions. And heightened gut permeability correlates with increased sepsis risk in critically ill patients due to bacterial translocation. These issues should be addressed during a future metabolic organ implementation program.

Another major potential concern is whether metabolic organ users might feel hungry[386] all the time, given that they may not be eating any solid food. Ghrelin, the primary **stomach-derived hunger hormone**, is suppressed rather than elevated during TPN. For instance, in rats on TPN for 8 days, serum ghrelin fell by ~50% (vs. fasted controls).[387] In humans fed only by TPN, fasting plasma ghrelin concentrations are nearly **five-fold lower** than in individuals fasting but still eating orally.[388]

However, exclusive intravenous feeding reduces the levels of **gut-derived luminal satiety signals** that would otherwise suppress feelings of hunger. Hunger is reported during in-patient infusion,[389] but for longer-term (~31 days) out-patient TPN, hunger was generally low for most of the day with moderate hunger sensations before the small amounts of allowed oral intake.[390] Enteric satiety-peptides remain at fasting levels during TPN because no luminal nutrients reach their secreting cells, so these hormones should be replaced in the circulation:

---

[384] Kooij IA, Sahami S, Meijer SL, Buskens CJ, Te Velde AA. The immunology of the vermiform appendix: a review of the literature. Clin Exp Immunol. 2016 Oct;186(1):1-9; https://pmc.ncbi.nlm.nih.gov/articles/PMC5011360/.

[385] https://en.wikipedia.org/wiki/Parenteral_nutrition#Complications.
[386] https://en.wikipedia.org/wiki/Hunger_(physiology).

[387] Qader SS, Salehi A, Håkanson R, Lundquist I, Ekelund M. Long-term infusion of nutrients (total parenteral nutrition) suppresses circulating ghrelin in food-deprived rats. Regul Pept. 2005 Nov;131(1-3):82-8; https://pubmed.ncbi.nlm.nih.gov/16102855/.

[388] Cummings DE, Shannon MH. Roles for ghrelin in the regulation of appetite and body weight. Arch Surg. 2003 Apr;138(4):389-96; https://jamanetwork.com/journals/jamasurgery/fullarticle/394661.

[389] Loss SH, Alves KM, Nunes AC, Stefani J, Loureiro GP, Píscopo A, Viana LV. Hunger and the transition from parenteral nutrition in hospitalized adults: A descriptive cohort study. JPEN J Parenter Enteral Nutr. 2025 Feb;49(2):256-266; https://pubmed.ncbi.nlm.nih.gov/39681539/.

[390] McCutcheon NB, Tennissen AM. Hunger and appetitive factors during total parenteral nutrition. Appetite. 1989 Oct;13(2):129-41; https://pubmed.ncbi.nlm.nih.gov/2508550/.

(1) **GLP-1** [3298 gm/mole][391] is secreted by distal-gut L-cells only in response to nutrients in the intestinal lumen. In conditions of prolonged lack of oral/enteral feeding, postprandial GLP-1 release is essentially abolished.[392] In a randomized, blinded crossover study in obese men, a four-hour IV infusion of GLP-1 (0.75 pmol/kg/min) reduced hunger ratings on visual-analogue scales and cut *ad libitum* energy intake at lunch + dinner by ~21% (-1.7 ± 0.5 MJ) compared to saline.[393]

(2) **Peptide YY** (PYY) [4310 gm/mole]:[394] In healthy volunteers, graded intravenous infusions of PYY (up to 0.8 pmol/kg/min) produced a dose-dependent reduction in food intake (maximal -35% vs. placebo), with subjects reporting less hunger and earlier fullness even before the test meal.[395]

(3) **Cholecystokinin** (CCK-8) [1142 gm/mole]:[396] A 20-minute IV infusion of cholecystokinin-octapeptide (4 ng/kg/min) given to fasted volunteers significantly lowered pre-meal hunger, slowed eating rate, and cut energy intake by ~45-57%, independent of any nausea or anxiety effect.[397]

GLP-1, PYY, and CCK act via receptors on vagal afferents and within the hypothalamus. None require a food bolus in the gut lumen. To best mimic natural physiological post-prandial hormone spikes, maximize satiety, and minimize hormone receptor desensitization and side effects such as nausea and tachyphylaxis,[398] the three peptides should be administered in three pulses per day (e.g., morning, afternoon, and night). Appropriate pulsed dosages from the metabolic organ might include **0.042 mg/day of GLP-1** (3 x 1 pmol/kg/min at 70 kg for 60 min), **0.043 mg/day of PYY** (3 x 0.8 pmol/kg/min at 70 kg for 60 min), and **0.017 mg/day of CCK-8** (3 x 4 ng/kg/min at 70 kg for 20 min), and should produce near-maximal satiety effects (e.g., 40-

---

[391] https://en.wikipedia.org/wiki/Glucagon-like_peptide-1.

[392] Beltrand J, Colomb V, Marinier E, Daubrosse C, Alison M, Burcelin R, Cani PD, Chevenne D, Marchal CL. Lower insulin secretory response to glucose induced by artificial nutrition in children: prolonged and total parenteral nutrition. Pediatr Res. 2007 Nov;62(5):624-9; https://www.nature.com/articles/pr2007290.

[393] Näslund E, Barkeling B, King N, Gutniak M, Blundell JE, Holst JJ, Rössner S, Hellström PM. Energy intake and appetite are suppressed by glucagon-like peptide-1 (GLP-1) in obese men. Int J Obes Relat Metab Disord. 1999 Mar;23(3):304-11; https://pubmed.ncbi.nlm.nih.gov/10193877/.

[394] https://en.wikipedia.org/wiki/Peptide_YY.

[395] Degen L, Oesch S, Casanova M, Graf S, Ketterer S, Drewe J, Beglinger C. Effect of peptide YY3-36 on food intake in humans. Gastroenterology. 2005 Nov;129(5):1430-6; https://www.gastrojournal.org/article/S0016-5085(05)01785-3/fulltext.

[396] https://en.wikipedia.org/wiki/Cholecystokinin.

[397] Greenough A, Cole G, Lewis J, Lockton A, Blundell J. Untangling the effects of hunger, anxiety, and nausea on energy intake during intravenous cholecystokinin octapeptide (CCK-8) infusion. Physiol Behav. 1998 Nov 15;65(2):303-10; https://pubmed.ncbi.nlm.nih.gov/9855480/.

[398] https://en.wikipedia.org/wiki/Tachyphylaxis.

60% hunger reduction with GLP-1, 30-50% fullness increase with PYY, and 45-57% intake drop with CCK). Because the TPN infusion continues from the metabolic organ, users should not experience true "hunger rebound" after the pulses end, though hunger ratings typically climb back toward baseline over 2-3 hr as the hormone levels fall.

Finally, long-term TPN patients can also experience hunger pangs driven by **interdigestive gastric contractions** involving gastric mechanoreceptors and the migrating motor complex (MMC)[399] – a fasting-state pattern of strong stomach and small-intestinal contractions that continues during TPN, with Phase III bursts correlating closely with the subjective sensation of hunger pangs.[400] More specifically, the MMC is a stereotyped, fasting-state pattern of stomach and small-intestinal contractions that recurs every 90-120 minutes and underlies the "hunger contractions" or pangs we feel when fasting. Because TPN bypasses the gut lumen, the MMC remains uninterrupted as long as no enteral nutrition is given, and thus these pangs may continue unless actively suppressed. Suppression may be accomplished by continuously adding to the intravenous feed either:

(1) **0.20-0.80 mg/day of human somatostatin**[401] (1.2-4.8 pmol/kg/min @ 70 kg; 1638 gm/mole) which completely abolishes all gastric motor activity including Phase III hunger contractions, by both inhibiting motilin release and directly blocking gastric smooth-muscle excitability.[402] **Octreotide**[403] (a long-acting somatostatin analogue) likewise suppresses MMC cycles in both stomach and small intestine.[404]

(2) **0.1-0.3 mg/day of native GLP-1** (0.3-0.9 pmol/kg/min @ 70 kg; 3298 gm/mole) which dose-dependently reduces both the frequency and amplitude of migrating motor complexes in healthy subjects (and IBS patients), slowing gastric and small-bowel motility that underpins hunger pangs.[405]

---

[399] https://en.wikipedia.org/wiki/Migrating_motor_complex.

[400] Deloose E, Janssen P, Depoortere I, Tack J. The migrating motor complex: control mechanisms and its role in health and disease. Nat Rev Gastroenterol Hepatol. 2012 Mar 27;9(5):271-85; https://pubmed.ncbi.nlm.nih.gov/22450306/.

[401] https://en.wikipedia.org/wiki/Somatostatin.

[402] Peeters TL, Janssens J, Vantrappen GR. Somatostatin and the interdigestive migrating motor complex in man. Regul Pept. 1983 Feb;5(3):209-17; https://pubmed.ncbi.nlm.nih.gov/6133316/.

[403] https://en.wikipedia.org/wiki/Octreotide.

[404] Romański KW. Mechanisms controlling the gastrointestinal migrating motor complex, J Pre-Clin and Clin Res 2009; 3(1):011-019; https://bibliotekanauki.pl/articles/3715.pdf.

[405] Marathe CS, Rayner CK, Jones KL, Horowitz M. Effects of GLP-1 and incretin-based therapies on gastrointestinal motor function. Exp Diabetes Res. 2011;2011:279530; https://pmc.ncbi.nlm.nih.gov/articles/PMC3124003/.

4.3.7 Biocompatibility and General Safety Issues

Biocompatibility is a key concern for any device intended to be implanted and to remain inside the human body for extended periods of time. Many important aspects of nanorobot biocompatibility have been reviewed in a previous publication.[406] An extensive discussion of biocompatibility issues specific to the proposed metabolic organ is beyond the scope of the present document, but key issues might include:

(1) **Immune**[407] **and Foreign-Body Response**[408] – preventing activation of macrophages, complement cascades or giant-cell formation against the nanofactory components, using strategies such as inert diamondoid surfaces[409] or PEGylation to minimize recognition and chronic inflammation. Wang *et al.*[410] provides a general overview of how nanomaterials interact with host proteins, lipids, and sugars to trigger innate and adaptive immune responses,[411] and discusses traditional design strategies to mitigate inflammation and complement activation.[412] Anderson *et al.*[413] reviews the cellular cascade leading to fibrous encapsulation of implants and discusses the traditional use of drug-eluting surfaces (e.g., dexamethasone) to modulate foreign

---

[406] Freitas RA Jr. Nanomedicine, Volume IIA: Biocompatibility, Landes Bioscience, Georgetown, TX, 2003; http://www.nanomedicine.com/NMIIA.htm.

[407] Freitas RA Jr. Nanomedicine, Volume IIA: Biocompatibility, Landes Bioscience, Georgetown, TX, 2003; Section 15.2.3, "Nanorobot Immunoreactivity"; http://www.nanomedicine.com/NMIIA/15.2.3.htm.

[408] Freitas RA Jr. Nanomedicine, Volume IIA: Biocompatibility, Landes Bioscience, Georgetown, TX, 2003; Section 15.4.3.5, "Foreign Body Granulomatous Reaction"; http://www.nanomedicine.com/NMIIA/15.4.3.5.htm.

[409] Freitas RA Jr. Nanomedicine, Volume IIA: Biocompatibility, Landes Bioscience, Georgetown, TX, 2003; Section 15.3.1.1, "Protein Absorption on Diamond Surfaces"; http://www.nanomedicine.com/NMIIA/15.3.1.1.htm; and Section 15.3.1.5, "Chemical Inertness of Diamond"; http://www.nanomedicine.com/NMIIA/15.3.1.5.htm.

[410] Wang X, Reece SP, Brown JM. Immunotoxicological impact of engineered nanomaterial exposure: mechanisms of immune cell modulation. Toxicol Mech Methods. 2013 Mar;23(3):168-77; https://pmc.ncbi.nlm.nih.gov/articles/PMC3773497/.

[411] Hussain S, Vanoirbeek JA, Hoet PH. Interactions of nanomaterials with the immune system. Wiley Interdiscip Rev Nanomed Nanobiotechnol. 2012 Mar-Apr;4(2):169-83; https://pubmed.ncbi.nlm.nih.gov/22144008/.

[412] Kyriakides TR, Raj A, Tseng TH, Xiao H, Nguyen R, Mohammed FS, Halder S, Xu M, Wu MJ, Bao S, Sheu WC. Biocompatibility of nanomaterials and their immunological properties. Biomed Mater. 2021 Mar 11;16(4):10; https://pmc.ncbi.nlm.nih.gov/articles/PMC8357854/.

[413] Anderson JM, Rodriguez A, Chang DT. Foreign body reaction to biomaterials. Semin Immunol. 2008 Apr;20(2):86-100; https://pmc.ncbi.nlm.nih.gov/articles/PMC2327202/.

body reaction and fibrosis.[414] Specific methods for reducing or eliminating phagocytic interest in blood-contacting component surfaces[415] and for suppressing fibrous capsule formation[416] around the device bulk that might impair nutrient or waste transport should be further investigated in the context of advanced diamondoid nanorobotics, including eluting[417] or coated surfaces. Inspirational present-day strategies for reducing or suppressing the foreign body response[418] and fibrous capsule formation around chemically inert implants include: (1) surface engineering with zwitterionic[419] or biomimetic[420] coatings to reduce initial protein binding and immune activation,[421] (2) incorporating localized immunomodulation such as PEG-PSL liposomes (reducing TGF-β1 from macrophages, producing thinner capsules and less giant cell formation)[422] or CSF1R inhibitors to block macrophage cascade (reducing giant cells and fibrosis),[423] (3)

---

[414] Carnicer-Lombarte A, Chen ST, Malliaras GG, Barone DG. Foreign Body Reaction to Implanted Biomaterials and Its Impact in Nerve Neuroprosthetics. Front Bioeng Biotechnol. 2021 Apr 15;9:622524; https://pmc.ncbi.nlm.nih.gov/articles/PMC8081831/.

[415] Freitas RA Jr. Nanomedicine, Volume IIA: Biocompatibility, Landes Bioscience, Georgetown, TX, 2003; Section 15.4.3.6, "Phagocyte Avoidance and Escape"; http://www.nanomedicine.com/NMIIA/15.4.3.6.htm.

[416] Freitas RA Jr. Nanomedicine, Volume IIA: Biocompatibility, Landes Bioscience, Georgetown, TX, 2003; Section 15.4.3.5, "Foreign Body Granulomatous Reaction"; http://www.nanomedicine.com/NMIIA/15.4.3.5.htm.

[417] Olbrich KC, Meade R, Bruno W, Heller L, Klitzman B, Levin LS. Halofuginone inhibits collagen deposition in fibrous capsules around implants. Ann Plast Surg. 2005 Mar;54(3):293-6;discussion 296; https://pubmed.ncbi.nlm.nih.gov/15725837/.

[418] https://en.wikipedia.org/wiki/Foreign_body_reaction#Engineering_biomaterial_to_resist_the_foreign_body_reaction.

[419] Dong D, Tsao C, Hung HC, Yao F, Tang C, Niu L, Ma J, MacArthur J, Sinclair A, Wu K, Jain P, Hansen MR, Ly D, Tang SG, Luu TM, Jain P, Jiang S. High-strength and fibrous capsule-resistant zwitterionic elastomers. Sci Adv. 2021 Jan 1;7(1):eabc5442; https://pmc.ncbi.nlm.nih.gov/articles/PMC7775767/. See also: https://en.wikipedia.org/wiki/Foreign_body_reaction#Zwitterionic_materials.

[420] https://en.wikipedia.org/wiki/Surface_modification_of_biomaterials_with_proteins.

[421] Kondyurina I, Kondyurin A. Foreign body reaction (immune respond) for artificial implants can be avoided. arXiv:1905.02500 [physics.chem-ph], 2019; https://arxiv.org/pdf/1905.02500.

[422] Kim Y, Wu L, Park HC, Yang HC. Reduction of fibrous encapsulation by polyethylene glycol-grafted liposomes containing phosphatidylserine. Biomed Mater. 2020 Sep 24;15(6):065007; https://pubmed.ncbi.nlm.nih.gov/32615550/.

[423] Mariani E, Lisignoli G, Borzì RM, Pulsatelli L. Biomaterials: Foreign Bodies or Tuners for the Immune Response? Int J Mol Sci. 2019 Feb 1;20(3):636; https://pmc.ncbi.nlm.nih.gov/articles/PMC6386828/.

enhancing mechanical and topographical design using controlled porosity[424] and micropatterning[425] to minimize fibroblast activation, and (4) optional gene therapy via siRNA nanofibers targeting collagen genes for high-risk or long-term implants (50-60% reduced capsule thickness).[426]

(2) **Thrombosis**[427] **and Hemocompatibility**[428] – avoiding platelet adhesion and clot formation on any blood-contacting surfaces (e.g., blood extraction filters, tubing, pump housings), using antithrombogenic coatings (e.g., heparin, nitric-oxide releasing polymers) and flow designs that minimize stasis. Litvinov and Weisel[429] review the thrombotic cascade from protein adsorption to platelet adhesion, activation, and clot formation on blood-contacting surfaces, emphasizing how surface chemistry and topography dictate thrombogenicity.[430] Kizhakkedathu *et al.*[431] discusses the thermodynamics of protein adsorption on polymers and the traditional design of antithrombogenic coatings (e.g., zwitterionic or nitric-oxide-releasing surfaces) to prevent clotting.[432]

---

[424] Taylor SR, Gibbons DF. Effect of surface texture on the soft tissue response to polymer implants. J Biomed Mater Res. 1983 Mar;17(2):205-27; https://pubmed.ncbi.nlm.nih.gov/6841364/.

[425] Han W, Chu Q, Li J, Dong Z, Shi X, Fu X. Modulating Myofibroblastic Differentiation of Fibroblasts through Actin-MRTF Signaling Axis by Micropatterned Surfaces for Suppressed Implant-Induced Fibrosis. Research (Wash D C). 2023;6:0049; https://pmc.ncbi.nlm.nih.gov/articles/PMC10076024/.

[426] Rujitanaroj PO, Jao B, Yang J, Wang F, Anderson JM, Wang J, Chew SY. Controlling fibrous capsule formation through long-term down-regulation of collagen type I (COL1A1) expression by nanofiber-mediated siRNA gene silencing. Acta Biomater. 2013 Jan;9(1):4513-24; https://pmc.ncbi.nlm.nih.gov/articles/PMC3523808/.

[427] Freitas RA Jr. Nanomedicine, Volume IIA: Biocompatibility, Landes Bioscience, Georgetown, TX, 2003; Section 15.2.5, "Coagulation and Thrombogenicity"; http://www.nanomedicine.com/NMIIA/15.2.5.htm.

[428] Freitas RA Jr. Nanomedicine, Volume IIA: Biocompatibility, Landes Bioscience, Georgetown, TX, 2003; Section 15.5.5, "Mechanocompatibility with Nontissue Cells"; http://www.nanomedicine.com/NMIIA/15.5.5.htm.

[429] Litvinov RI, Weisel JW. What Is the Biological and Clinical Relevance of Fibrin? Semin Thromb Hemost. 2016 Jun;42(4):333-43; https://pmc.ncbi.nlm.nih.gov/articles/PMC5536100/.

[430] Xu LC, Bauer JW, Siedlecki CA. Proteins, platelets, and blood coagulation at biomaterial interfaces. Colloids Surf B Biointerfaces. 2014 Dec 1;124:49-68; https://pmc.ncbi.nlm.nih.gov/articles/PMC5001692/.

[431] Ji H, Yu K, Abbina S, Xu L, Xu T, Cheng S, Vappala S, Arefi SMA, Rana MM, Chafeeva I, Drayton M, Gonzalez K, Liu Y, Grecov D, Conway EM, Zhao W, Zhao C, Kizhakkedathu JN. Antithrombotic coating with sheltered positive charges prevents contact activation by controlling factor XII-biointerface binding. Nat Mater. 2025 Apr;24(4):626-636; https://pmc.ncbi.nlm.nih.gov/articles/PMC11961369/.

[432] Crago M, Lee A, Hoang TP, Talebian S, Naficy S. Protein adsorption on blood-contacting surfaces: A thermodynamic perspective to guide the design of antithrombogenic polymer coatings. Acta Biomater. 2024 May;180:46-60; https://www.sciencedirect.com/science/article/pii/S1742706124001910.

The main medical risk in the Blood Extraction Subunit (Section 4.2.2) is probably blood clotting or embolism – if the device disturbs flow or creates low-flow eddies, clots could form. A clot in the renal vein interface could propagate or cause a pulmonary embolism if dislodged. While atomically smooth diamond surfaces and high flow might help keep clots at bay, real implants (even coated stents) often need anticoagulation initially. In the worst case scenario, use of the metabolic organ might necessitate the patient to be on anti-coagulant medication permanently, but good design should be able to avoid this. For example, the device's internal surfaces might be lined with endothelial cells (biological integration) or glycocalyx-mimicking coatings to fool the body into treating it as normal vessel. Additionally, the internal geometry maintains laminar flow above a minimum shear threshold to discourage stagnation. The need to redirect renal venous blood flow through the BES also indicates the need for careful attention to vascular mechanocompatibility.[433]

(3) **Hemolysis and Red-Cell Integrity**[434] – ensuring that micro- and nano-scale pumps or channels do not create shear stresses high enough to damage erythrocytes, by verifying that flow rates, channel geometries, and surface rugosities are within safe thresholds, and that sorting rotors produce nanomachine shear rates low enough to avoid erythrocyte lysis in the BES. The tangential shear stress imposed by the part of the sorting rotor exposed to blood is $\tau_{shear} \sim \rho_{blood}\ r_{rotor}\ (\nu_{rotor}\ \Omega_{rotor}^{3})^{1/2}\ G'(0) =$ **2 Pa**,[435] for $\rho_{blood} \sim 1060$ kg/m^3, $r_{rotor} \sim 5$ nm, $\nu_{rotor} = \mu_{blood} / \rho_{blood} \sim 2.8 \times 10^{-6}$ m^2/sec (blood at 310 K) and blood viscosity $\mu_{blood} \sim 3 \times 10^{-3}$ Pa-sec,[436] $\Omega = (2\pi)$ (86,000 rev/sec) $= 5.4 \times 10^5$ rad/sec, and the dimensionless shear-rate coefficient $G'(0) \sim 0.616$.[437] This is well below the no-trauma design limit of <**12 Pa** that ensures zero sublethal damage to red cells,[438] the physiological maximum of **15 Pa** in microvessels and the subhemolytic threshold of ~**30 Pa** for 2 min exposures, [439] and the hemolytic threshold of **300-400 Pa** that can be briefly

---

[433] Freitas RA Jr. Nanomedicine, Volume IIA: Biocompatibility, Landes Bioscience, Georgetown, TX, 2003; Section 15.5.3, "Vascular Mechanocompatibility"; http://www.nanomedicine.com/NMIIA/15.5.3.htm.

[434] Freitas RA Jr. Nanomedicine, Volume IIA: Biocompatibility, Landes Bioscience, Georgetown, TX, 2003; Section 15.5.5.1, "Mechanical Interactions with Erythrocytes"; http://www.nanomedicine.com/NMIIA/15.5.5.1.htm.

[435] https://en.wikipedia.org/wiki/Von_K%C3%A1rm%C3%A1n_swirling_flow.
[436] https://en.wikipedia.org/wiki/Hemorheology.

[437] Schlichting H, Gersten K. Boundary-Layer Theory. 8th ed., Springer, 2000; https://www.amazon.com/Boundary-Layer-Theory-H-Schlichting/dp/3540662707/. (Table of similarity solutions for the rotating disk) See also: White FM. Viscous Fluid Flow. 3rd ed., McGraw-Hill, 2005, §6.5 "Rotating Disk" (gives $G'(0) \sim 0.616$); https://www.amazon.com/Viscous-Fluid-MCGRAW-MECHANICAL-ENGINEERING/dp/0072402318/.

[438] https://www.heartrecovery.com/en-us/education/education-library/faq-hemolysis.

[439] Avc M, Edgar A. O'Rear EA, Foster KM, Papavassiliou DV. Sublethal Damage to Erythrocytes during Blood Flow. Fluids 2022; 7(2):66; https://www.mdpi.com/2311-5521/7/2/66.

tolerated in modern Ventricular Assist Devices (VADs).[440] Internal channels should exceed a few microns in diameter and avoid abrupt flow accelerations.

(4) **Protein Adsorption**[441] **and Biofouling**[442] – mitigating non-specific adsorption of plasma proteins that can lead to fouling, loss of device function, or immune activation, perhaps incorporating ultra-smooth (atomically flat) surfaces, zwitterionic coatings to resist protein layering, or other anti-biofilm surface treatments. The traditional approach is exemplified by Zhang *et al.*,[443] who critically review biomaterials for nano-encapsulation, highlighting how material properties (surface charge, hydrophilicity, roughness) influence non-specific protein adsorption and downstream fouling or immune activation,[444] and by Roach *et al.*,[445] who specifically analyze the "conditioning film" of adsorbed plasma proteins and its role in mediating cell-surface interactions.[446] Fouling and biofilm formation on rotor surfaces is a serious concern, as even diamond can get coated with proteins or cellular deposits. In practice, any filter that processes bodily fluids (blood or urine) tends to clog over time, so the design might require periodic self-cleaning or backflushing cycles, nanorobotic "windshield wiper" mechanisms, or occasional replacement of nanofilter elements.

(5) **Urine-Side Scaling and Encrustation**[447] – preventing deposition of mineral salts (e.g., calcium phosphate, magnesium ammonium phosphate) on components of the rotor system of the Urine Extraction Subunit (Section 4.2.1) that is placed inside the two ureters, by designing

---

[440] https://www.heartrecovery.com/en-us/education/education-library/faq-hemolysis.

[441] Freitas RA Jr. Nanomedicine, Volume IIA: Biocompatibility, Landes Bioscience, Georgetown, TX, 2003; Section 15.2.2, "Adhesive Interactions with Implant Surfaces"; http://www.nanomedicine.com/NMIIA/15.2.2.htm.

[442] Freitas RA Jr. Nanomedicine, Volume IIA: Biocompatibility, Landes Bioscience, Georgetown, TX, 2003; Section 15.3.6.6 "Biofouling of Medical Nanorobots"; http://www.nanomedicine.com/NMIIA/15.3.6.6.htm.

[443] Zhang L, Cao Z, Bai T, Carr L, Ella-Menye JR, Irvin C, Ratner BD, Jiang S. Zwitterionic hydrogels implanted in mice resist the foreign-body reaction. Nat Biotechnol. 2013 Jun;31(6):553-6; https://pubmed.ncbi.nlm.nih.gov/23666011/.

[444] Witika BA, Makoni PA, Matafwali SK, Chabalenge B, Mwila C, Kalungia AC, Nkanga CI, Bapolisi AM, Walker RB. Biocompatibility of Biomaterials for Nanoencapsulation: Current Approaches. Nanomaterials (Basel). 2020 Aug 22;10(9):1649; https://pmc.ncbi.nlm.nih.gov/articles/PMC7557593/.

[445] Roach P, Farrar D, Perry CC. Interpretation of protein adsorption: surface-induced conformational changes. J Am Chem Soc. 2005 Jun 8;127(22):8168-73; https://pubmed.ncbi.nlm.nih.gov/15926845/.

[446] Brash JL, Horbett TA, Latour RA, Tengvall P. The blood compatibility challenge. Part 2: Protein adsorption phenomena governing blood reactivity. Acta Biomater. 2019 Aug;94:11-24; https://pmc.ncbi.nlm.nih.gov/articles/PMC6642842/.

[447] Freitas RA Jr. Nanomedicine, Volume IIA: Biocompatibility, Landes Bioscience, Georgetown, TX, 2003; Section 15.2.2, "Adhesive Interactions with Implant Surfaces"; http://www.nanomedicine.com/NMIIA/15.2.2.htm.

nonadhesive nanorobot surfaces,[448] self-cleaning surfaces, hydrophilic surface grafts and periodic back-flush cycles[449] to avoid clogging. Traditionally, Teflon and PEG coatings have been studied in long-term urinary catheters to prevent mineral encrustation. Contemporary ureteral stents combine inert polymer substrates with anti-fouling coatings, novel surface chemistries, antimicrobial agents, optimized stent geometry, and, in some cases, biodegradable materials to minimize encrustation, biofilm-related infection and chronic tissue reaction.[450]

(6) **Bacterial Colonization and Biofilm Formation**[451] – guarding against urinary tract or bloodstream infection by ensuring sterile implantation and employing antibacterial surface treatments. Donlan and Costerton[452] provide a foundational review of biofilm biology on implanted devices and survey antimicrobial-release coatings that could be adapted for nanorobotic surfaces, and a controlled release of antimicrobial peptides or periodic local sterilization protocols are additional possible solutions. In the specific case of the metabolic organ, the transdermal port for recharging the battery is a pathway for bacteria, and any device components in the ureters or in contact with blood could serve as surfaces for biofilm formation. Nanoscale surface patterning combined with antibacterial coatings[453] and bottomless elutions[454]

---

[448] Freitas RA Jr. Nanomedicine, Volume IIA: Biocompatibility, Landes Bioscience, Georgetown, TX, 2003; Section 15.2.2.1, "Nonadhesive Nanorobot Surfaces"; http://www.nanomedicine.com/NMIIA/15.2.2.1.htm.

[449] Stickler DJ. Clinical complications of urinary catheters caused by crystalline biofilms: something needs to be done. J Intern Med. 2014 Aug;276(2):120-9; https://onlinelibrary.wiley.com/doi/10.1111/joim.12220.

[450] Chew BH, Denstedt JD. Technology insight: Novel ureteral stent materials and designs. Nat Clin Pract Urol. 2004 Nov;1(1):44-8; https://pubmed.ncbi.nlm.nih.gov/16474466/. Cauda F, Cauda V, Fiori C, Onida B, Garrone E. Heparin coating on ureteral Double J stents prevents encrustations: an in vivo case study. J Endourol. 2008 Mar;22(3):465-72; https://pubmed.ncbi.nlm.nih.gov/18307380/. De Grazia A, Somani BK, Soria F, Carugo D, Mosayyebi A. Latest advancements in ureteral stent technology. Transl Androl Urol. 2019 Sep;8(Suppl 4):S436-S441; https://pmc.ncbi.nlm.nih.gov/articles/PMC6790420/. Tomer N, Garden E, Small A, Palese M. Ureteral Stent Encrustation: Epidemiology, Pathophysiology, Management and Current Technology. J Urol. 2021 Jan;205(1):68-77; https://pubmed.ncbi.nlm.nih.gov/32856981/. Guo H, Yuan JB. New insights into the prevention of ureteral stents encrustation. Open Med (Wars). 2023 Dec 6;18(1):20230854; https://pmc.ncbi.nlm.nih.gov/articles/PMC10710215/.

[451] Freitas RA Jr. Nanomedicine, Volume IIA: Biocompatibility, Landes Bioscience, Georgetown, TX, 2003; Section 15.2.1.4, "Implant Infection and Biofilms"; http://www.nanomedicine.com/NMIIA/15.2.1.4.htm.

[452] Donlan RM, Costerton JW. Biofilms: survival mechanisms of clinically relevant microorganisms. Clin Microbiol Rev. 2002 Apr;15(2):167-93; https://pmc.ncbi.nlm.nih.gov/articles/PMC118068/.

[453] Cyphert EL, von Recum HA. Emerging technologies for long-term antimicrobial device coatings: advantages and limitations. Exp Biol Med (Maywood). 2017 Apr;242(8):788-798; https://pmc.ncbi.nlm.nih.gov/articles/PMC5407537/. das Neves RC, Mortari MR, Schwartz EF, Kipnis A, Junqueira-Kipnis AP. Antimicrobial and Antibiofilm Effects of Peptides from Venom of Social Wasp and Scorpion on Multidrug-Resistant *Acinetobacter baumannii*. Toxins (Basel). 2019 Apr 10;11(4):216; https://pmc.ncbi.nlm.nih.gov/articles/PMC6520840/. Zhao Y, Chen G, Yushanjiang S, Zhao M, Yang H, Lu R, Qu R, Dai Y, Yang L. In vitro and in vivo study of antibacterial and anti-encrustation coating on

(continuously synthesized by the NSU) at these interfaces should provide significant protection, but further research may be needed to completely resolve this risk.

(7) **Long-Term Material Stability and Wear** – all structural and moving components must resist corrosion, mechanical fatigue, and molecular degradation over years of use. Diamondoid components should be chemically inert[455] and extremely durable against corrosion,[456] wear,[457] and fatigue,[458] and generally biocompatible,[459] specifically including diamond,[460] sapphire,[461] and carbon fullerenes and nanotubes.[462]

---

ureteric stents. BJU Int. 2024 Jul;134(1):72-80; https://bjui-journals.onlinelibrary.wiley.com/doi/pdfdirect/10.1111/bju.16326.

[454] Bistolfi A, Massazza G, Verné E, Massè A, Deledda D, Ferraris S, Miola M, Galetto F, Crova M. Antibiotic-loaded cement in orthopedic surgery: a review. ISRN Orthop. 2011 Aug 7;2011:290851; https://pmc.ncbi.nlm.nih.gov/articles/PMC4063209/. Tande AJ, Patel R. Prosthetic joint infection. Clin Microbiol Rev. 2014 Apr;27(2):302-45; https://pmc.ncbi.nlm.nih.gov/articles/PMC3993098/. Tarakji KG, Mittal S, Kennergren C, Corey R, Poole JE, Schloss E, Gallastegui J, Pickett RA, Evonich R, Philippon F, McComb JM, Roark SF, Sorrentino D, Sholevar D, Cronin E, Berman B, Riggio D, Biffi M, Khan H, Silver MT, Collier J, Eldadah Z, Wright DJ, Lande JD, Lexcen DR, Cheng A, Wilkoff BL; WRAP-IT Investigators. Antibacterial Envelope to Prevent Cardiac Implantable Device Infection. N Engl J Med. 2019 May 16;380(20):1895-1905; https://pubmed.ncbi.nlm.nih.gov/30883056/. Barbar T, Patel R, Thomas G, Cheung JW. Strategies to Prevent Cardiac Implantable Electronic Device Infection. J Innov Card Rhythm Manag. 2020 Jan 15;11(1):3949-3956; https://pmc.ncbi.nlm.nih.gov/articles/PMC7192142/. Callahan TD, Tarakji KG, Wilkoff BL. Antibiotic eluting envelopes: evidence, technology, and defining high-risk populations. Europace. 2021 Jun 23;23(23 Suppl 4):iv28-iv32; https://pmc.ncbi.nlm.nih.gov/articles/PMC8221048/.

[455] Freitas RA Jr. Nanomedicine, Volume IIA: Biocompatibility, Landes Bioscience, Georgetown, TX, 2003; Section 15.3.1.5, “Chemical Inertness of Diamond”; http://www.nanomedicine.com/NMIIA/15.3.1.5.htm.

[456] Freitas RA Jr. Nanomedicine, Volume I: Basic Capabilities. Landes Bioscience, Georgetown, TX, 1999; Section 9.3.5, “Materials Disassembly for Disposal”; http://www.nanomedicine.com/NMI/9.3.5.htm.

[457] Drexler KE. Nanosystems: Molecular Machinery, Manufacturing, and Computation. John Wiley & Sons, New York, 1992; Section 10.10.2.b, “No wear, no contaminants”; https://www.amazon.com/dp/0471575186/.

[458] Drexler KE. Nanosystems: Molecular Machinery, Manufacturing, and Computation. John Wiley & Sons, New York, 1992; Section 10.10.2.c, “No fatigue, tolerance of high strains”; https://www.amazon.com/dp/0471575186/.

[459] Freitas RA Jr. Nanomedicine, Volume IIA: Biocompatibility, Landes Bioscience, Georgetown, TX, 2003; Chapter 15.3, “Biocompatibility of Nanomedical Materials”; http://www.nanomedicine.com/NMIIA/15.3.htm.

[460] Freitas RA Jr. Nanomedicine, Volume IIA: Biocompatibility, Landes Bioscience, Georgetown, TX, 2003; Section 15.3.1, “Biocompatibility of Diamond”; http://www.nanomedicine.com/NMIIA/15.3.1.htm.

Given the ability to manufacture atomically-precise and atomically-specified implant surfaces, it should be possible to minimize or largely eliminate all of the aforementioned biocompatibility risks, ensuring that the metabolic organ can remain safe, functional, and biocompatible over the long term – and always with the assurance that even if an entire subsystem (like the NSU) fails, the patient can still eat normally.

General safety issues. The metabolic organ must be designed to avoid or minimize any safety issues that might arise if its components are **physically damaged**, e.g., if the user falls onto concrete, is struck in the torso with a blunt object, is involved in a car crash, or a bullet or other projectile enters the abdomen and penetrates or ruptures the device, or an individual flywheel loses integrity and explodes. The exterior casing of the metabolic organ can be extremely rupture-resistant if made composed of multilayer nanotube-reinforced crystalline diamond with a sufficiency of internal energy-absorbing crumple layers. The Nutrient Storage Tank can be deployed as numerous smaller tanks to avoid single-point failure, providing redundancy in case one is ruptured.

The biggest general safety risk is probably the 480 cm^3 **flywheel battery** that contains ~17.3 MJ of stored energy (Section 4.3.3.1), roughly comparable to the energy contained in ~0.36 kg of gasoline[463] (which humans routinely carry in cars). The design must include methods for preventing rapid energy release if portions of the battery are disrupted or breached, perhaps by (1) subdividing the battery into multiple smaller subunits (compartmentalization), (2) adding energy-absorptive internal support infrastructure (e.g., internal compressible voids, shock absorbers, or "crumple zones"), (3) employing shock-resistant containment (ensuring any fragments from broken nanomachines remain trapped inside the device housing), and other similar techniques. The system should include fail-safes: if a flywheel malfunctions or if an impact is detected (via accelerometers), electromagnetic brakes or redundant bearings can rapidly decelerate the flywheels to dissipate energy gradually as heat, avoiding any explosive release. Simply providing a solid diamond shell ~1 mm thick surrounding the entire device, adding ~185 gm (or <8%) to total metabolic organ mass, would provide a blast containment vessel that could tolerate the simultaneous explosion of 5% of all flywheels in the battery.[464] The granular nature of the energy

---

[461] Freitas RA Jr. Nanomedicine, Volume IIA: Biocompatibility, Landes Bioscience, Georgetown, TX, 2003; Section 15.3.5, "Biocompatibility of Sapphire, Ruby, and Alumina"; http://www.nanomedicine.com/NMIIA/15.3.5.htm.

[462] Freitas RA Jr. Nanomedicine, Volume IIA: Biocompatibility, Landes Bioscience, Georgetown, TX, 2003; Section 15.3.2, "Biocompatibility of Carbon Fullerenes and Nanotubes"; http://www.nanomedicine.com/NMIIA/15.3.2.htm.

[463] Freitas RA Jr. Energy Density. IMM Report No. 50, 25 June 2019; Table 29, "Specific energy of fuel materials during ambient combustion"; http://www.imm.org/Reports/rep050.pdf.

[464] Crudely modeling the flywheel detonation as an ideal diatomic gas with a heat capacity ratio* of $\gamma \sim 1.4$, the explosive peak pressure is $p_{max} \sim f_{explode}\, E_{flybatt}\, (\gamma - 1) / V_{organ} \sim 3.15 \times 10^8$ N/m^2 and the required containment shell thickness is $t_{shell} \sim R_{organ}\, p_{max} / 2\, \sigma_w = 1.01$ mm, giving shell volume $V_{shell} \sim (4\pi/3)\, [(R_{organ} + t_{shell})^3 - R_{organ}{}^3] = 52.8$ cm^3 and shell mass $M_{shell} \sim \rho_{diamond}\, V_{shell} =$ **185 gm**, taking $V_{organ} = 1100$ cm^3, $E_{flybatt} = 17.3$ MJ, $f_{explode} = 5\%$, $\rho_{diamond} = 3510$ kg/m^3, and diamond failure strength $\sigma_w \sim 10^{10}$ N/m^2.
* https://en.wikipedia.org/wiki/Heat_capacity_ratio.

storage (e.g., ~600 pJ/flywheel) is actually a safety feature, as long as one failure doesn't cascade into neighboring rotors – interior "blast doors" or bulkheads can be placed at key locations throughout the battery volume to reduce the likelihood of explosive chain-reactions and to interrupt blast-wave propagation.

Installation presumably requires **major surgery** – e.g., in today's world, a laparotomy[465] to place the device and connect to vessels and ureters, similar to an organ transplant – but the surgical techniques available in a future era of advanced medical nanorobotics and metabolic organs will be far more sophisticated than today's and are outside the scope of this paper. The ~1100 cm^3 device sits in the abdomen, likely in the retroperitoneal space, and is smaller than a liver in volume but actually heavier, at ~2.4 kg. Surgeons would need to secure it to avoid pressure on other organs or sinking, possibly with some internal reinforcement or harness, requiring careful surgical technique to avoid compressing other organs or blood vessels. If necessary, device density could be reduced closer to normal tissue density by increasing device volume via internal voids without altering device mass, or by reducing mass by using less-dense materials or by redesigning atomically precise components such as sorting rotors and nanofabricators to have fewer atoms while achieving the same functionality. The device is essentially a multi-organ replacement (liver for nutrient synthesis, kidney for waste removal, lung for gas exchange), so post-operative intensive care, monitoring, and long-term maintenance would be expected just as in any multiple organ transplant or implant.

The device should fail-safe in the event of total **power failure**. If the battery dies suddenly, all active pumping stops, in which case the device must be configured so that blood flow is not blocked. Ideally, the BES would behave like a passive stent when unpowered, allowing blood through to the lungs normally. If any valves or pumps in the blood path freeze in a closed state, that would cause immediate harm (e.g., venous blockage). The same risk applies to the UES, which if unpowered should default to letting urine flow unprocessed to the bladder to prevent hydronephrosis (kidney back-pressure).[466] The design should employ nanoscale filters with no macroscale valves so there's no single point (like a clamp) that can stop flow if unpowered (whereupon continuous flow is maintained and extraction rotors simply stop removing molecules, safely reverting the user back to normal physiology). Further research is required to determine if the long-term presence of even a small rotor assembly in the ureter could lead to scarring or stone formation.

Thermal safety is another important design issue. Given the risk of hyperthermia, environmental conditions and hydration may be limiting factors for device use. Given known human thermal limits, 200 W extra in the core is at the edge of what can be dissipated continuously in temperate climate. A scenario where the user is in a hot environment or cannot increase the sweat rate (e.g., high humidity or wearing insulating clothing) could lead to overheating. The AMO might enable metabolic exertion that outstrips the body's normal thermoregulatory capacity. In effect, the user could potentially "overclock" their metabolism (since nutrients and oxygen are plentiful from the device) and may hit a heat-dissipation limit before a metabolic or nutritional limit. Thus the ultimate sustained performance limit might be set by thermoregulation rather than nutrient supply. In practical terms, the device may need safety governors – for example, if internal

---

[465] https://en.wikipedia.org/wiki/Laparotomy.
[466] https://en.wikipedia.org/wiki/Hydronephrosis.

temperature sensors detect overheating, the AMO could intentionally throttle nutrient release, temporarily reducing support for extreme exertion, to protect the user from heat stroke. In sum, the feasibility of sustained high-power operation might be limited in practice by human thermal tolerances: an AMO-equipped person might be nutritionally self-sufficient but would still need to remain mindful of hydration and cooling, similar to any person performing strenuous activity.

4.3.8 Above-Basal Performance

Except for the relatively small impact of Na^+/K^+-ATPase down-regulation if implemented as described above, there should be no major reduction in the maximum performance of users possessing baseline-design metabolic organs who choose to engage in vigorous physical exercise. This is because the original basic objective of the metabolic organ was to serve as a supplementary source of basal "survival" nutrition, not a complete and permanent replacement for all conventional nutrition (i.e., food). Having such an organ would permit the user to easily survive lengthy periods without access to conventional food, as long as air, water, electricity, and a few grams per day of supplemental minerals from internal stores remain available.

What is the effect on the baseline design of the metabolic organ if we want its effectiveness to continue when the user engages in physical activities requiring above-basal power and endurance? **Table 18** provides brief descriptions of the levels of physical effort that are characteristic of a range of metabolic power levels.

Table 18. Approximate physical effort required by 70 kg male to generate the indicated amount of metabolic waste heat (activity metabolism)

Metabolic Power Level (W)	Typical Physical Effort Required
100 (basal)	lying quietly or sitting at rest
200	strolling at ~3 km/hr
300	brisk walking at ~5 km/hr
400	slow jogging at ~8 km/hr
500	running at ~10 km/hr (~6 min/mile pace)
600	running at ~12 km/hr (~5 min/mile pace)[467]
700	running at ~14 km/h (~4.33 min/mile pace, very vigorous pace)
800	near-maximal sprinting at ~16 km/hr (~3.75 min/mile pace)[468]
900	30-60 sec sprint, trained track cyclist or elite rower
1000	a few-second burst by a world-class sprinter

[467] The men's world record time for a 26-mile marathon is 2:00:35, set by Kelvin Kiptum at the Chicago Marathon in 2023, an average speed of **4.6 min/mile**; https://en.wikipedia.org/wiki/Marathon_world_record_progression.

[468] The current male world record for running the mile is 3 min, 43.13 sec, set by Hicham El Guerrouj of Morocco at Rome's Stadio Olimpico on 7 July 1999, an average speed of **3.72 min/mile**; https://en.wikipedia.org/wiki/Mile_run.

Sustained exertions above 600-700 W of metabolic power for more than a few minutes are almost impossible, even for top competitors. Elite athletes can briefly hit metabolic rates of 900-1000 W, but only in all-out sprint efforts.

During physical exertion lasting some period of hours, basal protein and lipid resources are not significantly drawn down compared to available reserves. There is increased water loss from extra sweating that must be supplemented with increased water intake. Sweating loses salts and mineral electrolytes, and continuous high-rate metabolism depletes cofactors, vitamins and other micronutrients. But all of these items can be can be stored as extra reserves in the Nutrient Storage Tank of a user who is planning to do a lot of strenuous exercise, so sweating and heavy exercise should not unduly tax the resources of the baseline metabolic organ. No extra nanocomputers or other support infrastructure appear to be required.

In the context of a metabolic organ, supporting vigorous physical activity mainly requires faster recycling of glucose, the primary energy source, and carbon dioxide, the primary waste molecule.

Glucose. The basal glucose nutrient requirement is $m_x \sim 400$ gm/day (~17 gm/hr),[469] or $n_x \sim 5.58 \times 10^{22}$ glucose molecules/hr, at the 100 W metabolic level (**Table 1**). Each additional 100 W of physical activity will require the Nutrient Synthesis Unit or NSU (Section 4.1) to mechanosynthesize a similar increment of nutrient glucose. The NSU generates $R_{FS} = r_{organics} MW_{glucose} / N_A \sim 3 \times 10^{-17}$ gm/sec of glucose per Nanofabricator (Section 4.1.2), so at the 2 P_{BMR} ~ 200 W power level we'll need an extra $n_{xNF} = m_x R_{FS} \sim 157$ trillion Nanofabricators, of mass $n_{xNF} M_{FS} \sim 3.14$ gm and volume $n_{xNF} V_{FS} \sim 1.57$ cm^3. Assuming water is plentiful for the reaction, we'll also need 6 times as many CO_2 molecules (3.35×10^{23} CO_2 molecules/hr) supplied to the NSU to make this happen, along with ~(4658 zJ/glucose molecule) ($n_x / (\varepsilon_{MS})$ ~ 3.25 MJ/hr of energy input, or an additional ~90 W of power draw from the flywheel battery while the user is exercising. The supplementary mechanosynthesis will also produce a sufficiency of 3.35×10^{23} molecules/hr of **oxygen** to be fed to the Blood Extraction Subunit or BES (Section 4.2.2) to enable CO_2 extraction from the blood.

Carbon Dioxide. The main function of the BES (Section 4.2.2) is to extract CO_2 from, and then reoxygenate, the blood. A 2 P_{BMR} ~ 200 W exercise power level requires roughly doubling the amount of CO_2 processed for the duration of the 200 W exercise effort. Since the blood residence time $t_{cap} \sim 5$ sec (>> t_{carb}, t_{bicarb}), and because the total capillary-facing area of a tenfold-higher rotor count of 10 $A_{rotors} \sim 4$ m^2 is still 6 times smaller than the total capillary surface area $A_{cap} \sim 24$ m^2, then up to a 5-fold speedup of blood passing through the nanofilter might be possible without significantly degrading its performance. This means the nanofilter may not require increasing in size, perhaps up to a ~5 P_{BMR} ~ 500 W exercise effort. However, at P_{BMR} ~ 200 W the Nutrient Molecule Transport System must be doubled in size, adding ~40 cm^3, ~7 gm, and ~4.6 W to the total resource requirement, along with an extra ~2.5 mm^3 and ~4 mg of Nutrient Distribution Sorting Rotors (**Table 16**).

Table 19 shows the changes to the baseline metabolic organ that would be needed to sustain and fully recycle nutrients and waste products for a user engaging in vigorous physical exercise at

---

[469] The human body stores ~500 gm of glucose in the form of glycogen, including ~400 gm (~1600 kcal) in the muscles and ~100 gm (~400 kcal) in the liver, or roughly 1.25 day's basal metabolic burn rate.

metabolic power levels up to 500 W. The flywheel battery holds $E_{flybatt} \sim P_{MetOrg}\ t_{day} \sim 17.3$ MJ of stored energy, enough for ~1 day at the basal rate, ~16.3 hr at the 200 W metabolic rate, or 8.3 hr at the 500 W metabolic rate. The AMO can monitor core temperature, and possible skin temperature by direct or indirect means. If overheating is detected (e.g., during sustained 500 W output in a hot environment), the device could temporarily modulate nutrient output to reduce metabolic heat, or prompt the user (via a haptic or electronic alert) to rest or cool down. In an envisioned practical use, users might wear a light cooling garment or ensure hydration during extreme exercise.

Table 19. Metabolic organ modifications to accommodate higher activity power levels

System or Subsystem	Mass (gm)	Volume (cm^3)	Power (W)	Total Heat (W)	Sweat (L/hr)
Activity Metabolism: **200 W**					
157 trillion Nanofabricators (x10)	3.14	1.57	90		
Nutrient Molecule Transport System (x10)	7	40	4.6		
Nutrient Distribution Sorting Rotors (x10)	0.004	0.003	~0		
Total Additions to Baseline Organ	10.1	41.6	94.6		
Augmented Organ @ 200 W Metabolism	2410	1142	295	495	0.73
Activity Metabolism: **300 W**					
Total Additions to Baseline Organ	20.3	83.1	189.2		
Augmented Organ @ 300 W Metabolism	2420	1183	389	689	1.02
Activity Metabolism: **400 W**					
Total Additions to Baseline Organ	30.4	124.7	283.8		
Augmented Organ @ 400 W Metabolism	2430	1225	484	884	1.31
Activity Metabolism: **500 W**					
Total Additions to Baseline Organ	40.6	166.3	378.4		
Augmented Organ @ 500 W Metabolism	2441	1266	578	1078	1.60

Total heat production (metabolic plus augmented artificial organ), shown in the fifth column of **Table 19**, rises about twice as fast as metabolic heat production alone because recycling enough nutrients to produce each additional ~100 W of metabolic heat requires the enhanced metabolic organ to produce an additional ~96 W of nanomachinery waste heat, exacerbating the thermoregulatory challenge.

Evaporative cooling (sweat) can carry away $E_s \sim 2.43$ MJ/kg of water at body temperature,[470] so the $2\ P_{BMR} \sim 200$ W power level the body must dissipate 200 W + 295 W = 495 W via sweating, which requires evaporating $R_{sweat} \sim (495\ W) / E_s \sim 0.73$ L/hr assuming $\rho_{sweat} \sim 1$ gm/cm^3. Note

[470] Baker LB. Physiology of sweat gland function: The roles of sweating and sweat composition in human health. Temperature (Austin). 2019 Jul 17;6(3):211-259; https://pmc.ncbi.nlm.nih.gov/articles/PMC6773238/.

that the ISO-endorsed Thermal Work Limit[471] for "safe, indefinitely maintainable" work in hot environments is a **1.2 L/hr** sweat-rate ceiling, and an adult can sweat as much as **2-4 L/hr** for a short time under extreme conditions.[472] The mass and volume increases in the upgraded metabolic organ to sustain this extra capacity are minimal, but the practical limit for full nutrient recycling is probably in the 400-500 W range due to constraints on the maximum evaporative cooling capacity of the human body. Note that during periods of lighter physical activity or complete rest (i.e., basal rate), the power consumption of an augmented metabolic organ would revert to the lower levels consistent with nutrient demand – the slight extra mass and volume of the device would remain, but its waste heat would decline proportionately to the activity level.

If the goal was to enable superhuman endurance during lengthy periods (e.g., continuous ~8 hr exertions at the 500 W metabolic rate) of vigorous physical activity, additional internal nanorobotic augmentations to the human body beyond the metabolic organ would be required because many physiological and regulatory brakes remain in place:

(1) **Calcium-handling exhaustion**. SR Ca^{2+} pumps (SERCA)[473] and ryanodine receptors[474] fatigue under relentless cycling and may hit a ceiling where these biological "molecular machines" begin to misfold or oxidize and must be replaced, even with optimal supplies of Ca^{2+}, ATP and cofactors.

(2) **Lactate clearance from muscles**. Lactate[475] (and the associated H^+ load) is generated and buffered primarily inside active muscle fibers, and only then is exported into the blood. Lactate ($C_3H_5O_3^-$) exits muscle through MCT isoforms[476] (especially MCT4 in fast-twitch fibers), but this transport is saturable and limited by membrane transporter density and the trans-sarcolemmal H^+/lactate gradient. Even with lactate aggressively cleared from the blood,[477] the rate at which muscle can offload lactate is capped by local capillary perfusion (blood flow per muscle mass) and MCT transport capacity (i.e., V_{max} and K_m of the transporters), with time constants on the order of minutes at best – systemic clearance lowers blood lactate but can't instantly "vacuum" lactate (and H^+) out of the fiber.

(3) **Bone and tendon fatigue**. Every footstrike or push-off at high speed generates microcracks in bone and microtears in tendons and ligaments. Even with perfect nutrient delivery

---

[471] https://en.wikipedia.org/wiki/Thermal_work_limit. The index, which has been introduced into the United Arab Emirates and Australia, and has resulted in a substantial fall in the incidence of heat illness in the latter, is designed for self-paced workers and does not rely on estimation of actual metabolic rates.

[472] https://en.wikipedia.org/wiki/Perspiration.
[473] https://en.wikipedia.org/wiki/SERCA.
[474] https://en.wikipedia.org/wiki/Ryanodine_receptor.
[475] https://en.wikipedia.org/wiki/Lactic_acid.
[476] https://en.wikipedia.org/wiki/Monocarboxylate_transporter.

[477] The human blood volume contains 0.24-1.07 gm of L-lactate (4.5-19.8 x 10^{-5} gm/cm^3 venous plasma reference range) with a ~117 gm/day turnover rate,* virtually all of which is metabolized (either recycled into glucose or fully oxidized) rather than excreted intact.
* Gunnerson KJ. Lactic acidosis. Medscape, 22 Jan 2025; https://emedicine.medscape.com/article/167027-overview.

and cytokine clearance, remodeling those microinjuries[478] via osteoblasts/osteoclasts and collagen synthesis takes days to weeks, not hours. Continuous loading will therefore outpace repair, risking stress fractures and tendon rupture.

(4) **Rhabdomyolysis[479] and structural muscle damage**. Ultra-prolonged maximal contractions tear sarcolemmal membranes.[480] Even with perfect clearance of the resulting myoglobin and inflammatory debris, rebuilding connective tissue scaffolds and myofiber regeneration via satellite cells is still a multi-day process.

(5) **Mitochondrial and sarcomeric protein turnover**. High-frequency firing damages mitochondrial membranes and contractile proteins. Proteostasis[481] requires hours to days of low-intensity activity for mitophagy[482] and *in situ* protein synthesis.

(6) **Cardiovascular structural stress**. Maintaining near-maximal heart rates (~180 bpm) for many hours would push cardiac muscle to its mechanical limits, raising risk of arrhythmias, myocarditis-like injury,[483] and even acute heart failure, from prolonged tachycardia. Constant maximal vasodilation and high shear rates injure vessel linings, risking endothelial microinjury. Even with inflammatory molecules scrubbed from the bloodstream, repairing endothelium and basement membrane will be slow, risking microthrombosis.[484] Sustained near-maximal heart rates induce cardiomyocyte remodeling and oxidative damage; leukocyte clearance can't substitute for weeks-long cardiac tissue turnover.

(7) **Neurotransmitter and neuromodulator balance**. Serotonin, dopamine, GABA and endorphin pools get depleted or desensitized with continuous extreme exertion, degrading coordination, motivation and pain tolerance.

(8) **Psychological and sensory fatigue**. Eight hours of maximal pain and proprioceptive bombardment eventually collapse focus, reaction time and decision-making, limiting cognitive endurance. Sensory pathways adapt or desensitize, making it ever harder to sustain gait and limb coordination without stumbles or injury (e.g., central habituation).

4.3.9 Additional Functionality

Many optional functions could be added to the basic metabolic organ model, as detailed below.

---

[478] https://en.wikipedia.org/wiki/Microtrauma.
[479] https://en.wikipedia.org/wiki/Exertional_rhabdomyolysis.
[480] https://en.wikipedia.org/wiki/Sarcolemma.
[481] https://en.wikipedia.org/wiki/Proteostasis.
[482] https://en.wikipedia.org/wiki/Mitophagy.
[483] https://en.wikipedia.org/wiki/Myocarditis.
[484] https://en.wikipedia.org/wiki/Thrombotic_microangiopathy.

4.3.9.1 Low-Oxygen or Oxygen-Free Breathing

With the metabolic organ installed, a user will still feel the urge to breathe because pCO_2 is maintained close to 40 mmHg (Section 4.2.2), so involuntary respiration should continue as normal. However, within ~20 minutes of activating the device the venous blood arriving at the lungs should already be ~99% fully oxygenated,[485] so breathing is merely "topping off" the recycled internal oxygen inventory. A target for carbon dioxide removal and oxygen regeneration of 99% implies the system may only lose 1% of the 719 gm/day O_2 flux (**Table 5**), or ~7.19 gm/day. Adding 7.19 gm of oxygen to the Nutrient Storage Tank (**Table 16**), pressurized to 1000 atm, adds only $V_{O2tank} \sim 9.8$ cm^3 to Tank contents and would permit oxygen-free breathing for ~1 day at the basal rate, or until the flywheel battery runs out of power. The mechanical expansion energy available from discharging the oxygen tank down to $P_2 = 0.2$ atm (arterial pressure), or the energy cost to refill the oxygen tank to $P_1 = 1000$ atm from arterial pressure, is a fairly modest $W_{O2} \sim P_1 V_{O2tank} \ln(P_1/P_2) \sim 8.5$ kJ.

4.3.9.2 Blood Detoxification

A properly configured metabolic organ could be employed to rapidly detoxify the blood, or degrade airborne pollutants (benzene, formaldehyde) and heavy metals (lead, mercury), or persistent organic pollutants that have entered the bloodstream. For instance, a molecular sorting system operating on the entire blood volume could reduce a user's blood alcohol concentration (BAC) from "legally drunk" at $c_{drunk} = 0.08\%$ (~8 x 10^{-4} gm/cm^3) to "sober" at $c_{sober} = 0.01\%$ (~1 x 10^{-4} gm/cm^3) in $t_{extract} \sim 1$ min using $N_{sober} = n_{ethanol} / r_{sort} = 6.1 \times 10^{16}$ ethanol-binding-site-equipped sorting rotors, adding $M_{sober} = M_{rot} N_{sober} =$ **0.12 gm** of rotor mass, $V_{sober} = V_{rot} N_{sober} =$ **84 mm^3** of rotor volume, and $P_{sober} = n_{ethanol} E_{ethanol} \sim$ **7.3 W** of rotor power draw to the baseline metabolic organ, taking total sortation rate $n_{ethanol} = (c_{drunk} - c_{sober}) N_A / MW_{ethanol} t_{extract} \sim 8 \times 10^{20}$ molecules/sec; per-rotor sorting rate $r_{sort} \sim c_{molecule} r_{max} / c_{max} = 13{,}100$ molecules/rotor-sec for $c_{max} \sim 10^{-1}$ molecules/nm^3, $r_{max} \sim 10^6$ molecules/rotor-sec, and $c_{molecule} \sim c_{sober} N_A / MW_{ethanol} \sim 0.00131$ molecules/nm^3; and $E_{ethanol} = k_B T_{310K} \ln(0.08\%/0.01\%) \sim 8.9 \times 10^{-21}$ J/molecule, resulting in the removal of $M_{ethanol} \sim (c_{drunk} - c_{sober}) V_{blood} \sim 3.8$ gm of ethanol from the blood volume. However, progress toward sobriety will take a bit longer than $t_{extract}$ because only 20% of the total blood flow passes through the metabolic organ. Specifically, the $BAC \sim c_{drunk} - [(1 - (0.80)^{\tau}) (c_{drunk} - c_{sober})]$ reached after a sobering-up time period of τ will be BAC ~ 0.066% after τ ~ 1 min, BAC ~ 0.033% after $\tau \sim 5$ min, and BAC ~ 0.018% after $\tau \sim 10$ min.[486]

This same process could be employed to remove any identified drug or toxin from the blood if the metabolic organ is provided with (1) a rotor field equipped with fixed or variable-configuration binding sites keyed to the target toxin molecule, and (2) either a small mass of general-purpose

---

[485] Blood circulates once every ~1 min, and 20% of all blood passes through the renal veins, so after 20 circulations the blood should be $(0.80)^{20} \sim 1\%$ unoxygenated or $(1 - (0.80)^{20}) \sim 99\%$ oxygenated, if all venous blood passing through the metabolic organ is fully oxygenated.

[486] Various organs and tissues may have become saturated with ethanol after a night of binge drinking, and these molecules will gradually diffuse back into the bloodstream as BAC is drawn down by the metabolic organ, further slowing progress toward sobriety.

mechanodecomposition nanomachinery that could be remotely programmed to reduce the toxin molecule to harmless nutrient feedstock molecules, or temporary space in the Nutrient Storage Tank.

More generally, the AMO can prevent the accumulation of harmful wastes. Any identified unusable or truly toxic atoms or molecules can be excreted or rendered inert via decomposition. If not all cholesterol or bilirubin is needed for nutrients, the device can dispose of it safely.

4.3.9.3 Direct Blood Dosing

Specific drugs could be stocked in the Nutrient Storage Tank or synthesized *in situ* using a specialized bank of Nanofabricators (Section 4.1.1), then released into the bloodstream on a specific dosing schedule or under the direct intentional control of the user. The device could precisely regulate endocrine balance by synthesizing and releasing insulin, thyroid hormones, erythropoietin, growth hormone, or IGF-1 in direct response to physiological needs, or manufacture and deploy tailored antimicrobial peptides, monoclonal antibodies, or cytokine cocktails to fight infections, dampen autoimmunity, or support cancer immunotherapy. It could also provide rapid response therapeutics by storing small amounts of precursors for antidotes against nerve agents or arrhythmia-reversing compounds.

4.3.9.4 Metabolic and Physiological Augmentation

Beyond oxygen recycling, the metabolic organ could generate intermittent hypoxic or hyperoxic pulses to boost mitochondrial biogenesis – hypoxia and hyperoxia cycling could be useful for endurance training or altitude acclimation. The device could fine-tune electrolyte and pH homeostasis by monitoring and adjusting Na^+, K^+, Cl^-, Ca^{2+}, Mg^{2+} and blood pH continuously, and modulate dopamine, serotonin, GABA, acetylcholine, or endorphins on demand for mood stabilization, focus enhancement, or pain relief. With an expanded design the AMO could reverse its normal recycling mode of operation in order to generate a net excretion of excess nutrients (perhaps due to overeating), for purposes of weight loss – easier than traditional "dieting" – or to offset persistent or otherwise uncontrollable hypernutrition. Note that **water recycling**, while theoretically possible, seems not very useful because the large unrecoverable losses due to transdermal perspiration create an unavoidable need for regular water consumption even if all metabolic and urinary water could be recycled (which would also generate more waste heat during metabolic organ operation).

4.3.9.5 Communication and Control Interface

The metabolic organ could provide continuous biomarker surveillance via real-time sensing of blood markers (glucose, troponin, cytokines, tumor antigens, etc.) with onboard assays, enabling pre-symptomatic disease detection and automatic alerts to external devices or physicians (raising cybersecurity issues). It could run multiplexed assays analogous to PCR or ELISA on tiny blood

samples, reporting results wirelessly to healthcare providers or smartphone applications enabling continuous health records like a full-service implanted Lab-on-a-Chip. To accomplish all this, the metabolic organ will need some means to outmessage[487] to the user and the outside world, and some form of inmessaging[488] interface allowing the user to externally control the organ, the preferred options for both of which will vary by user and are outside the scope of this document.

4.3.10 Additional Enabled Applications

Several applications missions could be enabled by the basic utility of the artificial metabolic organ.

4.3.10.1 Space Exploration and Long-Duration Missions

The metabolic organ's ability to recycle internal waste into nutrients is especially appealing for space travel. Astronauts normally require ~1.7 kg/person/day of food,[489] which amounts to hundreds of kilograms per year that must be lifted and stored. An astronaut with a metabolic organ and access to plenty of electrical power would need far less consumable mass – mainly water and perhaps a small O_2 cartridge – significantly cutting launch weight and resupply needs. This could enable longer missions (to Mars or beyond) and smaller spacecraft, as the metabolic organ would generate much of the crew's food internally. Additionally, the "low-oxygen or oxygen-free breathing" mode (Section 4.3.9.1) could let astronauts survive in emergencies if cabin oxygen is compromised. In essence, the metabolic organ would be a game-changer for both space habitation and planetary exploration, allowing unsuited humans to live off recycled resources in closed ecosystems (or even carry the organ as a backup life-support system in spacesuits[490] for extended EVAs).

Alternatively, a version of the metabolic organ with access to the astronaut's urine collection system and air scrubber apparatus in an EVA suit[491] could revolutionize astronaut life support by making the suit function as a self-contained ecosystem[492] rather than a one-time-use kit. In such a "perpetual spacesuit", the metabolic organ attachment would take the astronaut's urine and exhaled CO_2 captured by the suit and regenerate oxygen to breathe and nutrients to drink or eat, vastly extending the duration of spacewalks and reducing reliance on resupply. Current EVA

---

[487] Freitas RA Jr. Nanomedicine, Volume I: Basic Capabilities. Landes Bioscience, Georgetown, TX, 1999; Section 7.4.6, "Outmessaging to Patient or User"; http://www.nanomedicine.com/NMI/7.4.6.htm.

[488] Freitas RA Jr. Nanomedicine, Volume I: Basic Capabilities. Landes Bioscience, Georgetown, TX, 1999; Section 7.4.2, "Inmessaging from Patient or User"; http://www.nanomedicine.com/NMI/7.4.2.htm.

[489] "Food for Space Flight", 28 Dec 2020; https://www.worldspaceflight.com/bios/spacefood.php.

[490] https://www.nasa.gov/reference/11-0-spacesuits-vol-2/; https://en.wikipedia.org/wiki/Space_suit.
[491] https://www.space.com/39710-orion-spacesuit-waste-disposal-system.html.
[492] https://www.syfy.com/syfy-wire/sci-fi-bioreactor-can-make-food-and-water-in-space-from-algae.

suits do capture waste (using diapers and LiOH scrubbers), but **t**hey don't recycle it.[493] In the fully advanced configuration (including feces and sweat), the metabolic organ attachment approaches closed-loop perfection, with almost zero net loss of matter except for a trickle of inert residues. This concept aligns with the goals of future long-duration missions where efficiency and self-sufficiency are paramount. The mass, volume and power characteristics of the suit attachment should be comparable to those of the artificial metabolic organ (Section 4.3.4), except that water closure would need to be added to the design. The required thermal radiator surface area of $A_{radiator}$ ~ **0.6 m^2** (Section 4.3.5(2)) for waste heat disposal should be available on EVA suits of exterior surface area ~**3.25 m^2**,[494] as should up to ~400 W of power be available to a suited astronaut in Earth orbit equipped with a ~**1 m^2** of ~30% efficient solar cells oriented normal to the solar direction. NASA's design specifications for EVA suits accommodate up to ~2000 BTU/hr (580 W) maximum metabolic load for short periods, but average ~1000 BTU/hr (290 W), during an EVA.[495]

4.3.10.2 Military and Special Operations

Soldiers operating in remote areas or behind enemy lines could greatly benefit from not needing regular rations. A metabolic organ would free troops from carrying days' worth of MREs (Meals Ready-to-Eat) and reduce their dependence on supply drops, making units lighter, faster, and harder to starve out. Historically, "an army marches on its stomach," but with these implants soldiers would march on water and electricity, which might be easier to secure in the field (e.g., via portable solar chargers or generators). Beyond nutrition, the organ's blood detoxification function could serve military needs, e.g., quickly clearing chemical or biological toxins from a soldier's bloodstream. If the metabolic organ stores or can manufacture antidotes to nerve agents, or can deploy tailored immune boosters on command, military medics could use this capability to protect personnel from biochemical warfare or to enhance performance (through controlled release of stimulants, nootropics, or stabilizing hormones). Elite special forces might operate for days in extreme environments (desert, arctic, high altitude) using the organ to manage physiology (e.g., maintaining oxygenation, hydration balance, and energy without regular food) – a strategic advantage in endurance and resilience. Extra shielding is probably required in the military context due to the high risk of damage by offensive combat ordnance.

---

[493] Sofia E, Bielski L, Rose J, Morales K, Belman A, Alexander E, Li E, Lin R, Patel K, Rakhmonova S, Walter C, Mason CE. Enhanced astronaut hygiene and mission efficiency: a novel approach to in-suit waste management and water recovery in spacewalks. Front Space Technol. 2024 Jul 11; 5:01-07; https://www.frontiersin.org/journals/space-technologies/articles/10.3389/frspt.2024.1391200/full.

[494] Jones RJ, Daley MF. NASA Advanced Space Suit xEMU Development Report – Environmental Protection Garment. 51st International Conference on Environmental Systems, 10-14 July 2022, St. Paul MN, ICES-2022-265; https://ttu-ir.tdl.org/bitstreams/da2078f1-6e2d-49ce-8e46-0f7dda027ce9/download.

[495] https://forum.nasaspaceflight.com/index.php?topic=36150.0#:~:text=EMU%20Q%26A%20,7%20by.

4.3.10.3 Habitation in Remote or Extreme Environments

The metabolic organ could be invaluable for explorers and workers in harsh environments, such as polar researchers, deep-sea submersible crews, mountain climbers, or submarine sailors. In many of these situations, supplying food is challenging or adds considerable weight and complexity. With an artificial metabolic organ, an expedition team in Antarctica or on a months-long submarine tour would require only air, water, and electricity (which nuclear subs already produce) to stay nourished. High-altitude climbers could endure longer on mountains where carrying food is heavy and appetite wanes at altitude. The organ could even modulate oxygen and hematocrit levels for altitude acclimatization. Similarly, long-distance sailors or truckers in desolate regions could traverse greater distances without needing to restock food, provided they can generate power via solar panels or otherwise. Essentially, any scenario where humans are cut off from fresh supplies for extended periods could be revolutionized: the artificial metabolic organ turns the body into a largely self-sustaining system, as long as minimal inputs (which could be cached or harvested from the environment) are available.

5. Conclusions

The **artificial metabolic organ** (AMO) is a compact special-purpose diamondoid nanofactory, intended to be implanted in the human body, that could efficiently recycle metabolic waste products into nutrients. By this means, the human user becomes a nutritionally self-sufficient entity needing only air, water, and occasional access to electric power and a few grams per day of stored supplemental minerals to survive indefinitely at metabolic power levels ranging from the basal or resting rate of ~100 W (~2000 kcal/day) up to ~500 W, a fairly vigorous level of physical exertion. The device doesn't prevent eating, it just makes eating unnecessary, adding a capability (nutritional self-sufficiency) that can be used as needed.

The basic objective of the metabolic organ is to serve as a supplementary source of basal "survival" nutrition, not a complete or permanent replacement for all conventional nutrition (i.e., food). Having such an organ would permit the user to easily survive lengthy periods without access to conventional food, but the organ is intended to function in concert with natural digestive and excretory processes – if the user eats food as normal, the metabolic organ has less work to do. However, the monetary cost of normal food may be ~25 times higher than the 2025 cost of the electricity needed to power the device.

Users can still consume food for pleasure, in which case the AMO would simply supplement or idle accordingly, with excess nutrients from food handled by normal physiology or temporarily stored. Over-reliance on the AMO could lead to a very efficient metabolism – e.g., weight gain from eating would be more directly caused since the device ensures no nutrient deficits. Note that if a user with an AMO eats a big meal, the body will try to use that and the AMO must scale back nutrient release to avoid oversupply, in extreme cases causing the person to experience pathological hypernutrition.[496] Ideally the AMO will detect external nutrient inflow (e.g., rising blood glucose after a meal) and correspondingly pause its own nutrient production until the excess is absorbed, preventing "double-feeding".

The metabolic organ is 2400-2441 gm in mass and 1100-1266 cm^3 in volume – a bit smaller than the liver (~1470 cm^3) or brain (~1350 cm^3) – and installed in the central abdomen with proximal

---

[496] Abe K, Kuo L, Zukowska Z. Neuropeptide Y is a mediator of chronic vascular and metabolic maladaptations to stress and hypernutrition. Exp Biol Med (Maywood). 2010 Oct;235(10):1179-84; https://doi.org/10.1258/ebm.2010.009136. Nakagawa H, Umemura A, Taniguchi K, Font-Burgada J, Dhar D, Ogata H, Zhong Z, Valasek MA, Seki E, Hidalgo J, Koike K, Kaufman RJ, Karin M. ER stress cooperates with hypernutrition to trigger TNF-dependent spontaneous HCC development. Cancer Cell. 2014 Sep 8;26(3):331-343; https://pmc.ncbi.nlm.nih.gov/articles/PMC4165611/. Bernardi MM, Macrini DJ, Rodrigues PdS, Kirsten TB, Chaves-Kirsten GP, Florio JC, Reis-Silva TM, Bondan EF, Suffredini IB, Rocha PRD, Bonamin LV. Overweight induced by hypernutrition in juvenile rats dysregulates the central monoamines in the adult age. Psychol Neurosci. 2021; 14(1):34-48; https://repositorio.unip.br/wp-content/uploads/tainacan-items/79420/90960/2021-Bernardi-et-al.pdf. Wang X, He Q, Zhou C, Xu Y, Liu D, Fujiwara N, Kubota N, Click A, Henderson P, Vancil J, Marquez CA, Gunasekaran G, Schwartz ME, Tabrizian P, Sarpel U, Fiel MI, Diao Y, Sun B, Hoshida Y, Liang S, Zhong Z. Prolonged hypernutrition impairs TREM2-dependent efferocytosis to license chronic liver inflammation and NASH development. Immunity. 2023 Jan 10;56(1):58-77; https://pmc.ncbi.nlm.nih.gov/articles/PMC9839616/.

access to the two renal veins and the ureters exiting both kidneys. It has full bloodstream access and the ability to efficiently extract waste molecules from both blood and urine, chemically transform these wastes into nutrient molecules, then release the nutrient molecules back into the bloodstream, creating a closed-circuit nutrient recycling system. The power draw of the device ranges from 200 W to supply basal-level nutritional recycling for ~1 day before recharging the battery, up to 578 W at the peak rated exercise level for ~8 hours of continuous activity, exhausting the onboard battery.

The artificial metabolic organ design described in this paper is hypothetical and relies on future advances in molecular manufacturing and nanorobotics, and assumes the development of diamondoid nanofabrication technology in a future where atomically precise manufacturing is available. Key enabling technologies would include atomically precise manufacturing of diamondoid components, high-density energy storage, and safe biointegration of nanosystems. Current research in DNA origami, molecular motors, and biocompatible materials are stepping stones in this direction. While implementation awaits advances in molecular manufacturing, several component technologies are on the horizon. For example, medical devices that remove CO_2 from blood (e.g., dialysis-like extracorporeal CO_2 scrubbers)[497] or implantable insulin/glucagon pumps[498] already tackle parts of the problem. The AMO can be seen as an ultimate integration of such technologies at the nanoscale. Early prototypes might focus on recycling a single nutrient (such as a device to convert lactic acid back into glucose in muscles) or on supplemental artificial organs[499] (like an implant to assist liver function by detoxifying blood). Each success will pave the way toward the full artificial metabolic organ described here.

The present work demonstrates that, in principle, there are no evident physical impossibilities in meeting human metabolic needs with a ~2.4 kg nanotech device, apart from the need to invent and perfect a suite of technologies beyond what we have today. The general availability of such an organ would open new frontiers in how and where humans can live, and how we tackle hunger and dependency in the future.

---

[497] Staudinger T. Update on extracorporeal carbon dioxide removal: a comprehensive review on principles, indications, efficiency, and complications. Perfusion. 2020 Sep;35(6):492-508; https://pubmed.ncbi.nlm.nih.gov/32156179/. Hanks J, Fox S, Mehkri O, Lund LW, Dill T, Duggal A, Krishnan S. On the horizon: Extracorporeal carbon dioxide removal. Cleve Clin J Med. 2022 Dec 1;89(12):712-718; https://www.ccjm.org/content/89/12/712.long. Combes A, Brodie D, Aissaoui N, Bein T, Capellier G, Dalton HJ, Diehl JL, Kluge S, McAuley DF, Schmidt M, Slutsky AS, Jaber S. Extracorporeal carbon dioxide removal for acute respiratory failure: a review of potential indications, clinical practice and open research questions. Intensive Care Med. 2022 Oct;48(10):1308-1321; https://pureadmin.qub.ac.uk/ws/files/369400138/R1_ECCO2R_for_ICM.pdf.

[498] Rimon MTI, Hasan MW, Hassan MF, Cesmeci S. Advancements in Insulin Pumps: A Comprehensive Exploration of Insulin Pump Systems, Technologies, and Future Directions. Pharmaceutics. 2024 Jul 15;16(7):944; https://pmc.ncbi.nlm.nih.gov/articles/PMC11279469/.

[499] Moon SJ, Jung I, Park CY. Current Advances of Artificial Pancreas Systems: A Comprehensive Review of the Clinical Evidence. Diabetes Metab J. 2021 Nov;45(6):813-839; https://pmc.ncbi.nlm.nih.gov/articles/PMC8640161/.